Looking into the past: A Mid to Late Holocene Sea-Level History for Okains Bay, Canterbury, New Zealand using Ground Penetrating Radar

By

Mitchell Robert Dingwall

A Thesis submitted in fulfilment of the partial requirements for the degree of Master of Science in Geography

The University of Otago, 2022.

This thesis is for examination purposes only and is confidential to the examination process.

Abstract

Okains Bay, New Zealand, provides a sequence of 48 defined beach and 10 dune ridges through a process of progradation with the deposition of sediment derived from the continental shelf (Stephenson and Shulmeister, 1999). Investigation of past sea-level variation in this area shows that the sequence of beach ridges dates approximately back to the beginning of the Holocene when the infilling of the Bay began 7.5 Ka. The Canterbury coastline has not seen significant sea-level work performed in the past, creating a major gap within New Zealand's Holocene sea-level history. Looking at past sea levels can further help comprehend the impacts of localised sea-level variations in the present day and in the future. A transect cut through the middle of Okains Bay over 1.7 km allows for accurate data collection. The use of Ground Penetrating Radar (GPR) enabled a look into the subsurface using electromagnetic reflective pulses. Radiocarbon dating (^{14}C) from shell fragments and thermoluminescence (TSL) dates from quartz grains are supplied from Stephenson and Shulmeister's (1999) paper which deliver further observations into the timing of events at Okains Bay. The results from GPR show past sea-level changes through the prograding sequence of where the high and low stands occurred, as well as providing an insight of erosional events through scraping and storm surge of beach ridges. ^{14}C dates are 672 ± 63 and 1674 ± 76 BP, and TSL dates are 7.5 ± 1.2 ka and 13.5 ± 1.6 ka BP respectively. However, these dates are not in chronological order irrespective of dating methods, potentially due to the mixing of sediment, lag time between death and deposition, or the re-exposure of grains to light. The primary data collected within this research contain a fragmented history of localised sea-level on the Canterbury coastline, aiding in covering an unstudied area within New Zealand's sea-level history. Sea levels dated back to 7.5 ± 1.2 ka show that average sea levels were 1.2 m higher than present day. Furthermore, sea levels varied between present day sea-level and 1 m in height between 7.5 ± 1.2 ka and present day. Such can ultimately contribute to providing a relevant framework for understanding mid to late Holocene sea levels, which in turn, can help with future management of coastal regions.

Keywords: Okains Bay, Beach ridges, Sea-level variation, Ground penetrating radar, Holocene.

Acknowledgements

I would like to thank my supervisor, Associate Professor Wayne Stephenson for his guidance and help throughout this process. I would also like to extend my thanks to Professor Sean Fitzsimons for his help throughout learning how to use GPR and answering GPR related questions. Thank you to the School of Geography for providing me with this chance to write this thesis.

A huge thank you to the people of Okains Bay, with special thank you to Reagan Knapp for helping me get in touch with the rest of the farmers to allow me property access.

A special thank you to Sebastien, Tilly and Chelle, who's motivation to keep me going has led me to finish this research.

Thank you to my parents, Helen and Greg Dingwall for always being there when I needed to have a chat.

Finally, thank you to all of my family and friends that supported me on this journey, it would not have been possible without your support.

Table of Contents

Contents

Chapter One: Introduction **1**

1.1 Context **2**

1.2 Problem Statement **4**

1.3 Purpose of Study **4**

1.4 Thesis structure **6**

Chapter Two: Literature Review **8**

2.1 Introduction **8**

2.2 Global sea-level rise **8**

2.2.1 Causes of Sea-level rise 9

2.2.2 Eccentricity 10

2.2.3 Obliquity 10

2.2.4 Precession 11

2.3 The Impacts of global warming **11**

2.3.1 The Northern Hemisphere 12

2.3.2 Antarctica 13

2.3.3 8000 years to present day 14

2.4 New Zealand's sea-level **15**

2.4.1 New Zealand Holocene sea-level debate 15

2.4.2 No Holocene sea-level highstand at 8ka 16

2.4.3 No spatial variation in sea-level change 16

2.4.4 Refinements of earlier studies 17

2.4.5 Unconventional dating methods 17

2.5 Regional New Zealand sea-level variation over the Holocene **18**

2.5.1 The Northern Section of the North Island. 18

2.5.2 The south-eastern section of the North Island 19

2.5.3 The Canterbury Coastline 20

2.5.4 The Otago coastline 22

2.6 Causes of sea-level rise in New Zealand **23**

2.7 Beach ridges **24**

2.7.1 Swash built beach ridges 25

2.7.2 Settling lag ridges 25

2.7.3 Aeolian formed ridges 25

2.7.4 Storm surge ridges 26

2.7.5 Understanding the internal structure of beach ridges. 26

2.7.6 Using OSL Dating alongside GPR to understand sea-level variation on Beach Ridges 27
2.8 Ground Penetrating Radar 28
2.8.1 Electromagnetic waves 28
2.8.2 Electrical Permittivity of substances 29
2.8.3 Electrical conductivity 32
2.8.4 GPR Antennas 32
2.8.5 Signal Frequencies 32
2.8.6 GPR Pulses 33
2.8.7 Vertical and Horizontal Resolution 34
2.8.8 Data Display 35
2.9 Summary 36
Chapter Three: Field Setting 38
3.1 Introduction 38
3.2 Geological setting 38
3.2.1 Okains Bay 40
3.2.2 Sediment Characteristics of Okains Bay 42
3.3 Progradation at Okains Bay 42
3.3.1 Wave and Tides Characteristics at Okains Bay 42
3.3.2 Sediment Transport 43
3.3.3 Banner Bank 44
3.4 Summary 45
Chapter Four: Methodology 47
4.1 Introduction 47
4.2 Preliminary studies and validation of GPR on Okains Bay beach ridges 48
4.3 Study sites 50
4.3.1 Transect one 51
4.3.2 Transect two 52
4.3.3 Transect three 52
4.4 Description of GPR 52
4.4.1 The Weather and timing of year 54
4.4.2 Type of GPR Survey 54
4.4.3 Electrical Permittivity of Okains Bay 54
4.4.4 Choice of Antennas 55
4.4.5 Timezero 55
4.4.6 Distance between scans 56
4.4.7 Choice of band width between antennas 56
4.4.8 Type of cables used to connect the GPR system to the Antennas 57
4.4.9 Time constraints of data 57
4.5 Real Time Kinematic (RTK) 58
4.6 Processing of Data 60

4.6.1 Static correction 60
4.6.2 Dewowing of datasets 60
4.6.3 Inclusion of Topography 61
4.6.4 Post processing data analysis 61
4.7 Limitations of Methodology 62
4.7.1 Estuary and timing 62
4.7.2 Powerlines and Electric Fences 63
4.7.3 Underground Pipes 63
4.7.3 Anthropogenic change of the Landscape 64
4.7.4 Ethical consideration 64
4.8 Summary 64
Chapter Five: Results 65
5.1 Introduction 65
5.2 Analysis of beach ridge formation using GPR 65
5.3 Transect One of Okains Bay 68
5.4 Transect Two of Okains Bay 70
5.5 Transect Three of Okains Bay 82
5.6 Other GPR images Obtained in Okains Bay 84
5.7 Sea-level curve for Okains Bay 85
5.7.1 Transect Three 85
5.7.2 Transect Two 85
5.7.3 Transect One 86
5.8 Summary 88
Chapter Six: Discussion 89
6.1 Introduction 89
6.2 Okains Bay sea-level history 89
6.2.1 Toplapping and Downlapping surfaces 90
6.2.2 Sea-level analysis 91
6.3 Holocene coastal evolution of Okains Bay 92
6.3.1 Future changes of coastal evolution at Okains Bay 97
6.3.2 Historic storm events on Okains Bay 98
6.4 Comparing Okains Bay sea-level history to Gibb (1986) and Clement et al. (2016) 99
6.4.1 Comparing to Gibb (1986) national sea-level curve 99
6.4.2 Comparison of Okains Bay sea-level history to Clement et al. (2016) Canterbury Holocene sea-level curve 101
6.5 Future Research 103
Chapter Seven: Conclusion 105
7.1 Key Findings 107
7.2 Implications of Findings 108
Reference list 109

Appendix A: GPR image for Okains Bay showing 37.5 m 120
Appendix B: GPR image for Okains Bay showing 100 m 121
Appendix C: GPR image for Okains Bay showing 31 m 122
Appendix D: GPR image for Okains Bay showing 72 m 123
Appendix E: GPR image for Okains Bay showing 85 m 124
Appendix F: GPR image for Okains Bay showing 100 m 125
Appendix G: GPR image for Okains Bay showing 72.5 m 126
Appendix H: GPR image for Okains Bay showing 35 m 127

List of Figures

Figure 1.1. Map indicating the location of Okains Bay in Canterbury, New Zealand… 5

Figure 2.1. Showing where the Laurentide ice sheet was situated over Canada, alongside the former great lake of Lake Agassiz-Ojibway (Original image from Lajeunesse and St-Onge, 2008, redrawn by Smith et al., 2011) 13

Figure 2.2. Sea-level curve for the northern section of the North Island, New Zealand. (Image from Clement et al., 2016) 18

Figure 2.3. Image of sea-level curve for the southeastern section of the North Island New Zealand (Image from Clement et al., 2016) 19

Figure 2.4. Image of sea-level curve for Canterbury coastline, New Zealand (image from Clement et al., 2016) 21

Figure 2.5. Image of sea-level curve for the Otago coastline, New Zealand (Image from Clement et al., 2016) 22

Figure 3.1. Map locations of Banks peninsula as well as Pegasus Bay and the Canterbury Blight..... 39

Figure 3.2. Geomorphic map of Okains Bay showing the beach and dune ridges, as well as the dating sites used in this thesis from Stephenson and Shulmeister, 1999 (Image from Stephenson and Shulmeister,1999) 41

Figure 3.3 Map of the Canterbury region and the flow direction of currents (taken from Carter and Herzier, 1979; adapted by Stephenson and Shulmeister, 1999) 44

Figure 3.4. Bathymetry map off coast of Banks Peninsula showing Banner Bank outside of Okains Bay extending North (Image from Carter and Herzier, 1979: Adapted by Stephenson and Shulmeister, 1999) 45

Figure 4.1. Showing the preliminary work achieved by Harry Jol (Pers. Comm), a) is at 200 MHz while b) is 100 MHz (Images are from Harry Jol Pers. Comm)..... 50

Figure 4.2. Aerial Map of Okains Bay showing the three different transects that are used within this thesis..... 51

Figure 4.3. Image of RTK base station (right) and rover (left) 59

Figure 5.1. Image of GPR through section one of Okains Bay. 5.1a shows imagery from GPR with no analysis. 5.1b shows a schematic of GPR. Red; erosional areas with landward dipping stratigraphy. Green; areas of progradation with downlapping and toplapping points. Orange; areas where stratigraphy is horizontal. Cyan; large hyperbolae, unknown the causes of why this occurred. Brown; unobtainable data 69

Figure 5.2 GPR Image of 61 m of transect in Okains Bay. a) shows data without annotation. b) shows annotation where green = prograding sequence, red = erosional features, = yellow = unobtainable data 71

Figure 5.3: Images of GPR transect in Okains Bay showing 185 m. a) is post processed data with no annotation. B) shows annotations. Green = prograding sequence with downlapping points, red = erosional features, yellow = unreadable data 73

Figure 5.4: Images of GPR transect in Okains Bay showing 222.5 m. a) is post processed data with no annotation. B) shows annotations. Green = prograding sequence with downlapping points, red = erosional features 75

Figure 5.5: GPR image of part of the Okains Bay transect showing 100 m. a) non-annotated image. b) showing annotations. Green = prograding sequence, red = erosional sequence and orange showing horizontal stratigraphy 76

Figure 5.6: GPR image of part of the Okains Bay transect showing 104 m. a) non-annotated image. b) showing annotations. Green = prograding sequence, red = erosional sequence 77

Figure 5.7: GPR image of part of the Okains Bay transect showing 120 m. a) non-annotated image. b) showing annotations. Green = prograding sequence, Blue = Showing aeolian sediment deposition and Purple = showing a mix between an artifact within the ground as well as aeolian deposition 79

Figure 5.8 GPR image of part of the Okains Bay transect showing 71 m. a) non-annotated image. b) showing annotations. Green = prograding sequence, and orange showing horizontal stratigraphy 80

Figure 5.9: GPR image of part of the Okains Bay transect showing 32.5 m. a) non-annotated image. b) showing annotations. Orange = horizontal stratigraphy and cyan = unreadable imagery due to electrical disturbances 81

Figure 5.10: GPR image of part of the Okains Bay transect showing 57.5 m. a) non-annotated image. b) Showing annotations. Green = prograding sequence, red = erosional sequence and orange showing horizontal stratigraphy, Blue/green = area where RTK results misread topography 82

Figure 5.11: GPR image of part of the Okains Bay transect showing 100 m. a) non-annotated image. b) showing annotations. Green = prograding sequence, Blue = aeolian deposition and pink = mix between aeolian and swash zone mixing 84

Figure 5.12. Image of the sea-level history using the downlapping and toplapping surfaces from GPR data collected in this research. Dates from Stephenson and Shulmeister (1999) 87

Figure 6.1. schematic of Okains Bay sea-level history. The red arrows represent consistent amounts of progradation. The green box represents the area of unknown time due to a rising sea-level and progradation only occurred through the building of dune ridges 93

Figure 6.2. Aerial photograph of Okains Bay showing the area where a higher sea-level had the potential to flood during 1674 date, as well as where the coastline would have been 1674 years ago (date from Stephenson and Shulmeister, 1999) 95

Figure 6.3. Showing the sea-level curve. The red line represents point A and the red square represents point B 96

Figure 6.4. Sea-level curve produced by Gibb (1986) further dates and heights added by Shulmeister and Kirk, 1993) 100

List of Tables

Table 4.1. Dates from Stephenson and Shulmeister (1999) 49

Table 5.1. Key features found within the GPR data with definitions 67

List of Equations

Equation 2.1 29
Equation 2.2 29
Equation 2.3 30
Equation 2.4 30
Equation 2.5 31

Glossary

Key abbreviations used

GPR – Ground Penetrating Radar

^{14}C – Radiocarbon dating

OSL – Optical Stimulation Luminescence

RTK – Real Time Kinematic

AIS – Antarctic ice sheet

PMSL – Present mean sea-level

GPS – Geographic positioning system

TSL – Thermoluminescence Dating

Chapter One: Introduction

This thesis investigates a Holocene sea-level record preserved in a prograding beach and dune sequence in Okains Bay on New Zealand's Canterbury coastline. With coastal populations rising at exceptional rates over the last 20 years (Neumann et al., 2015), understanding past occurrences of sea-level can provide insights and contribute to the success of future planning for adaptation and mitigation strategies to sea-level rise.

Globally, sea-level is constantly changing. At a local scale, locations experience different rates of change, dependent on the regional climate and local environmental factors. Thermal expansion of water, and melting ice sheets and glaciers generate eustatic changes, whereas seismic events generating isostatic shifts of coastlines are the major causes of both localised and eustatic sea-level change (Smith et al., 2011). Only a small number of studies have been conducted in New Zealand to explore sea-level change over the Holocene epoch (e.g. Gibb, 1986; Hayward et al., 2010a; Clement, 2011; Clement et al., 2016). Gibb (1986) work, is considered the benchmark study in New Zealand which presented New Zealand's sea-level as a unified system, suggesting that national changes in sea-level occurred at the same time around New Zealand. However, later examinations of New Zealand's sea-level history revealed that it was highly variable and called into doubt whether New Zealand's sea-level history was truly uniform or if regional fluctuations in sea-level occurred (Pirazzoli 1991; Hayward et al., 2010a; Clement, 2011; Clement et al., 2016).

Most studies in New Zealand have used shell fragment identification and radiocarbon dating (^{14}C) to determine the magnitude and timing of changes in sea-level during the Holocene; however, recent global studies (Tamura et al., 2008; Nielsen and Clemmensen, 2009; Clemmensen and Nielsen, 2010) have shown that ground-penetrating radar (GPR) produces higher quality results. Ground Penetrating Radar (GPR) allows the analysis of the subsurface of prograding beaches, within which there is a series of swash zone-produced beach ridges indicative of sea-level at the time of formation. This thesis will explore a beach ridge sequence at Okains Bay, using GPR, as well as ^{14}C, and thermoluminescence (TSL) dates from an earlier investigation by Stephenson and Shulmeister (1999), to observe sea-level fluctuation during the Holocene. This work will indicate whether sea-level change can be observed on the Canterbury coastline. This will allow us to see if the sea-level record here

reflects the national curve of Gibb (1986) or is regionally different as suggested by Clement (2011) and Clement et al. (2016).

1.1 Context

Beach ridges are an important natural feature that has been overlooked in New Zealand sea-level change studies. Beach ridges are comparatively rare systems compared to the usually found dune ridge and marine terrace platforms in New Zealand due to the prograding nature needed to be achieved for beach ridges to become preserved. In general, beach ridges in New Zealand are found on Banks Peninsula, Canterbury (Dingwall, 1966; Stephenson and Shulmeister, 1999), Kaitorete Spit in Canterbury (Soons, Shulmeister and Holt, 1997), Turakirae Head on the South Wellington coast (McSaveney, Graham and Begg, 2006) and beaches south of Auckland such as Miranda (Dougherty and Dickson, 2012) and Whakatiwai (Scholfield, 1960). Beach ridges are landforms found on prograding beaches that arise because of a variety of geomorphological processes (Isla et al., in press). Beach ridges are often described as elongated mounds which run parallel to the shoreline (Otvos, 2000). As progradation progresses, beach ridges become part of the land where they are preserved (Stapor, 1975). Beach ridges are used as a tool for indicating previous shoreline position and shape, as well as for recording internal coastal dynamics (Tamura, 2012). Beach ridges reveal sea-level processes through the way sand is deposited, forming what is known as a downlapping surface (Tamura et al., 2008). Downlapping surfaces occur during low tides, sands and will begin to overlap, creating an overlap in stratigraphy (Tamura et al., 2008; Nielsen and Clemmensen, 2009). ^{14}C dating and OSL is the two primary dating techniques that are used when employing GPR to look at downlapping surfaces of prograding coastlines.

GPR is a non-destructive analytical technique that allows the examination of the internal structure of beach ridges without disturbing the subsurface. GPR uses electromagnetic energy to detect variations in attenuation caused by changes in electrical conductivity, electrical permittivity, and dielectric permittivity, which helps to visually reconstruct internal sedimentary structures. Due to complexities in beach ridge development and beach progradation, a sound understanding of the GPR method on beach ridges is imperative (Tamura, 2012). Globally, many studies have misinterpreted GPR observations, which has resulted in variability in overall data analysis. Ultimately, this has produced some erroneous

data when investigating paleoenvironmental records (Tamura, 2012). Only a few studies (e.g. Tamura et al., 2008; Nielsen and Clemmensen, 2009; Clemmensen and Nielsen, 2010) on beach ridges globally have begun to use GPR to its full extent to understand how sea-level has changed in within their localised studies throughout the Holocene, potential for GPR to reveal New Zealand's sea-level history from prograded beach ridges remains untapped.

Over the last 40 years, various research has been conducted on sea-level change in New Zealand, with the leading paper published by Gibb (1986). Gibb (1986) characterised New Zealand's sea-level change as a consistent process by examining two areas: one on the South Island and the other on the North Island. This publication elevated Gibb to the status of one of the foremost sea-level fluctuation researchers in New Zealand. Based on Gibb's (1986) paper, additional investigations were carried out in similar locations across New Zealand. (e.g. Davies and Healy, 1993; Brown, 1995; Heap and Nichol, 1997; Kennedy, 2008). However, these studies were conducted irrespective of other New Zealand sea-level change studies, resulting in conflicting Holocene sea-level history (Hayward et al., 2007).

Hayward et al. (2007) and Clement et al. (2016) have characterised New Zealand's Holocene sea-level history in a widely fragmented manner. Clement et al. (2016) analysed Gibb (1986) findings by consolidating all investigations done in New Zealand, which revealed sea-level was not uniform but varied locally; the North Island reached its highstand 600 -1400 years earlier than Gibb's (1986) findings, however, the South Islands highstand point was unable to be formed due to lack of evidence. Clement et al. (2016) also revealed that there were numerous gaps in New Zealand's sea-level, especially on the Canterbury and Otago coastlines. Their findings called for further research, particularly on the Canterbury and Otago coastlines where there is relatively little data, to better understand how sea-level changed throughout the Holocene. With predictions of future warming temperatures and rising sea-levels (IPCC, 2021), understanding how past sea-level have varied is imperative to the future development of communities that reside on and near these coastlines. Localised sea-level curves are highly important as they help predict rises and falls that can occur in the future. The variation in localised sea-levels creates complex situations for managing sea-levels. Using a single national sea-level curve likely creates misconceptions about what has occurred in the past and therefore provides inadequate knowledge on areas that were overlooked, such as the Canterbury coastline.

1.2 Problem Statement

During the past 40 years, studies of New Zealand beach ridges have been predominantly carried out using ^{14}C, TSL dating to investigate sea-level fluctuation. Using only dating techniques has several drawbacks, notably ^{14}C dating, which records the time of death of organisms with carbon shells rather than the moment of deposition (Shulmeister and Head, 1993). While GPR does not provide dates, it does provide accurate information on the changes that occur in the stratigraphy in the subsurface of beach ridges. However, interpreting the subsurface requires an understanding of beach ridge and prograding beach processes, in addition to the interpretation of GPR radargrams. Little research has been carried out on the Canterbury coastline, which has hindered a developed understanding of how the eastern section of the South Island of New Zealand's sea-level has changed throughout the Holocene. This highlights a gap in our knowledge of New Zealand sea-level variation over the Holocene. The beach ridge sequence in Okains Bay, therefore, presents an opportunity to employ GPR on a prograding coastline with a long succession of beach ridges that have been previously dated to the Mid-Holocene, 7500 years ago (Stephenson and Shulmeister, 1999).

1.3 Purpose of Study

The objective of this thesis is to extend the preliminary research conducted by Stephenson and Schulmeister (1999) in Okains Bay. Okains Bay is located on New Zealand's east coast, situated on Banks Peninsula in Canterbury (Figure 1.1). The bay is facing a northeast direction and is approximately 3 km long and 1 km wide. From the beach face, the bay extends a further 2 km, where the bay's head enters open water. Investigation of the Okains Bay beach ridge system was conducted using a multi-technique approach to determine a sea-level curve. This will be accomplished through GPR, real-time kinematic GPS surveying (RTK), and ^{14}C and TSL dates from Stephenson and Schulmeister (1999).

Okains Bay's beach ridge system, which consists of 48 beach ridges and 10 dune ridges, is a suitable location for studying beach ridges to observe Holocene sea-level fluctuation using GPR. The bay has been subject to a modest degree of anthropogenic modification, with a small village within the bay, as well as conversion to farm fields, enabling the preservation of most beach ridges to occur across the bay. Dingwall (1974) followed by Stephenson and

Shulmeister's (1999) initial study at Okains Bay revealed that the origin of the beach sand is the continental shelf rather than the catchment or cliff erosion at Banks Peninsula and that sediment originated from the erosion of the Canterbury coast to the south of the peninsula. Stephenson and Shulmeister (1999) also noted a change in sediment supply from the coastlines, with a slowing progradation between 6000 and 2000 years BP associated with changing erosion rates of the Canterbury coast.

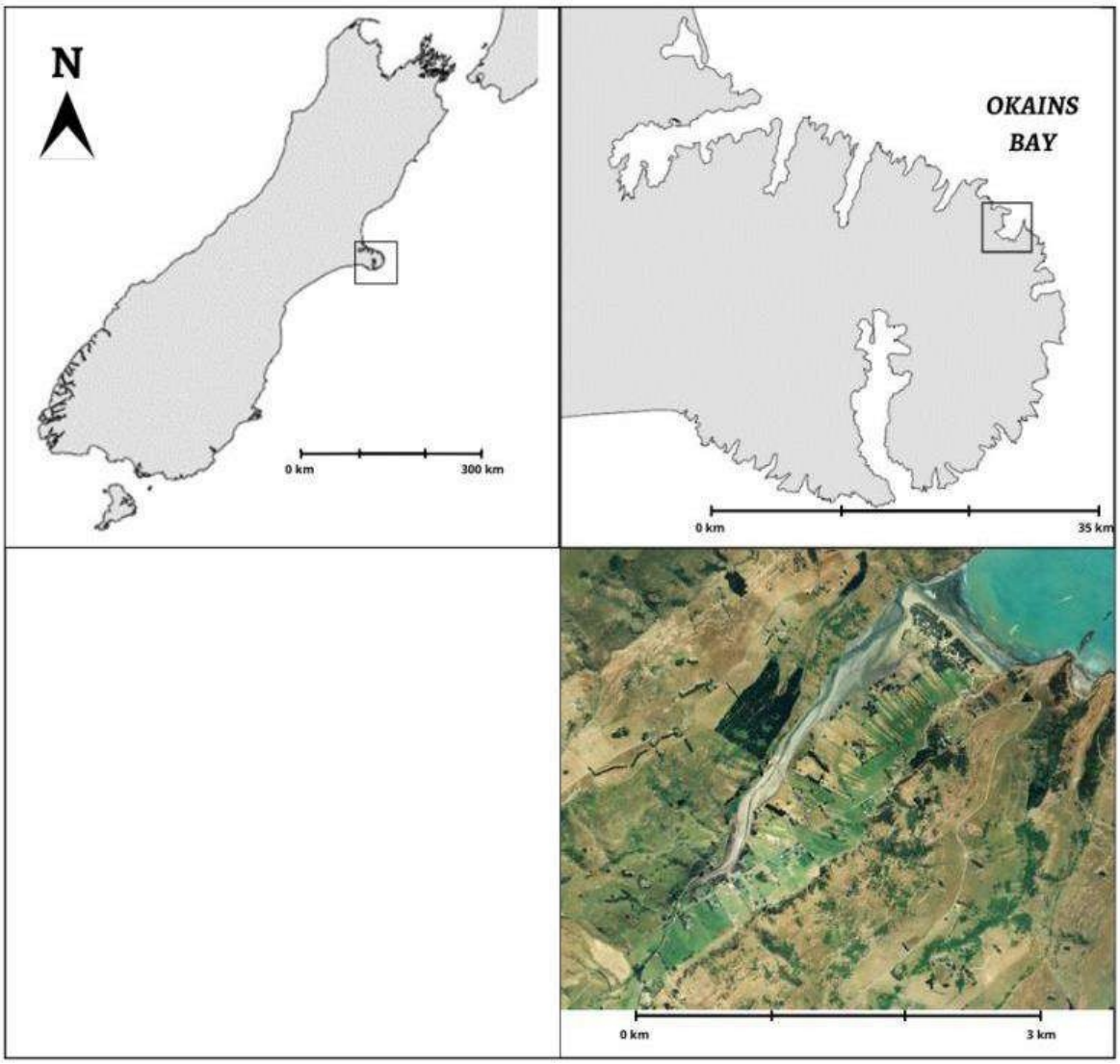


Figure 1.1. Map indicating the location of Okains Bay in Canterbury, New Zealand.

This research will investigate evidence of sea-level history preservation at Okains Bay, Canterbury, New Zealand. This study will offer reliable knowledge on the timing and magnitude of sea-level fluctuation at Okains Bay, in turn helping to predict how Canterbury's coastline has evolved through the Holocene. This study will therefore contribute to the developing understanding of New Zealand's overall sea-level history.

This thesis aims to answer the following research questions:

1. Does Okains Bay hold a preserved and intact sea-level curve for the Canterbury coastline line and what does this sea-level curve look like?
2. What are the changes in coastal evolution that have occurred with a changing sea-level over the Holocene at Okains Bay?
3. Does the sea-level curve at Okains Bay fit more to Gibb (1986) or Clement et al. (2016)?

1.4 Thesis structure

This thesis will follow a multi-step approach in the investigation of sea-level change at Okains Bay. Chapter Two will provide a comprehensive discussion of previous and contemporary literature on sea-level fluctuation over the Holocene. Then a discussion of how beach ridges originate and the mechanisms that occur during progradation, leading to preservation is presented. The current and historical literature on New Zealand's sea-level history will be examined and compared to what has been researched in the Southern Hemisphere, notably Antarctica, Australia, and the Pacific Islands. Following that, a method review will look at how GPR is utilised, as well as why GPR approaches are crucial when researching beach ridges. Chapter Three provides a description of the field location, covering the geology and geomorphology of Okains Bay and Banks Peninsula in Canterbury, New Zealand. The fourth chapter explains the methodologies employed in this thesis, as well as the setup, calibration, and validity of GPR and real-time kinematic (RTK). Chapter Five presents the results of GPR and RTK investigations into the subsurface of Okains Bay's beach ridges and provides the key findings from the research area. Chapter Six provides a discussion of the primary findings reported in Chapter Six and will answer the research questions formed for this study.

Limitations faced during this research project and suggestions for future studies will then be reported and suggested respectively. Finally, Chapter 7 concludes by commenting on this thesis in its entirety.

Chapter Two: Literature Review

2.1 Introduction

Chapter Two provides a discussion of the current sea-level literature for both global and localised sea-level change over the Holocene. Understanding global sea-level changes are of utmost importance as it is the main driver of these localised changes. Sea-level is known to not be uniform, and changes occur down to a localised scale, for instance in New Zealand, there are four main regions (northern section of North Island, south-eastern section of North Island, the Canterbury coastline and the Otago coastline) with subtle changes between them. These changes have been theorised to occur through the melt of the Antarctic ice sheet through the Holocene as well as change in isostatic loading from hydro, glacial, and sedimentary changes. Localised sea-level change within New Zealand has been described as highly fragmented with large gaps in the Canterbury region making it extremely difficult to produce any type of sea-level curve for the region (Clement et al., 2016). Beach ridges on Okains Bay will be used extensively and therefore discussion on the formation and type of beach ridges will follow the discussion on sea-level change. Finally, a detailed explanation of ground penetrating radar (GPR) will be discussed, as well as the different types of ways GPR can be used to produce results that will further increase the chances of a sea-level curve being produced for Okains Bay, Canterbury, New Zealand.

2.2 Global sea-level rise

The history of global sea-level change is extremely complex, with several theories on the origins and consequences of global sea-level change (e.g. Pirazzoli, 1991; Carlson et al., 1991; Lambeck et al., 2002; Smith et al., 2011; Ullman et al., 2016) as well as contrasting models by the likes of (e.g. Flemming et al., 1998; Bard et al., 2010). Based on research previously mentioned, global sea-level has increased around 130 m since the Last Glacial Maximum (LGM), which occurred between 26.5 and 19 ka. The reasons for this variation in sea-level from the LGM to the present day have been identified as changes in the orbital shape of Earth around the sun, the tilt of the Earth's axis, and the wobble of the Earth's axis, also known as the Milankovitch cycles (First addressed within sea-level studies by Munk and Revelle, 1952).

The shift of the earth's axis focused more solar energy on the poles, melting massive ice caps closer to the poles, and therefore rising global temperatures of the planet (Denton and Hughes, 2017). These ice sheets, especially the Laurentide and Antarctic, with minor contributions from the Cordilleran; Fennoscandian, Barents-Kara, Patagonian, and Innuition ice sheets, created a total sea-level increase of 70 m from the beginning of the LGM to the start of the Holocene, and 60 m between 12,000- and 8000-years BP (Smith et al., 2011). After 8000 years, sea-level reached a highstand and has been fluctuating dependent on the location on the Earth till the current day. The melting of these ice sheets has a significant influence on the Earth's ocean circulation cycle. With the inundation of about 10 million km^2 of continental shelves, current flow directions are altering, hence influencing the earth's climate and global temperatures (Smith et al., 2011). Numerous studies (e.g. Fairbanks, 1989; Edwards et al., 1993; Bard et al., 1996; Liu et al., 2004) have claimed that three large meltwater pulses occurred after the initial melting of ice sheets, indicating that sea-level rise was not stable, but varied between rapid rates of rise during the times of these meltwater pulses (MWPS) (30-60 mm/yr) and slower rates outside of MWPS giving rise of 6-9 mm/yr (Smith et al., 2011).

2.2.1 Causes of Sea-level rise

Theoretical and empirical studies of the drivers of glacial and interglacial cycles are ongoing; One ongoing theory of the causes of climate change over the Holocene is though the Milankovitch theory of global climatic change which is affected by the change in the amount of solar radiation received on the poles by a change in Earths orbital cycle, first addressed by Munk and Revelle, 1952) and later Ritchie, Cyrnar and Spear (1983). The effects from the Milankovitch thermal maximum are seen to have occurred with higher amounts of solar radiation in the Northern Hemisphere leading to the retreat of large ice caps. Ritchie and his co-workers predicted that summer solstice radiation was 9-10 % greater than seen today by using tree pollen records from the MacKenzie River Delta that was freed from the Laurentide ice sheet, 14,000 years ago (Ritchie et al., 1983).

2.2.2 Eccentricity

Eccentricity is defined as the change in orbital shape during a 100,000-year cycle. The earth's orbit around the sun varies throughout time from an elliptic cycle to a more radial cycle and back again (Berger, 1988). As such, has had a direct impact on the quantity of constant solar energy that the earth receives. When the eccentricity cycle is at its greatest elliptic cycle, the variation in solar energy is at its peak, with the summer season receiving around 23 % more solar radiation than the winter seasons (Berger, 1988). When the planet is at its most elliptical cycle, the temperature is substantially lower due to reduced radiation during the winter months, enabling more ice to develop and driving the planet towards a glacial period. With 6.8 % solar energy during the summer and winter months, Earth is presently nearing its more circular revolution around the sun (Laskar et al., 2011). This indicates that until the LGM, which occurred at 26 Ka and before that, Earth has been slowly approaching the sun, and as a result, temperatures have been somewhat more constant, resulting in a warmer environment on Earth (Laskar et al., 2011). Eccentricity is considered to have the least influence on the Earth's climate because of the long period it takes to change, resulting in a situation where changes are more gradual and develop slowly.

2.2.3 Obliquity

The second Milankovitch hypothesis is obliquity, which is the shift in the tilt of the earth's axis between 22.1 and 24.5 degrees (Berger, 1988). Across 41,000-year cycles, the hypothesis of obliquity is thought to occur. When obliquity declines and approaches the 22.1-degree axis, warmer winters and cooler summers occur, allowing ice caps to form around the poles and as such, cools down the globe. The reflection of ice sheets and snow increases albedo, further cooling the earth and driving the planet towards an ice age (Berger, 1988). Maximum tilt promotes warmer temperatures in the summer and lower temperatures in the winter, resulting in the reverse effect, with ice caps melting and global average temperatures rising. The major cause of glacial and interglacial cycles is assumed to be obliquity (Berger, 1988; Denton and Hughes, 1983; Fairbridge, 1982). According to the literature (Berger, 1988), ice ages occur on a 41,000-year cycle. The earth is now at a 23.4-degree axis tilt, midway between both extremes, and is gradually reverting to a more upright posture. As a result, the greatest tilt occurred around 10,700 years ago, around the beginning of the Holocene (Buis, 2020). This also implies that the LGM occurred when the Earth's axis was at its highest tilt. As a result, Obliquity is the

source of global warming and as such the reason for the melting of the greatest ice caps from the LGM, which thereafter leads to the dramatic rises of eustatic sea-level (Berger, 1988).

2.2.4 Precession

The final Milankovitch cycle is precession, which is the wobble of the earth's axis, comparable to a slowing spinning, spinning top. The wobble is generated by the oceanic tidal pull from the sun and the moon's gravitational pull, which causes the earth to bulge in the centre (Berger, 1988). As a consequence of precession, the Northern Hemisphere currently experiences less seasonal change than the Southern Hemisphere, resulting in warmer temperatures and more ice melt in the Southern Hemisphere. This was the opposite 10,000 years ago, with the Northern Hemisphere receiving more solar energy through precession in addition to the tilt from obliquity (Denton and Hughes, 1983). The orbital cycle of obliquity and precession had a direct influence on the melting of Northern Hemisphere ice caps during the main melt from the LGM, as explained in the next portion of this thesis.

2.3 The Impacts of global warming

The increase in global ocean volume in the early Holocene was driven by climatic changes that warmed the Earth’s atmosphere (Ritchie, Crywir and Spear, 1983; Smith et al., 2011). While much is unclear about Holocene sea-level rise, melting ice sheets triggered three significant episodes of sea-level rise, as evidenced by coral reef deep core drilling (See Smith et al., 2011 for further explanation). MWPS are another name for these significant phenomena. Over 600 years, MWPS was responsible for 27.5 m of fast increase in sea-levels. The first MWP, also known as MWP 1a, occurred between 14,600 and 14,300 years ago, right before the Holocene (Deschamps, 2009). During these 300 years, eustatic sea -level rose by 13.5 metres. However, as it occurred outside of the Holocene boundary, MWP 1a is not included in Holocene sea-level literature (such as Smith et al., 2011). MWP 1b was thus the first significant MWP that occurred during the Holocene, occurring between 11,400 and 11,100 years ago. The precise chronology is uncertain, but (Blanchon and Shaw, 1995) claimed that it happened over 160 years and resulted in a 7.5-meter rise in eustatic sea-level. Sea-level rise rates were much slower between MWP 1b and MWP 1c, ranging from 6.0 to 9.9 mm/yr (Smith et al., 2011). The most debated and last reported significant MWP that occurred throughout the Holocene

was MWP 1c. MWP 1c occurred between 8.2 and 7.6 ka, with a centre at 8 ka (also known as the 8ka cooling event) (Nesje et al., 2004; Barber et al., 1999). Within about 140 years, MWP 1c observed a sea-level rise of 6.5 m, raising sea-level (3 m) above the present mean sea-level (PMSL). The fundamental cause of MWP 1c is still debated, with (Peltier and Fairbanks, 2006) arguing that the Laurentide ice sheet collapse was the key reason, while (Leventer et al., 2006; Blanchon and Shaw, 1995; Yu et al., 2007) argue that the Antarctic ice sheet retreat was the primary cause. However, it should be highlighted that because both episodes had significant effects on sea-level and happened around the same period, they should both be represented as significant contributors to MWP 1c.

2.3.1 The Northern Hemisphere

During the Early Holocene, ice sheets and glaciers were still widespread over the Northern Hemisphere with stable ice retreat occurring since the LGM (Smith et al., 2011). In North America, the main ice sheets that dominated the area were the Cordilleran ice sheet, Laurentide ice sheet and the Innuitian ice sheet (Clague and James, 2002; England et al., 2006; Smith et al., 2012). The Cordilleran ice sheet, over northern parts of America and on the Pacific coastline was retreating due to the rise in sea-level and climate temperatures, releasing large amounts of water into the Pacific Ocean. As sea-levels rose, the retreat of the ice sheet became more rapid, especially on the southern sections of the Cordilleran ice sheet (Clague and James, 2002). Both the Innuitian and Laurentide ice sheet began to melt rapidly by 11,600 years due to both climate change and rising sea-levels (England et al., 2006).

The Laurentide ice sheet is thought to be one of the largest causes of sea-level rise during the early to Mid-Holocene, however, the total amount of sea-level rise is still uncertain (Peltier and Fairbanks, 2006). As the ice sheet continued to melt, a large deep channel opened, known as the Hudson Bay (Andrew and Peltier, 1976), further forcing the discharge of large amounts of water into the Atlantic Ocean. Opening of Lake Agassiz carved out underneath the Laurentide ice sheet is thought to have formed by 13,400 yr/BP (Figure 2.1), joining Lake Ojibway to the East (Leverington et al., 2002; Teller and Leverington, 2004). Discharge from these two lakes, fully draining them was thought to have occurred by 8470 BP (Barber et al., 1999) significantly increasing sea-levels. Drainage of the two lakes into the Tyrrell Sea was thought to have occurred in episodes of 113,110 km^3 to 49,900 km^3 (Clark et al., 2004).

Changes in ice sheets over Europe and Asia were thought to have occurred with Holocene sea-level rise only having a minor effect on the ice sheets (Smith et al., 2012). Most glacial and ice sheet-locked water was landlocked, which melted over time due to the change in atmospheric heat, eventually discharging into the northern oceans and seas (Smith et al., 2012).

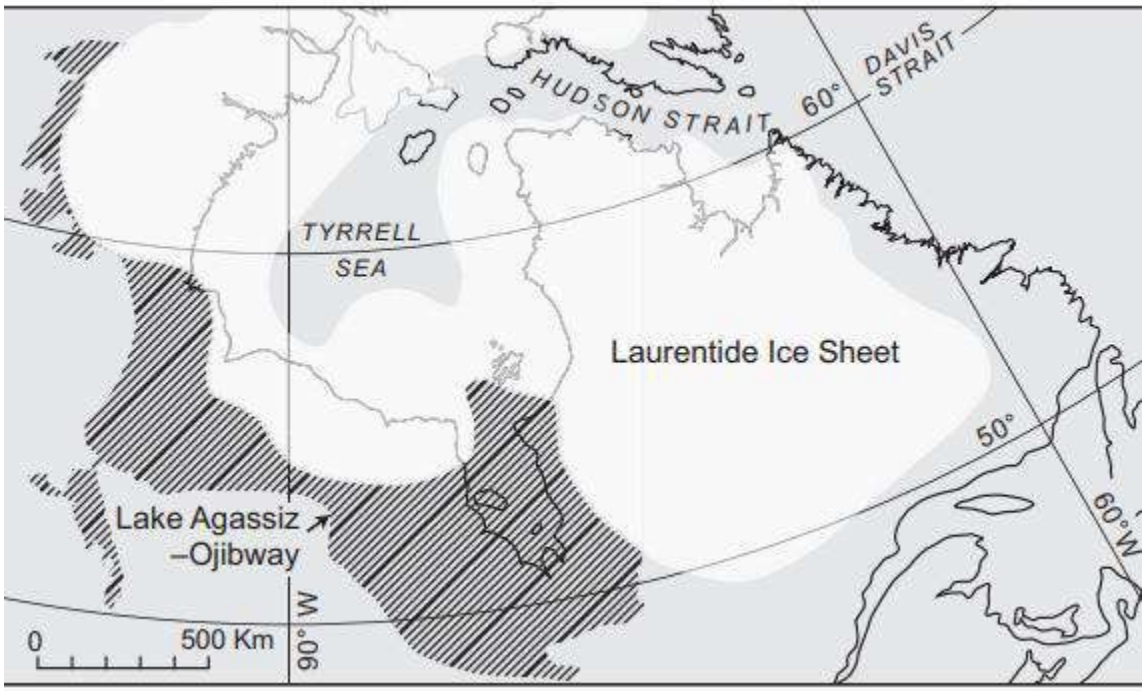


Figure 2.1. Showing where the Laurentide ice sheet was situated over Canada, alongside the former great lake of Lake Agassiz-Ojibway (Original image from Lajeunesse and St-Onge, 2008, redrawn by Smith et al., 2011)

2.3.2 Antarctica

The loss of Antarctica's west ice sheet was also one of the key sources of Holocene sea-level increase during the early and mid-Holocene. The amount of eustatic sea-level rise caused by the Antarctic ice sheet (AIS) retreat is still unknown since the MWPs are still undetermined (Smith et al., 2011). However, research suggests a significant impact on the MWP 1b and 1c, as well as accounting for world sea-level increase (Leventer et al., 2006; Blanchon and Shaw, 1995). The AIS retreat began is thought to have occurred on the western side of Antarctica, with a change in latitude in the Southern Hemisphere westerly wind belt (SHWW) between 12 and 8 Ka, when the SHWW was farther south, closer to Antarctica (McGlone et al., 2010). The shift of the SHWW had a direct impact on the upwelling of Circumpolar Deepwater (CDW) beneath the glacial sea ice sheets. Higher temperatures of water rising from the ocean's depths,

along with worldwide ice sheet melting, had the potential to destabilise the AIS, forcing the melting and retreat of the Antarctic ice sheet between 12 and 8 ka (Mackintosh et al., 2011). Because the west of Antarctica was partially melted by upwelling of CDW as well as a rising sea-level, the melting of the AIS would have had an impact on local sea-level datum throughout the southern hemisphere, namely in Australia, New Zealand, and the Pacific (Clement et al., 2016). The isostatic shift would have occurred after ice melt, with isostatic bulge contributing to sea-level changes in areas such as Australia, and New Zealand, raising the surface of the land more in the south than in the north (Clement et al., 2016). As such, this rise would see fewer amounts of sea-level rise within the southern sections of Australia and New Zealand and more rise within the northern sections, as well as the Pacific.

2.3.3 8000 years to present day

Between 8000 years ago and today, sea levels became more stable than they had previously been since the LGM. After the catastrophic collapse of the Laurentide ice sheet and the partial melt of AIS, as discussed in section 2.3.1 and 2.3.2, there were no significant changes in eustatic levels (Smith et al., 2011). The melting of polar ice caps continues to this day but has little influence on eustatic sea-level as it previously did, most likely due to the Milankovitch cycle of obliquity beginning to return to 22.1 degrees, therefore reducing the amount of solar radiation on Earth's poles. Following this point, the literature on Holocene sea-level change turned from eustatic sea-level variation to localised sea-level change.

Localised sea-level change happens depending on the precise place on the planet. While there is no major difference between two nearby locations, the variances are critical to understanding where sea-level rise originated, therefore aiding to understand previous sea-level changes and helping with the future management of changing coastlines. Australia, New Zealand, and the Pacific islands are some of the most important study locations for sea-level fluctuation in the Southern Hemisphere, as these locations were directly impacted by the melting of the AIS (Anderson et al., 2002) as well as feeling the effects from the Laurentide and Cordilleran ice sheet collapse.

2.4 New Zealand's sea-level

Sea-level change takes place both worldwide and locally. Global variations in sea-level are caused by mechanisms such as the thermal expansion of water and the collapse of large ice sheets near the poles, as previously described. It is well understood that sea-level is not uniform but rather fluctuates locally (Clement et al., 2016). Such differences between sea levels are seen in New Zealand as described by Clement et al. (2016). These small fluctuations in sea-level are caused by seismic processes, namely isostasy, rather than by climate change. However, it should be recognised that climate change can have an impact on these seismic shifts. There are five different types of isostasy sea-level shifts that might occur (Smith et al., 2011). These are Glacio-isostasy changes, which are caused by the loading or unloading of surface ice on the crust. The loading or unloading of water on the crust is known as hydro-isostasy. Thermal- isostasy is the change in temperature and/or density of the planet's interior, locally lifting or subsiding areas. Sediment-isostasy refers to the deposition or erosion of vast volumes of sediments that have a direct influence on the earth's crust. Finally, volcanic isostasy is achieved by magmatic extrusions. Throughout the Holocene, the primary drivers of localised sea-level change have been glacial, hydro, sedimentary, and some volcanic isostasy. Thermal isostasy is not considered a significant cause of sea-level variation through the Holocene in New Zealand as such process can take millions of years to create internal change. Sedimentary processes can have little influence on Holocene sea-level change, although only by 4 mm/yr (Clement et al., 2016).

2.4.1 New Zealand Holocene sea-level debate

The study by Gibb (1983), and further investigated by Gibb (1986), has long been the benchmark study of New Zealand's Holocene sea-level trend. Gibb (1986) published study focused on two New Zealand locations, one on the South Island at Blueskin Bay, just north of Dunedin, and the other on the North Island at Weiti River Estuary which was used as zero datum sites for the other ^{14}C locations used in Gibb's work around New Zealand. Through the investigation of the numerous locations around New Zealand, Gibb (1986) proposed that sea-level in New Zealand reached current PMSL at 6. Ka though the use of ^{14}C. After Gibb's study, little research was done to critically evaluate this finding, mainly due to the limited understanding of New Zealand's sea-level during the time. Pirazzoli (1992) (research done

outside of New Zealand), Clement (2011) and Clement et al. (2016) were the only studies which critically analysed Gibb (1983) and Gibb (1986) work. The study by Clement et al. (2016) has been well acknowledged in New Zealand's Holocene sea-level change, as such study synthesised past literature over the period of 30 years to explain localised sea-level changes within New Zealand. Within Clement et al. (2016), Clement and his co-workers critiqued Gibb (1986) research in the following ways:

2.4.2 No Holocene sea-level highstand at 8ka

Many researchers using geography information analysis (GIA) models (e.g. Nakada and Lambeck, 1989; Gehrels et al., 2012), geomorphic investigations (e.g. Hicks and Nichol, 2007; Kennedy, 2008; Schallenberg et al., 2012), sea-level reconstructions (e.g. Clement et al., 2016; Clement, 2011), and studies done in the Pacific and Australia (e.g. Baker et al., 2001a; Woodriffe, 2009; Lewis et al., 2013 for the Pacific Islands and Sloss et al., 2007; Lewis et al., 2013 for Australia), have revealed that there was a mid-level highstand on coastal New Zealand throughout the Holocene (Clement et al., 2016). To uncover sea-level references in New Zealand, the east coast of Australia and the Pacific islands to the north of New Zealand were locations of investigation as they share the same currents and are in the same sea-level zone. Findings (Baker et al., 2001a; Woodriffe, 2009; Lewis et al., 2013; Sloss et al., 2007; Lewis et al., 2013) in Australia and the Pacific area both suggested a Mid Holocene sea-level rise of varying magnitudes. Gibb (1983) and Gibb (1986) found no evidence of a mid-Holocene sea-level high stand. Clement et al. (2016) claimed that Gibb (1986) misunderstood his data, interpreting a mid-level highstand as tectonic uplift, and potentially did not use data that would have reflected sea-level height (Clement et al., 2016).

2.4.3 No spatial variation in sea-level change

Using sea-level indicator sites from throughout New Zealand, Gibb (1986) attempted to demonstrate that New Zealand's sea-level was uniform. However, evidence of localised changes is seen by Clement et al. (2016), showing that sea-level in New Zealand is not uniform, thus contesting Gibb's (1986) findings. The sea-level around the east coast of Australia and the Pacific Islands north of New Zealand is also not consistent, with localised differences

occurring. Such is supported through geographic information analysis (GIA) models of sea-level change exhibiting degrees of geographical and temporal variations (Clement et al., 2016).

2.4.4 Refinements of earlier studies

Clement et al. (2016) claimed that Gibb's changed his work between 1983 and 1986. Gibb's (1986) final reconstruction had multiple alterations with no justification or argument for why these changes occurred. Pirazzoli (1991) previously claimed that these variations in Gibb's work between 1983 and 1986 give the reader the impression that there is a greater level of vertical uncertainty than Gibb's (1986) inferred. Gibb's sea-level curve was displayed as a single line rather than two separate lines that would have shown vertical uncertainty, indicating that vertical uncertainty may have been ignored (Clement et al., 2016; Pizzaoli, 1991).

2.4.5 Unconventional dating methods

Three studies (Clement et al., 2016; Wilson et al., 2007a; Clark et al., 2011) sought to recalibrate (Gibb, 1986) radiocarbon dates into sideral years. Clement (2011) stated that this was not feasible since the dates used in Gibb's (1986) were obtained using unusual dating procedures, however, Clement et al. (2016) did suggests that dates from Gibb (1986) are erroneous and should not be utilised as a depiction of sea-level history over New Zealand.

From Gibb (1986), Clement et al. (2016) showed that New Zealand's sea-level data was highly fragmented and there was no cohesive document that provided insight into all localised sea-level changes that occurred on the coastlines of New Zealand. In doing so, Clement et al. (2016) compiled 30 years of past sea-level research previously done into one document and sectioned localised sea-level into regional sea-level. These sections are:

1. The northern section of the North Island
2. The south-eastern section of the North Island
3. The Canterbury region on the east coast of the South Island
4. The Otago region on the south-eastern coast of the South Island.

2.5 Regional New Zealand sea-level variation over the Holocene

The following section of this chapter introduces the sea-level change over the four regions as studied by Clement et al. (2016).

2.5.1 The Northern Section of the North Island.

The majority of studies on New Zealand's Holocene sea-level fluctuation have been achieved in this the northern section of the North Island of New Zealand. Twenty-four studies have been reviewed in Clement et al. (2016) paper on the northern sections of the North Island, providing for high-quality outcomes. Present mean sea-level (PMSL) was achieved between 8100 - 7340 yr/BP, 600 - 1400 years before Gibb's'(1983) and Gibb's (1986) findings (Figure 2.2). Sea-level rose until 4000 yr/BP, reaching approximately 2.5 m above PMSL. Afterward sea-level began to decline until it reached its current level (Clement et al., 2016).

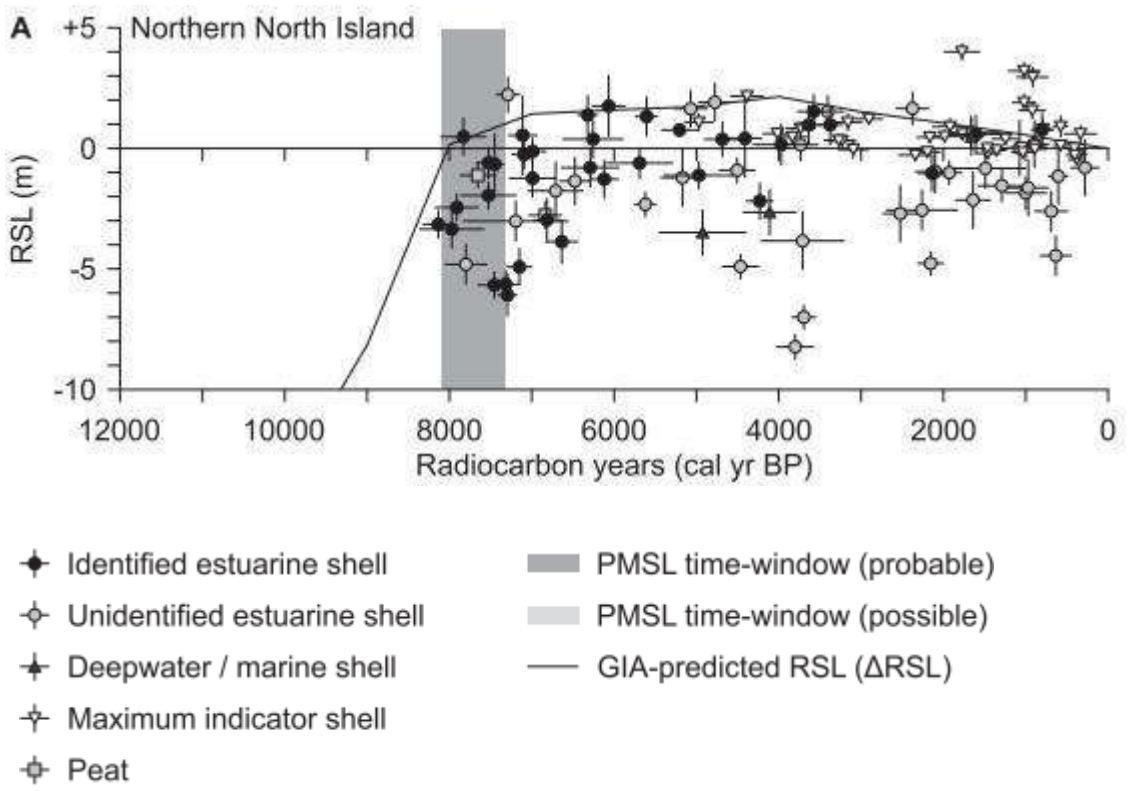


Figure 2.2. Sea-level curve for the northern section of the North Island, New Zealand. (Image from Clement et al., 2016)

2.5.2 The south-eastern section of the North Island

The south-eastern region of the North Island sees the second most activity through Clement et al. (2016) research, allowing for quality data to be obtained by aggregating all work done in the area. PMSL was obtained between 7780-7270 cal yr BP, which is 320 – 70 years later than what is shown on the northern North Island (Clement et al., 2016), demonstrating variance between the north and south of the North Island (Figure 2.3). As sea-level rose above PMSL, a mid-Holocene highstand of 3 m was reached at 7 ka, significantly higher than in the northern North Island (Clement et al., 2016). As such, it is seen within Figure 2.3 that the highstand of 3m continued to stay at this point until 4000 years BP, before declining in a similar fashion to the northern North Island.

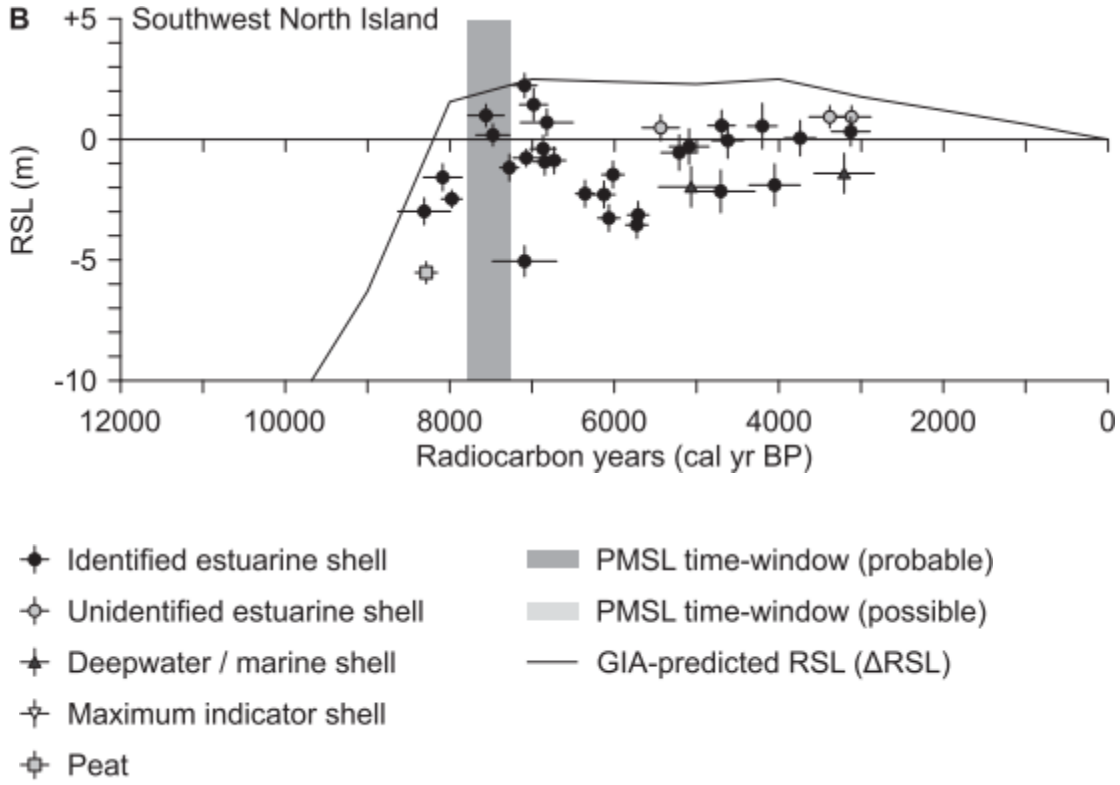


Figure 2.3. Image of sea-level curve for the southeastern section of the North Island New Zealand (Image from Clement et al., 2016).

2.5.3 The Canterbury Coastline

The Canterbury area is substantially less researched than areas on the North Island. The investigation of sea-level in Canterbury is very fragmented and subjective rather than conclusive due to the small number of studies currently available for the Canterbury coastline. Clement et al. (2016) stated that due to a lack of information, it is currently hard to estimate the exact time of PMSL in Canterbury during the Holocene, thus providing an opportunity for this thesis to further investigate the Canterbury coastline, specifically Okains Bay, Canterbury. However, Clement et al. (2016) has placed PMSL attainment at 7000 – 6400 cal yr BP (Figure 2.4). A mid-Holocene sea-level highstand may still be visible (Figure 2.4), but approximately 1 m less than on the North Island. Nevertheless, the mid-to-late-Holocene phase of Canterbury's sea-level curve is less conclusive via dating evidence of shell pieces. Clement et al. (2016) proposed that further study on the Canterbury coastline is needed to get important conclusions about New Zealand's Holocene sea-level history. The majority of work seen within Clement et al. (2016) Canterbury sea-level curve is seen to predate when PMSL was obtained during the mid-Holocene. Future work, such as this research topic will provide further insight into sea-level between 7.5 ka and present day, further aiding towards Canterburies sea-level curve.

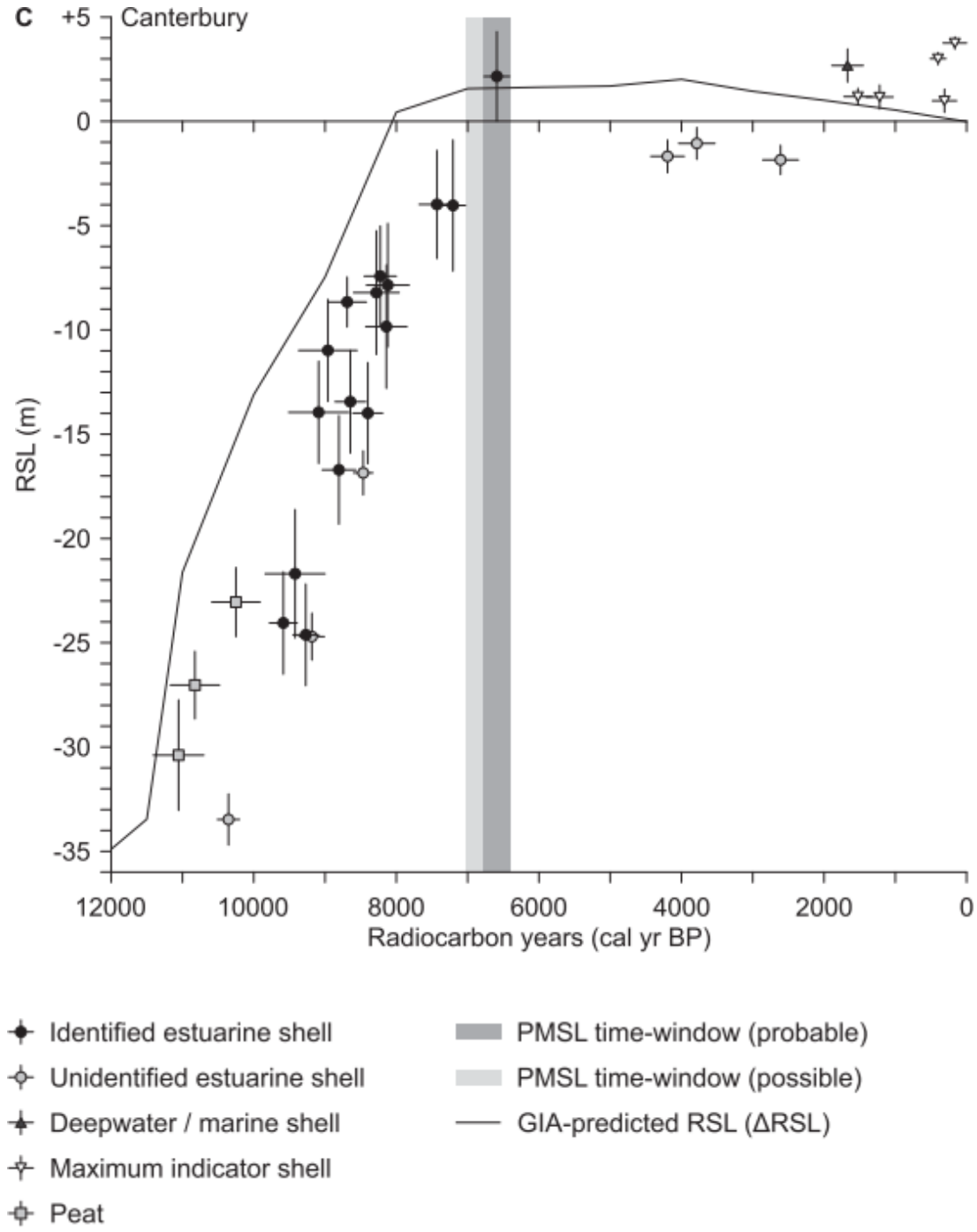


Figure 2.4 Image of sea-level curve for Canterbury coastline, New Zealand (image from Clement et al., 2016).

2.5.4 The Otago coastline

Clement et al. (2016) final part of the research focused on the Otago region, which, like the Canterbury region, has received little attention. Using 28 dates, a fragmented sea-level curve may be investigated. The Otago area attained PMSL between 7360 - 6630 cal yr BP, which is the closest match to Gibb's (1986) findings. The Otago region, like the Canterbury region, needs additional research to develop a more organised and robust sea-level curve. It is then evident that a detailed understanding of sea-level for the South Island of New Zealand is lacking when compared to the North Island's sea-level history. The PMSL on the Otago coastline was difficult to obtain as all dates in the Otago region utilised in Clement et al. (2016) were between 8000 years BP and present day.

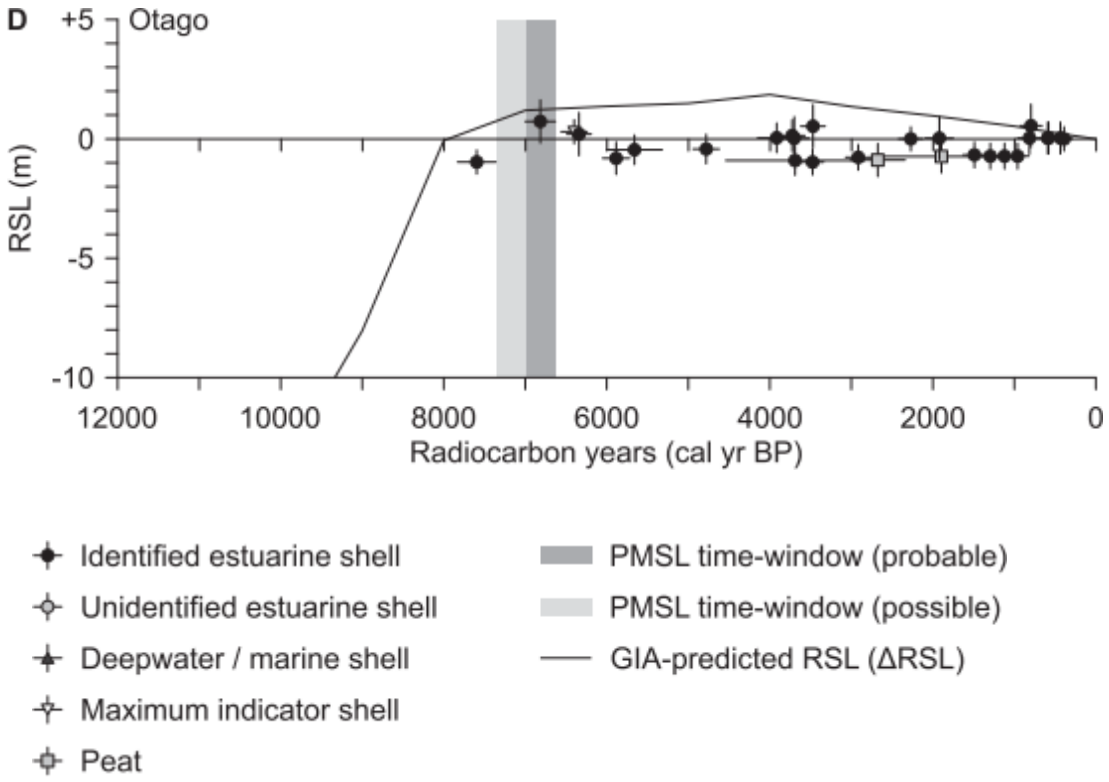


Figure 2.5. Image of sea-level curve for the Otago coastline, New Zealand (Image from Clement et al., 2016).

2.6 Causes of sea-level rise in New Zealand

Various theories have been proposed as to why New Zealand's sea-level followed its pattern through the Holocene. This section will look into the theories about what happened and the resulting controversy around it. The causes of New Zealand's sea-level rise are diverse, with the North Island seeing earlier and greater levels of increase and the South Island experiencing less.

The release of gravitational pull from the Antarctic ice sheet during its melt over the Holocene is one of the likely explanations for sea-level rising in New Zealand. This impact would have elevated sea-levels inside the Southern Hemisphere, resulting in greater sea-levels on New Zealand's South Island and lower sea-levels on the North Island. The likely explanation is the contrary to what has been observed in Clement et al. (2016) work comparing all sea-level studies in New Zealand, with Clement et al. (2016) proving that the North Island has a larger RSL than the south. Recent studies by also revealed that this release in gravitational pull release was not observed in Australia, hinting that it may not be a major driver of sea-level in New Zealand. With this being said, the release of the large amounts of water from the west AIS would have had direct impacts on New Zealand, therefore it should be noted that it is possible that isostatic change from the partial melt of the west AIS could have affected the gravitational pull release from AIS.

Throughout the Holocene, New Zealand would have seen variations in solid earth deformation, as well as changes in sediment regimes and local wave climates. Due to the differences in timing and magnitude of sea-level in the four separate locations, these localised solid earth changes might have a considerable impact on sea-level. This idea is exceedingly difficult to demonstrate the influence that changes in isostasy as well as flooding from rivers and ice melt had independently because each event would have occurred at equal times and at different magnitudes (Clement et al., 2016). More localised research is required not only on Holocene sea-level change, but also on the causes of sea-level change, particularly in the South Island, where the lack of evidence of sea-level within the Canterbury region from the last 6700 years makes it difficult to ensure precise timings, magnitudes, and durations of the mid-level Holocene highstand (Clement et al., 2016).

The dating using radiocarbon shell fragments in order to determine the changes in sea-level has dominated New Zealand's sea-level history. However, beach ridges provide a different and

albeit, more accurate methodology of understanding sea-level change over the Holocene (Tamura, 2012). As such, beach ridges have been exploited in research conducted in Japan and the Northern Hemisphere to study how sea-level change happened through time (Tamura et al., 2008; Tamura, 2012; Nielsen and Clemmensen, 2009). Because beach ridges are created on prograding shorelines, they are recognised as relics of former sea-levels (Tamura, 2012). Tamura (2008) alongside Nielsen and Clemmensen (2009) use of GPR on these ridges demonstrated that examining the subsurface of beach ridges can offer insight into the fluctuations of low tides in the past in order to generate a historic sea-level curve in a localised place (Nielsen and Clemmensen, 2009). The following portion of this thesis will analyse beach ridges and how they are produced, as well as the procedures of constructing beach ridges during low and high tides to examine sea-level variance through the Holocene.

2.7 Beach ridges

Beach ridges are low-lying mounds that occur on a prograding coastline (Otvos, 2000; Tanner, 1995). Beach ridges are semi-parallel structures that can occur in large systems of up to 250 ridges and indicate where ancient coastlines were in the past (Tanner, 1995). Beach ridges have been used to study historical sea-levels and geomorphic history in a specific location since they are considered to be relics of the past (Otvos, 2000). Since the 1950s and 1960s (Davies, 1957; Bird, 1960; McKenzie, 1958; Thom, 1964), the development of beach ridges has been a cause of conflict attributed to the reason that there are numerous techniques of formation each of which can take a long time to develop (10-50 years). This disagreement stems mostly from the fact that beach ridges go through several stages before being formed, as well as significant processes through swash and aeolian sediment deposition, and so beach ridges across the world are made differently. Jack, L. Davis has been considered to have formed the most accepted theory of beach ridge formation, forming the Davis model of cut and fill formation of beach ridges (Oliver et al., 2016). Beach ridge formation is considered to begin through berm formation within the swash zone, where sediment is cut from the base of the berm and due to progradation, more sand is then deposited onto the crest of the berm. This formation process occurs of numerous years (10-50) (Davis, 1957; Oliver at al., 2016).

Because of the variances in beach ridge creation, the terminology of beach ridges is quite complex, adding to the study controversy. Otvos (2000) proposed that any mound like ridge

developed on a prograding shoreline can be referred to as a beach ridge. For the sake of this thesis, the definition of beach ridges by (Otvos, 2000) is used, and so beach ridges may be classified into four categories as follows:

2.7.1 Swash built beach ridges

Swash-made ridges are developed on a typical low-angle fair-weather beach with crossbedding (Otvos, 2000). Beach ridges generated by swash zone occur in the intertidal and supratidal zones (Clemmensen and Nielsen, 2010; Otvos, 2000). These ridges can fluctuate in height from little or no elevation to up to 2 m depending on the tidal range and wave climate. Swash-formed ridges are the most common type of beach ridge to form and run parallel to or subparallel to the coastline; they may also occur in groups of 5-25 ridges or as part of a system of up to 250 ridges (Tanner, 1995). Each beach ridge within the system is a relic of an older beach face that was abandoned due to the development of a new beach seaward of the previously built ridge (Tanner, 1995).

2.7.2 Settling lag ridges

The outward aspects of settling lag ridges are similar to those of swash-built ridges, but their inside structures are significantly different. Horizontal bedding rather than poorly defined cross-bedding characterises settling lag ridges. This is due to the fact that there is no wave action to help in the creation of the ridges. The creation of these ridges is due to postma, a settling lag process (Tanner and Demirpolat, 1988). The formation of settling lag ridges is typical in the landward regions of tidal inlets because suspended sediment requires no wave energy and a certain length of time to settle out of suspension, resulting in postma setting lag (van Straaten and Kuenen, 1958; Postma, 1961). Basic field examination is insufficient to identify a settling lag ridge since granulometry determines whether or not ridges are caused by settling lag rather than wave or swash work; this can be performed by sample analysis, GPR, or trenching.

2.7.3 Aeolian formed ridges

Wind, rather than water, creates aeolian ridges, also known as dune ridges. The internal structure of dune ridges is cross-bedding, resulting in a distinct hummocky environment

(Otvos, 2000). Dune ridges are usually found inside and on top of a network of swash or settling lag ridges. Aeolian constructed ridges are limited by the amount of aeolian sand deposited onto the ridge itself rather than the height of sea-level at the time of deposition. Therefore, it is paramount within sea-level studies to avoid aeolian sediments as they can disrupt data collection and validation.

2.7.4 Storm surge ridges

Finally, storm surge ridges are clearly distinguished from other types of beach ridges because they are distinct landforms that appear between 5 and 10 metres in height. Storm surge ridges occur with concentric convex-up bedding because to the nature of the energy required for their formation (Tanner, 1995). Due to enormous levels of erosion caused by storm occurrences, grain size can range from sand to gravel, and it is not part of a set or system (Tanner, 1995).

Although there are two other types of ridges: namely ice-driven ridges and cheniers, the four types of ridges defined above are the most common in prograding systems used for historic sea-level and climate studies.

Swash zone, settling lag, and aeolian ridges can all form as a large system of ridges whereas storm ridges only form as a singular ridge. As such, this thesis looked at a mix of swash, aeolian and settling lag ridges in order to understand sea-level change on the Canterbury coastline. Swash-built ridges will normally occur only in situations of steady or dropping sea-level, although it is possible to see swash-constructed ridges on rising sea-levels if progradation can still outrun rising sea-levels. Aeolian dunes arise in reaction to fluctuations in sea-level height along a prograding shoreline, most notably when sea-level rise outpaces progradation, generating conditions in which swash-built ridges cannot form. Storm-made ridges are excluded because they can only be developed in full isolation from everything else; if they formed on a swash or settling lag ridge, erosional characteristics would most likely demolish previously built ridges in order to generate storm surge ridges.

2.7.5 Understanding the internal structure of beach ridges.

As mentioned, beach ridges may be utilised as paleoenvironmental records, the interior structure of beach ridges reveals significantly more than observations of the surface (Tamura, 2012). Using ground-penetrating radar (GPR) to capture subsurface information offers an in-

depth view into the subsurface and demonstrates how the sands migrated and generated the beach ridges (Tamura et al., 2008, Nielsen and Clemmensen, 2009). Beach ridge creation, more specifically swash zone generated beach ridges, is reliant on sea-level at the time of formation since it occurs within the intertidal and supratidal zones. Due to this, the low tide marks within beach ridges may be constrained throughout history, as long as the beach ridges are maintained. Tamura et al., (2008) and Clemmensen and Nielsen (2010) investigated the applicability of comparing down laps inside beach ridges to known sea-level heights throughout history.

Down lap surfaces are found on beach ridges nearing low tide in the intratidal zone. These down laps are thought to represent the beach face and upper shoreface border at the period of deposition (Tamura et al., 2008; Nielsen and Clemmensen 2009). Nielsen and Clemmensen (2010) used a 159 m long GPR line to test Tamuras et al., (2008) theory. Nielsen and Clemmensen (2009) discovered 19 down laps throughout their series that supplied the border between the shoreface and the upper shoreface, and these down laps were 95 % accurate in relating to sea-level (Nielsen and Clemmensen, 2009). More data would be required to confirm this notion of downlaps generating low tide locations, as errors are easily made while investigating GPR work on beach ridges. Tamura et al. (2008), alongside Nielsen and Clemmensen (2009) did not investigate the highest point of sea-level, which can be regarded as a top lapping surface. When high tide markings are unable to protrude above the present beach ridge, a top lapping surface can be constructed at the maximum height of the beach ridge. Such is critical when investigating a beach ridge with an aeolian sand element on top of a swash build ridge.

2.7.6 Using OSL Dating alongside GPR to understand sea-level variation on Beach Ridges

Over the past 20 years, GPR is considered to be the most robust methodology to understand the internal structure of beach ridges. Being able to construct the internal structure of beach ridges without trenching or disturbing the ground allows for quick and easy access to the subsurface. In addition to the benefits of utilizing GPR, there has been a change from using ^{14}C dating towards OSL dating in order to understand the timing of the event. OSL dating uses trapped photons within quartz structure to be able to date the last time that these specific quartz grains were subjected to light sources. In doing so, using OSL dating can accurately

date the timing of deposition of beach ridges, affirming the timing of events of creation, shoreline evolution and pauses within progradation if OSL dating methods are used within a sequence (Oliver et al., 2015; Oliver et al., 2017; Oliver et al., 2020). A high-quality study achieved by Oliver et al., (2018) is a prime example of the accuracy that GPR and OSL can achieve when examining coastal progradation and beach ridges. Oliver and his co-workers studied the internal structure of beach ridges at Pedro beach, South Australia and performed OSL dating to gather accurate information on the timing of events. Within Oliver's paper, it was observed that sea-level rise was gradual over the past 6000 years and using the truncations within the beach ridges (such as toplaps and downlaps discussed is section 2.6.5), and the topography of the beach, further concluding that sea-level was rising throughout the Holocene within Pedro Beach, South Australia.

2.8 Ground Penetrating Radar

With advances in coastal geomorphology technology and knowledge, particularly in GPR and other dating techniques, such as ^{14}C, OSL (Tamura, 2012), delving into the subsurface of beach ridges for paleoenvironment reconstruction is becoming significantly more accessible than it was previously. Trenching was the primary method utilised prior to GPR, but it was limited owing to cost and practicality (Tamura, 2012). GPR is a non-invasive technology that lies on the surface of the water. It then sends an electromagnetic energy pulse into the ground, which reflects paleoenvironment changes in the subsurface. The section that follows will go into the physics and understanding of GPR and how it may be used on beach ridges to exploit these paleoenvironmental traits previously described.

2.8.1 Electromagnetic waves

GPR generates electromagnetic waves (EM waves) that propagate in an oscillating electric field; these EM waves are composed of alternating magnetic and electrical waves. The EM spectrum, like a colour spectrum, is made up of many different types of EM waves. Different forms of EM waves are created by variations in frequency, and EM waves are measured by the number of cycles of electrical and magnetic fields per second (Hz) (Daniels, 2004). The wavelength is governed by the material's transit speed as well as the frequency of the wave oscillation. Within the EM wave spectrum, the lowest frequency waves have wavelengths of 1 km, while the highest frequency waves have wavelengths of 0.001 nm (0.001 x 10-9 m)

(Daniels, 2004). The term 'radar' is frequently used in GPR; however it was initially intended to refer to radio frequency waves. GPR's 'radar' operates at the lower end of the microwave frequency spectrum, where wavelengths are on the order of a few centimetres. Using these waves, GPR allows the operator to view the subsurface. Dielectric substances are required since this word refers to a material with little to no electrical conductivity yet may sustain electrical fields (Davis and Annan, 1989). The substance response of a material to an EM wave is determined by the dielectric characteristics of the material. Electrical permittivity (e), magnetic permeability (u), and electrical conductivity are the three qualities (o).

2.8.2 Electrical Permittivity of substances

The quantity of EM energy that a material can store after an electrical field is applied is referred to as its electrical permittivity. This function is complicated, as it includes both real and imaginary components.

$$\epsilon = \epsilon_r - i\,\epsilon'_r$$

Equation 2.1

Where ε is the complex dielectric permittivity, ϵ_r is the real part of the complex permittivity, ϵ_r' is the imaginary part of the complex permittivity and i = V-1 (Equation from Evans, 2009).

While 'Er' is regarded as the imaginary portion of the complex, it is also known as the 'loss factor,' which is determined by the amount of energy lost due to radar signal attenuation and dispersion. The relative permittivity, often known as the dielectric constant of a specific substance, is represented by the following equation (2.2). Here, ϵ_r is the ratio of space permittivity to material permittivity.

$$\epsilon_r = \frac{\epsilon_s}{\epsilon_o}$$

Equation 2.2

Where ϵ_r is the dielectric constant, ϵ_s is the permittivity of the substance under investigation and ϵ_o is the permittivity of a vacuum (Equation from Evans, 2009).

Several factors are required for data interpretation in GPR, therefore understanding the dialectic constant is critical. As shown in Equation 2.3 below, the velocity of a GPR signal through the material is proportional to the dielectric constant:

$$v = \frac{c}{\sqrt{\mu_r \in_r}}$$

Equation 2.3

Where v is the velocity of the GPR signal through the material, C is the velocity of light in free space (= 300,000 Km^{-1}) and μ_r is the relative magnetic permittivity (Equation from Evans, 2009).

When estimating depths using GPR data, the velocity of the signal through the material is necessary. GPR depth is measured in time (also known as two-way transit time) rather than distance. Thus, the measurement is made from the beginning points (antenna) to the subsurface structure, which is then reflected back to the GPR. This time can also be turned into distance values.

$$d = v \times \frac{t}{2}$$

Equation 2.4

Where *d* is the depth of the feature, and *t* is the two-way travel time of reflected signal recorded by the GPR system (Equation from Evans, 2009).

When EM waves are pulsated out of the GPR system, they reflect when they hit a difference between two materials, which have different dielectric constants. As a result, portion of the EM wave will be reflected off the material barrier and back towards the GPR, while the remainder of the energy will continue to penetrate further into the ground. Sometimes neighbouring materials will have comparable dielectric constants, resulting in less reflections off the material in the subsurface, making it difficult to establish and identify a material border upon interpretation. The quantity of energy reflected off the subsurface material is seen in Equation 2.5. As previously noted, the variations in dielectric characteristics of the two materials dictate

this.

$$R = \frac{(\sqrt{\epsilon_1}) - (\sqrt{\epsilon_2})}{(\sqrt{\epsilon_1}) + (\sqrt{\epsilon_2})}$$

Equation 2.5

Where R is the reflection coefficient and ϵ_1 and ϵ_2 are the dielectric constants of the adjacent materials (Equation from Evans, 2009).

When comparing dielectric constants, there is a significant discrepancy between various subsurface materials. Most geological materials will have a dielectric constant between 2 and 30, however, water in the subsurface would have a dielectric constant of 81 (Daniels et al., 2004). Air has the lowest dielectric constant, which is 1 (Daniels, 2004). One of the most difficult principles to grasp is the capacity to recognise the boundary of two different materials. Tamura (2012) claims that there is a significant knowledge gap while studying GPR, which might mean the difference between a correct interpretation and a misunderstanding. The magnetic permeability (u) of the subsurface can influence how EM energy is stored and subsequently released back to the surface. This can be an essential component during GPR work since it depends on how EM energy behaves within a magnetic dipole magnetically bound. Through magnetic permeability, this impact can alter EM wave velocity and attenuation. Steelwork and other materials can also influence the velocity and attenuation of electromagnetic waves.

2.8.3 Electrical conductivity

Electrical conductivity (o) defines how electrical charges move across an EM wave passage, influencing the energy attenuation of an EM signal. In general, this will result in significant energy losses. Signal attenuation is primarily influenced by conductivity and signal frequency. These two factors influence the quantity of signal penetration depth; higher conductivity signals attenuate faster than lower conductivity signals (Daniels, 2004). Because of its propensity to conduct electrical energy, saltwater existing in the subsurface considerably enhances the amount of conductivity of GPR signals when used on coasts. Most clay minerals can also accomplish this due to larger levels of exchangeable cations, albeit clay minerals are uncommon near coastal borders (Daniels, 2004). This indicates that salt water and clay materials can drastically impact EM wave penetration depth and should be avoided iffeasible. Working on beaches with GPR should be undertaken at the conclusion of a long dry period when the water table has been decreased in height, as this will allow for less disturbance from salt water and hence more penetration depth with better levels of resolution.

2.8.4 GPR Antennas

Antennas on a GPR are the equipment that allows EM waves to be transmitted and received. The reception antenna converts EM waves to current, whereas the transmitter antenna converts current to EM waves (Daniels et al., 2004). The signal intensity of a GPR is assessed by monitoring the voltage associated with the EM wave's current. Modern GPR systems will have two different antenna systems, one to emit the EM signal and the other to receive the signal once it has been reflected off subsurface materials. While it is feasible to have a single antenna system when employing GPR, there are major technical issues connected with switching between transmission and reception. This is owing to the speed with which EM waves bounce back from subsurface materials.

2.8.5 Signal Frequencies

GPR antennas can broadcast EM signals over a wide variety of frequencies. GPR antennas are wide bandwidth transmitters that enable greater data collection than a narrow bandwidth transmitter. The common frequencies utilised for beach ridges range from 20 to 200 MHz.

Higher frequencies cause increased attenuation of EM waves, resulting in less penetration of the subsurface (Jol and Bistow, 2003). Lower frequency antennas, on the other hand, penetrate deeper into the earth. While this is true, lower frequency signals have significantly poorer vertical resolution than high-frequency signals, making it difficult for the user to differentiate between individual reflections, particularly when dielectric constants are identical (Jol and Bistow, 2003). Due to this trade-off, the user must decide whether deep penetration or data resolution is more relevant to the research when selecting an antenna frequency. As a result, requiring additional understanding regarding the subject is critical. When choosing a signal frequency, keep in mind that increases in attenuation from saline water and clay minerals reduce penetration depth as well, therefore higher frequency antennas may be preferable in these locations (Jol and Bistow, 2003).

2.8.6 GPR Pulses

Pulses emitted by a GPR antenna generally consist of two peaks, one positive and one negative. This would be an ideal referral for data collection by GPR. In most circumstances, however, GPR will broadcast pulses that are positive - negative - positive (GSSI, 2006). The pulse delivered by GPR antennas normally takes a nanosecond to complete its whole cycle, however, this varies depending on the frequency of the signal. The duration of the GPR pulse is monitored from zero till it returns to zero at the conclusion of the pulse under ideal conditions (going through a positive-negative cycle). However, due to variations in attenuation through the subsurface, pinpointing the exact site of zero in actual EM pulses before and after the pulse can be challenging in real-time. When this occurs, the pulse length is measured from 50% of its greatest (positive) to 50% of its minimum (negative).

2.8.7 Vertical and Horizontal Resolution

Vertical and horizontal resolution are critical aspects to understand when utilising GPR to collect data. If they are not known, features inside the subsurface may be ignored owing to feature merging. If one of the signals is substantially stronger than the other and there are two vertically separated features, they will usually merge as one reflected signal rather than two (Jol and Bistow, 2003). The minimal distance between two separated features in a vertical sequence, which is controlled by signal wavelength, is also known as vertical resolution. When two vertically separated features are present, the reflected signal from one interface can get occluded and merge with the reflected signal from the other, especially when one signal is stronger than the other. GPR's vertical resolution (the smallest distance between two vertically separated features) is heavily determined by the signal wavelength (which is impacted by the dielectric characteristics of the material), with higher frequency signals having better resolution. GPR's vertical resolution is typically assumed to be between one-half and one-quarter of a signal wavelength (Daniels, 2004; GSSI, 2006; Martinez and Byrnes, 2001). Horizontal resolution minimum distance When two features within the subsurface are distinguishable, they must be separated horizontally. If the features are closer than the horizontal resolution, they will be shown as a single feature rather than two distinct features.

Horizontal resolution is affected by a variety of things. The first element is the number of scans performed per metre; if more scans are performed per metre, the horizontal resolution will be higher. In general, a 100 MHz antennae scan should have a step size between 0.25 m and 0.5 m dependent on the subsurface, whereas a larger step size can be used if the horizontal features of the subsurface are continuous (Jol and Bistow, 2003). Another factor is the EM radiation pattern, which determines the size of the antenna's footprint. While the number of scans per metre can be controlled, the footprint of the antenna is determined by the size of the antenna as well as the material properties of the subsurface; thus, horizontal resolution is a site-specific system that must be interchangeable depending on the materials present in the subsurface. Rial et al. (2007) may be consulted for further information on generally used formulae used to approximate the area of an antenna footprint. Horizontal resolution can be enhanced by a variety of means, including a higher frequency signal if the material has a high dielectric constant, greater signal attenuation, and shallower subsurface structures.

2.8.8 Data Display

The way data is shown after processing might vary depending on what features are sought in the subsurface.

The first, and most basic, method of displaying data is by a single scan line, often known as a 'wriggle.' This method of showing data compares the amplitude of a single scan to the time it takes for the EM signal to return to the antenna (Daniels et al., 2004). This is also referred to as an A-scan. When analysing individual GPR scans, A-scan wiggles provide the greatest information since they reveal the velocity with which it passes through different materials, providing the user with correct information about what is happening under the surface. When viewing numerous scans from a distance, however, a colour or grey-scale display is preferable (Annan, 2002). Colour or grey-scale displays are identical to individual scans, but variations in reflection amplitude are recorded as a change in colours. The data is then collated for each subsequent scan to generate a cross-section through the beach ridge. When the GPR EM energy velocity within the targeted ground material is known, the depth may be calculated using the recorded signal travel durations. This can happen when the scan is performed at predetermined lengths in a straight line.

A and B scans are raw data gathered straight from the GPR, allowing the user to view what lies under the surface in real time. However, there is also post-processing that occurs after data gathering in current GPR software packages. The following are examples of typical post-processing changes:

1. Static correction - Lowers the surface of beach ridges slightly below time zero so that the creation of the surface and subsurface may be seen.

2. Background removal - Removes random noise from the data.

3. Conversion of travel periods to depth - this needs information of the GPR pulse's velocity through the material.

4. Topography - Because certain GPR systems lack an in-built method for providing topography, GPS systems are also necessary.

The presentation of GPR data is critical when investigating what happened/happens beneath the surface. (Annan, 2002). Annan addresses how, for some uses of showing information, displaying information that has already been understood, rather than merely displaying data, would provide a clearer representation of information. However, if the data is relatively basic (for example, pavement layer depths), the interpreted formation of showing data will be preferable (E.G dielectric constant values of material moisture).

2.9 Summary

Evidence of sea-level variation has been seen throughout the Holocene, both globally and locally. Meltwater pulses occurring from the melting of large ice caps, such as the West Antarctic ice sheet as well as the Laurentide ice sheet collapse and drainage of Lake Agassiz-Ojibway released vast amounts of water that affected global current systems and raised sea-levels during MWPs 1b and 1c. Evidence for these pulses is still currently being worked out with discussion occurring about what had the largest effects on eustatic sea-level rise.

Within New Zealand, sea-level debates have been occurring for the Holocene over the past 30 years, since the benchmark study achieved by Gibb (1986), criticism of Gibb's work was done by Clement et al. (2016), suggesting that New Zealand sea-level is high fragmented and not well understood, especially within the South Island. Clement et al. (2016) also showed the importance of understanding localised sea-level change and that it was not a uniform change over New Zealand, with the northern sections of the North Island reaching PMSL 800-1400 years earlier than previously suggested by Gibb's (1986). This fragmented sea-level is especially seen within Clement et al. (2016) on the Canterbury coastline where PMSL, as well as Holocene highstands, are highly misunderstood with a lack of data showing that sea-levels cannot be calculated. This gap within New Zealand's sea-level research opens up chances to explore sea-level on the Canterbury coastline of New Zealand, especially within Okains Bay.

Okains Bay holds a large series of beach ridges that represent paleoenvironmental history of sea-level and coastline evolution through the Holocene. Both Tamura (2008) and Nielsen and Clemmensen (2009) have previously shown that using down lapping surfaces within beach ridges allows for low tide benchmarks to be seen using GPR systems on beach ridges, as well as seeing historical evidence of geomorphic change. GPR represents a reliable technique to

observe sea-level changes on beach ridges, and therefore can be the prime methodology to observe sea-level change over the Holocene time period in Okains Bay.

The next chapter of this thesis will investigate the field site of Okains Bay in order to gather information on sea-level variation over the Holocene for the Canterbury coastline. Okains Bay was the area of choice for this study as it provides an ideal location to exploit beach ridges, such as Tamura (2008) and Nielsen and Clemmensen (2009) used to look at down lapping surfaces in the subsurface of beach ridges to produce a sea-level curve.

Chapter Three: Field Setting

3.1 Introduction

Chapter Three presents the study site, Okains Bay, Canterbury. Specifically, this chapter describes the geological setting of Banks Peninsula as well as the coastlines of Pegasus Bay to the north and the Canterbury Coastline to the south. Then the morphology and geology at Okains Bay is explained, specifically looking into the geomorphology of beach ridges, as well as the hydrology and tidal changes of the studied area. A discussion of previously published and unpublished literature is provided to justify why Okains Bay was chosen as the field area for this thesis.

3.2 Geological setting

Banks Peninsula is located on the east coast, South Island Aotearoa, in the centre of the Canterbury coastal region (Figure 3.1). Pegasus Bay lies to the north and the Canterbury blight to the south. Both Pegasus Bay and Canterbury Blight have direct effects on the hydrology and the sediment transport onto the Peninsula (Stephenson and Shulmeister, 1999). Banks Peninsula was formed during the Miocene-Pliocene epoch by the eruptions of two major calderas (Dingwall, 1966). The peninsula is defined by a radial pattern comprising of flooded valleys which feature exceptionally sheer cliffs that end along slope interfluves, and divide the bays surrounding the peninsula (Dingwall, 1966). The eruptive centres of the two volcanos which formed Banks Peninsula reside in what is now Lyttleton and Akaroa, Canterbury (Liggett and Gregg, 1965). These eruptions are a mix of both Andesitic and basaltic flows. Steep valleys and ridges now dominate the entire area that was formed by the distinct lava flows, with deep valleys forming inside interflow zones. Isostatic changes occurred throughout this time alongside the adjustments in sea-level and began to drown the lower sections of the peninsula (Dingwall, 1966). Throughout the quaternary, there has been no record of subsidence of Banks Peninsula. This is demonstrated by marine terraces on the western side of Banks Peninsula residing +6 and +8 m above present-day sea-level (Lawrie, 1993). Lawrie (1993) were found to be attributed to higher last interglacial sea-levels.

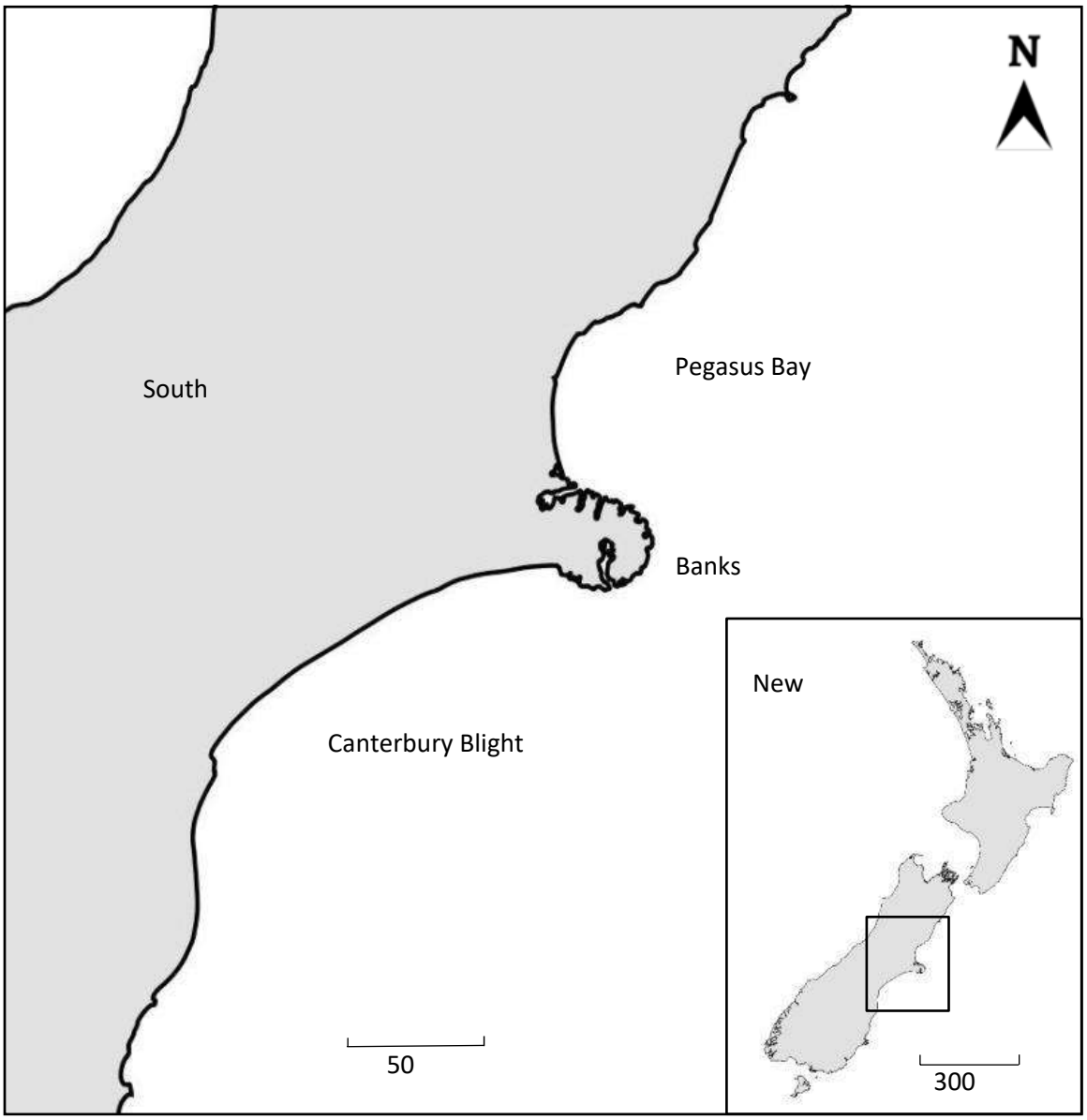


Figure 3.1. Map locations of Banks peninsula as well as Pegasus Bay and the Canterbury Blight.

Banks Peninsula has undergone several landlocked and isolated periods from the mainland of New Zealand's South Island through the Pleistocene as a result of successive glaciations and changes in relative sea-level. In addition, the Waimakariri River, which currently flows out to the north of the Peninsula, has been shown to have exited to the south (Dingwall, 1966). The flow of Waimakariri River deposited alluvial gravels to the western parts of the Peninsula, which are currently attaching Banks peninsula to the South Island (Dingwall, 1966). Most of the bays on Banks Peninsula contain marine sediments with a mix of clays and silts (Dingwall,

1966). There are however some beaches, such as Okains Bay which are purely fine to medium-grained sands (Dingwall, 1966). All the bays on the Banks Peninsula are impacted by different degrees of exposure to wave action, currents, and climate, through the orientation of each individual bay.

3.2.1 Okains Bay

Okains Bay lies on the north-eastern side of Banks Peninsula. The bay is constricted within a steep basaltic valley. The entrance to the bay is also orientated to the northeast, with an opening of 1.3 km in width. From the Mouth of Okains Bay, the latter then opens into a 2 km wide section that has been infilled with water before going back to a 1 km width section where the current beach resides. Infilling of Okains Bay has previously occurred throughout the quaternary, however, recent infilling of the bay occurred from 8 ka (Dingwall, 1966; Stephenson and Shulmeister, 1999), with gaps in infill occurring between 6 – 2 ka (Stephenson and Shulmeister, 1999). The formation of sands within Okains Bay occurs through a prograding nature, creating a series of beach and dune ridges. There is a total of 58 ridges within Okains Bay, with 48 of which are beach ridges and 10 are Dune ridges (Figure 3.2) (Stephenson and Shulmeister, 1999). The beach ridges at Okains Bay do not have any regularity within their spacing of one another and the heights of these ridges range from 0.15 to 1.2 m from the foot to the crest of the ridge (Dingwall, 1966; Stephenson and Shulmeister, 1999). There are three sets of dune ridges within Okains Bay (See Figure 2 for reference). These two different types of ridges within Okains Bay have been interpreted to be two different coastal environments which Stephenson and Shulmeister (1999) understood to be changed in sediment delivery rates that would have been dependent on sea-level change (Stephenson and Shulmeister, 1999). There are some larger ridges that have formed within Okains Bay, with two of the ten dune ridges reaching a height of 1.5 m and the middle ridge reaching 3.0 m in height (Dingwall, 1966, 1974; Stephenson and Shulmeister, 1999).

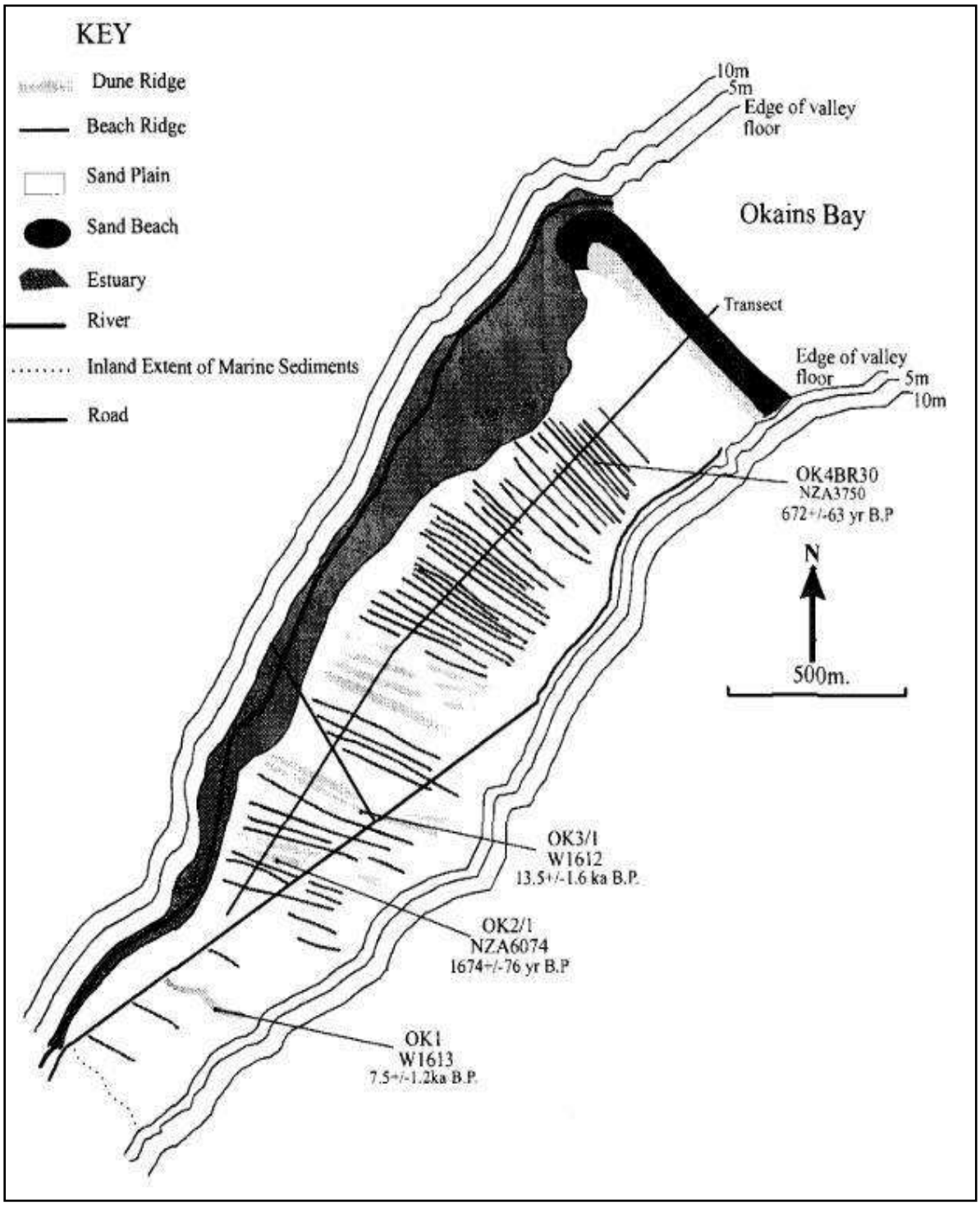


Figure 3.2. Geomorphic map of Okains Bayshowing the beach and dune ridges, as well as the dating sites used in this thesis from Stephenson and Shulmeister, 1999 (Image from Stephenson and Shulmeister,1999).

To the northern side of valley floor, a small river called the Opara River occurs. Opara River has also created a small estuary which occupies most of the valley floor at it widest point on the northern side of the Bay (Figure 3.2). Okains Bay village sits within the middle of the bay, while the rest of the bay is currently used for farming, thus preserving the beach and dune ridges.

3.2.2 Sediment Characteristics of Okains Bay

Okains Bay is made up of predominantly medium grain-sized quartz sands, along with a small percentage of feldspar (Dingwall, 1966). Despite Okains Bay being surrounded by cliff faces made of basalt, there is no presence of the latter within the sand complex of Okains Bay, as quartz grains do not form within basalt. This is evidence that the sand must come from offshore sites rather than local sites (Dingwall, 1966).

3.3 Progradation at Okains Bay

Progradation rates at Okains Bay are characterised as rapid, with Dingwall (1966) calculating rates of progradation at 2.3 m per year, while Martin (1969) calculated progradation rates at 2.4 – 3.6 m per year. Later, Stephenson (1992) provided progradation rates from 3.9 m per year. While these progradation rates are dissimilar to each other, both indicate the rapid progradation that occurs at Okains Bay. Okains Bay has not always been progradation at the rates seen today. Stephenson and Shulmeister (1999) concluded that progradation slowed between 6000-2000 Ka based on ^{14}C and TSL dates. The slow of progradation in Okains Bay brought forward aeolian-dominated sands, seen within the dune ridges at Okains Bay. The slowing of progradation observed by Stephenson and Shulmeister (1999) represents a potential and reliable reason for the different coastal dynamics observed in Okains Bay.

3.3.1 Wave and Tides Characteristics at Okains Bay

The waves within Okains Bay hold very little energy and thus do not produce currents strong enough to cause sand erosion from the beach. Spring and Neap tidal range for Okains Bay is between 2.17 m and 1.19 m respectively as modelled by NIWA tidal forecaster (NIWA, 2022).

Large waves within Okains Bay (>1 m) have been observed at 14-second intervals. Common wave heights are only 0.3 m in height with a wave period of 5-6 seconds (Brown, 1976). This also affects sand being deposited at the beach. Due to the orientation and the small mouth of Okains Bay, only waves coming from the northeast can penetrate the bay itself, creating a very sheltered environment from larger waves. Instead of waves being built purely off wind conditions, Banks Peninsula is subjected to swell-dominated waves that are altered through wind processes.

The swell-dominated waves are produced by storm conditions within the Pacific. Localised changes in climate over Banks Peninsula and off the coast of the peninsula also have effects on wave energy and orientation (Dingwall, 1966, 1974). The dominant wave direction to the north of Banks Peninsula, where Okains Bay is located, is from the north-east. It is very rare to observe large waves entering Okains Bay due to the shallow depth of the water. Such causes the refraction and the loss of most of the wave energy at the mouth, rather than at the beach face.

3.3.2 Sediment Transport

The origin of the sand in Okains Bay is greywacke, brought down by the rivers from the Canterbury hinterlands, with the main river outputs being the Ashburton and Rakaia Rivers (Figure 3.3) (Stephenson and Shulmeister, 1999; Dingwall, 1966). Sediments from the south of Banks Peninsula come from the coastal cliffs and coastal erosion observed in South Canterbury (Stephenson and Shulmeister, 1999). These sediments are then moved northwards through the Southland current that resides up the east coast of the South Island of New Zealand (Figure 3.3). As the current passes Banks Peninsula, a small channel is seen just off the Eastern coast of Banks Peninsula (see Figures 3.3 and 3.4). This increases the speed at which water moves and therefore moves sediments very efficiently. When the southland current passes Banks Peninsula, this channel opens which evidently decreases the speed, resulting in substantial sediment falling out of suspension. Such subsequently traps sediment onto the continental shelf to the north of Banks Peninsula.

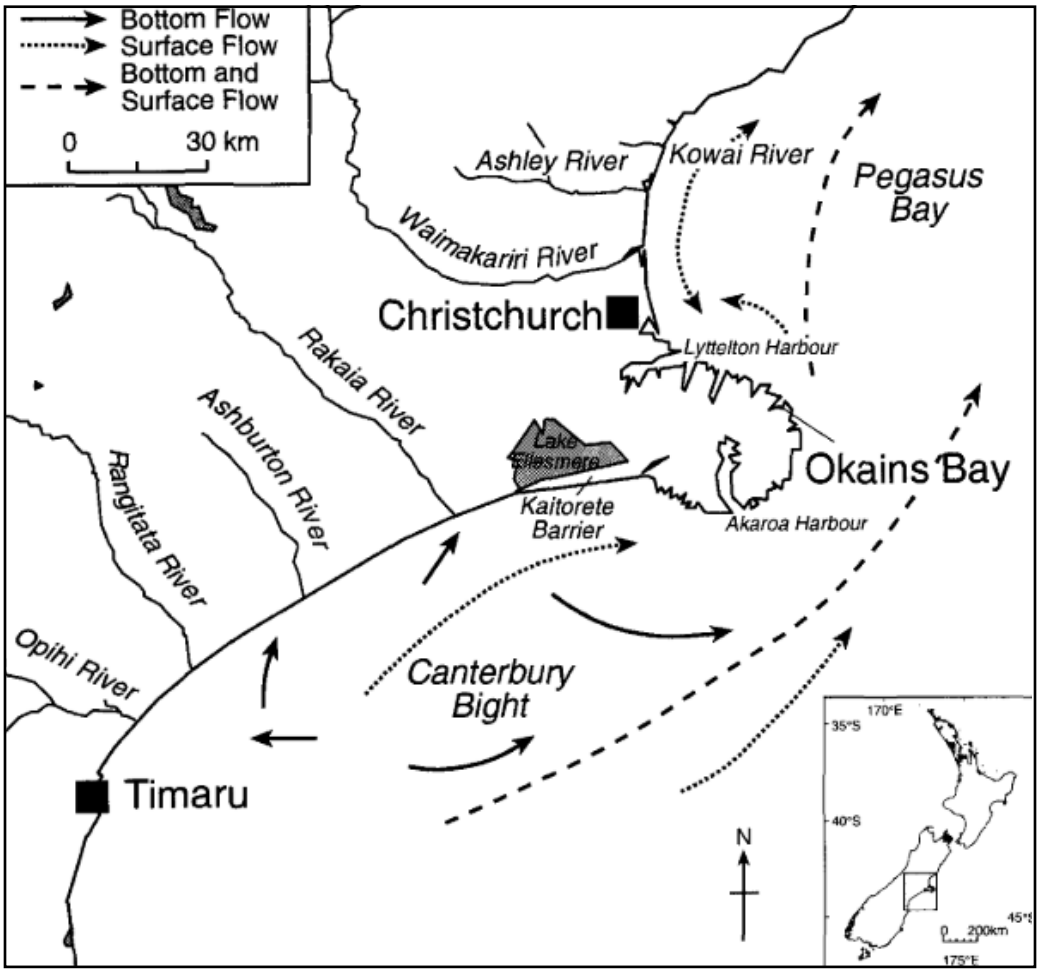


Figure 3.3 Map of the Canterbury region and the flow direction of currents (taken from Carter and Herzier, 1979; adapted by Stephenson and Shulmeister, 1999).

3.3.3 Banner Bank

An area of higher relief compared to off coast of the north-Eastern section of Banks Peninsula is found directly outside of Okains Bay and continues 20km to the North as seen in Figure 3.4 (Stephenson and Shulmeister, 1999). This area of high relief is called Banner Bank and was first documented by Herzer (1972). Herzer (1972) showed that Banner Bank is made up of fine quartz sands, similar to what is found at Okains Bay. Stephenson and Shulmeister (1999) showed that wind-generated and tidal currents take sediment off Banner Bank and shoal them onto the north-eastern bays of Banks Peninsula. As Banner Bank is found directly outside the mouth of Okains Bay, the latter experiences most of the shoaling of sediments and is most likely the reasoning as to why there is such a large sediment flux onto its coastlines.

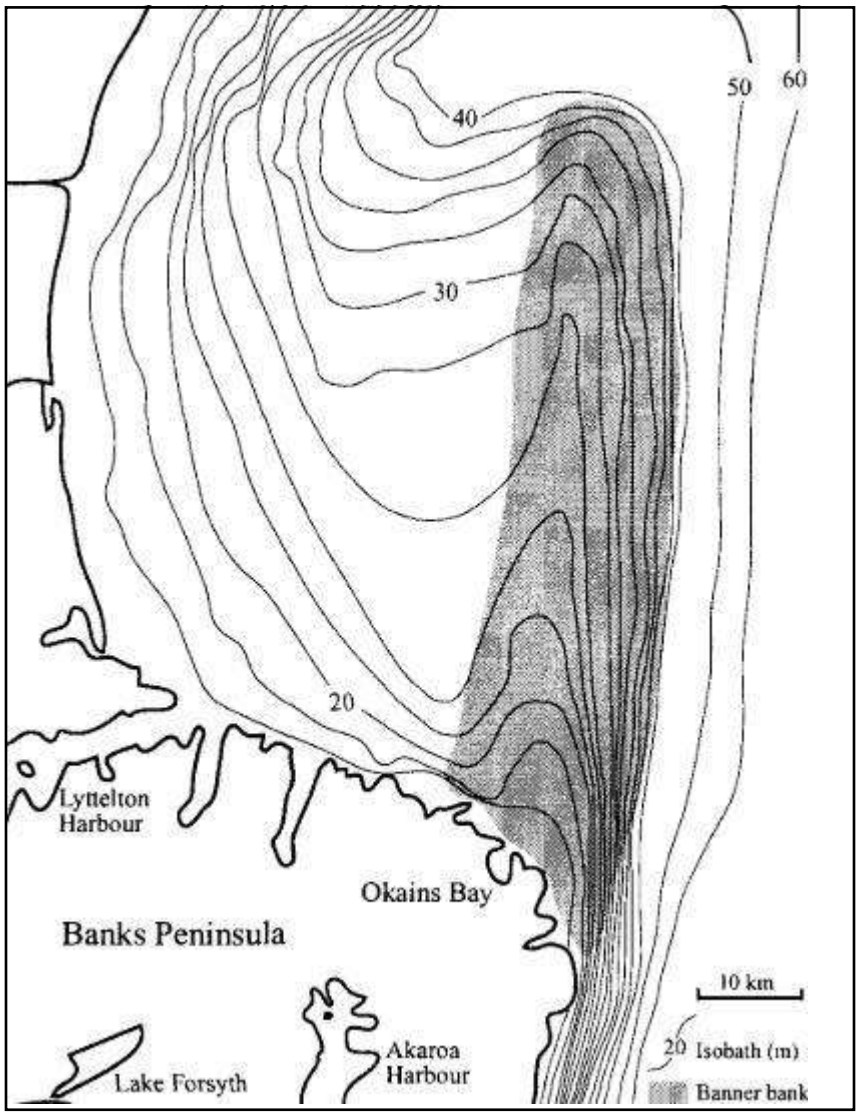


Figure 3.4. Bathymetry map off coast of Banks Peninsula showing Banner Bank outside of Okains Bay extending North (Image from Carter and Herzier, 1979: Adapted by Stephenson and Shulmeister, 1999).

3.4 Summary

This chapter investigated the field setting for this study. Firstly, the geological setting was examined surrounding Okains Bay through the investigation of Banks Peninsula, Pegasus Bay, and the Canterbury Blight (Dingwall, 1966; Stephenson and Shulmeister, 1999). The geology and geomorphology of Okains Bay were also described, as well as the progradation rates of the beach ridges and wave characteristics of the surrounding region (Stephenson and Shulmeister, 1999). The origin and the characteristics of the sediment grains in Okains Bay were identified

to be greywacke, with supporting evidence of the grains coming from offshore sites such as Banner bank (Stephenson and Shulmeister, 1999).

The next chapter will examine the validity, justification and methodological approach taken to provide a basis of how sea-level variation on the Canterbury coastline is found on Okains Bay, Canterbury.

Chapter Four: Methodology

4.1 Introduction

Recall from Chapter Two, there is a need to study sea-level fluctuations on the Canterbury coastline (Clement et al., 2016). With large gaps in New Zealand's sea-level history, it is difficult to comprehend the timing and severity of events that shaped New Zealand's sea-level during the Holocene. Stephenson and Shulmeister (1999) demonstrated that Okains Bay has been prograding since at least 8 ka, making it a good candidate for this argument. Fifty-eight beach and dune ridges were used, along with GPR and RTK, and prior dated approaches from Stephenson and Shulmeister (1999). This will give more insight into Canterbury coasts, as well as a look at a comparatively new approach employing GPR, rather than merely dating and shell fragment analysis, to understand historic tidal patterns, allowing historical sea-levels to be constrained.

Chapter Four aims to explain the methodology used to construct this thesis on Okains Bay in Canterbury, New Zealand. The first section of this chapter discusses the reasons for the specific locations where the transects for GPR were placed/selected. When employing GPR, transects are especially crucial over longer distances, such as for this thesis, as there are potential risks for lost data, erroneous readings, or other events if transects are not distanced appropriately. Following the explanation of transects, a brief introduction to GPR is provided, as well as how GPR will be utilised to address the problems raised by this thesis. The onsite calibration of GPR will be explained as well as the reasons behind why each component of GPR was chosen for this research project. The proper onsite calibration of GPR is critical for valid data as inappropriately choosing the components of GPR may lead to inaccurate outcomes, such as misinterpreted data, low vertical and horizontal resolution, and inability to gather any data. Following that, a brief look at RTK will be covered, as will the location of the base station in Okains Bay. Finally, the processing of GPR and RTK is explained, as well as how the corresponded information is interpreted.

4.2 Preliminary studies and validation of GPR on Okains Bay beach ridges

The research by Stephenson and Shulmeisters (1999) is used as a basis for the preliminary study for this thesis. ^{14}C and TSL dating techniques from Stephenson and Shulmeister were essential for this thesis as it was not possible to generate new dates due to the Covid-19 pandemic. Stephenson and Shulmeister (1999) gathered four dates in total throughout Okains Bay, with two of which are ^{14}C dates, while the remaining two were thermoluminescence (TSL) dates. The dates produced by Stephenson and Shulmeister (1999) will be used for this thesis' study to provide more information on the performance and analysis of GPR.

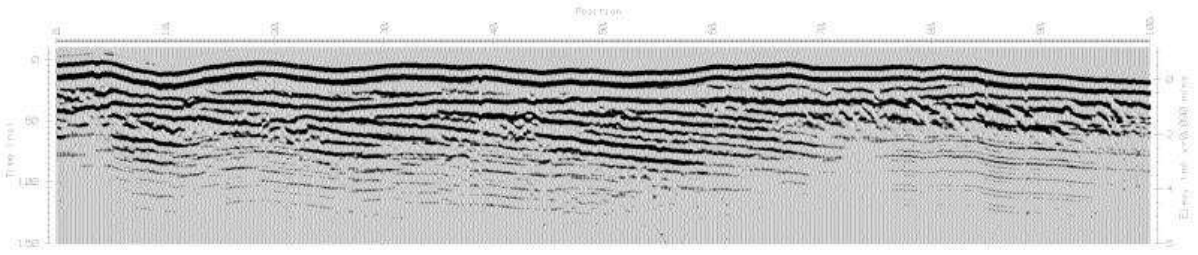
Jol (pers. comm) probed Okains Bay to investigate the possibility to obtain a GPR signal throughout the bay area. Specifically, Jol (pers. comm) performed GPR from the beach face of Okains Bay to midway through the Okains Bay camping ground, and produced two GPR lines, with one at 100 MHz and the other are 200 MHz. The two GPR lines revealed a strong enough signal at Okains Bay in order for this thesis to carry through (Figure 4.1a and 4.1b). Such therefore provided indications of the reliability of the frequencies of 100 MHz and 200 MHz to consider for the purpose of this study.

As shown in Table 4.1, the dating techniques that Stephenson and Shulmeister (1999) used throughout their 1999 research paper was two ^{14}C dates and two TSL dates. Date W1612 suggests that there was a 13 Ka midway through the sequence (See figure 3.2 for reference). However, this is highly unlikely and was potentially due to an incorrect dating technique. Furthermore, date NZA6074 directly after this is 11,826 years younger than date W1612, further supporting that there might have been an incorrect dating methodology. The three other dates used within Stephenson and Shulmeister (1999) are in chronological order when observing how the bays sands were deposited. The spacing between the dates show that Okains Bay has had geomorphological changes with speeding up and slowing down of progradation, or possibly a shift in already deposited sediments which may have caused these changes to occur.

Table 4.1 Dates from Stephenson and Shulmeister (1999)

Name	Type of dating technique	Age before present day (years)	Range of error (+\-) (years)
NZA3750	Radiocarbon	672	63
NZA6074	Radiocarbon	1674	76
W1612	Thermoluminescence	13,500	1600
W1613	Thermoluminescence	7,500	1200

A)



B)

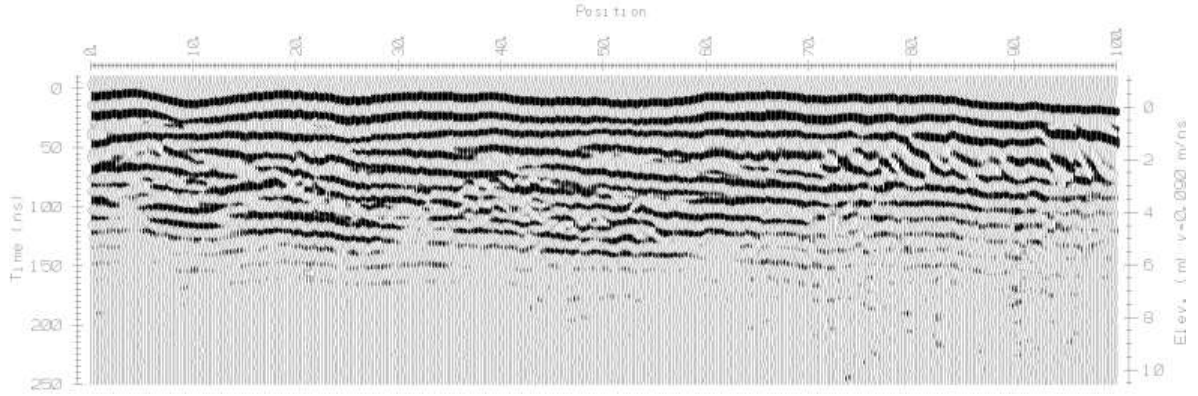


Figure 4.1. Showing the preliminary work achieved by Harry Jol (Pers. Comm), a) is at 200 MHz while b) is 100 MHz (Images are from Harry Jol Pers. Comm).

4.3 Study sites

This section explains the areas of interest within Okains Bay from the preliminary study achieved by Stephenson and Shulmeister (1999) (Figure 4.2). Some areas of Okains Bay are unable to be surveyed through GPR due to reworked land, powerlines, underground pipelines, and fallen trees. Okains Bay was therefore split into three separate sections for this thesis, which allows for three main transects to be used as described below.

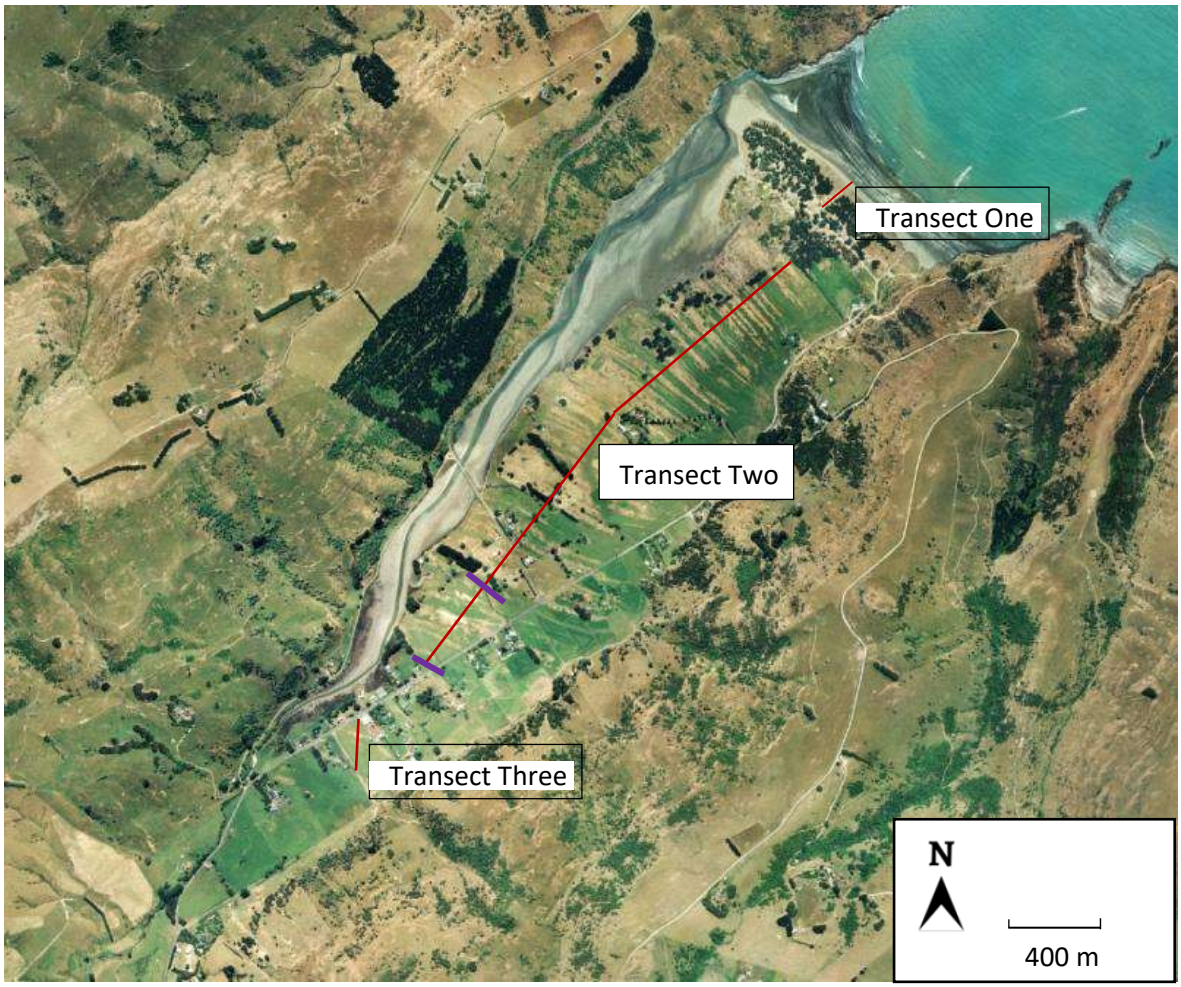


Figure 4.2. Aerial Map of Okains Bay showing the three different transects that are used within this thesis.

4.3.1 Transect one

The first transect of Okains Bay begins at the current beach face, starting at the position of the low tide until mid-way through the Okains Bay camping ground (See Figure 4.2). The orientation of the transect is NE – SW and follows the beach ridges in a perpendicular fashion. The transect was limited to Okains Bay camping ground due to the presence of underground pipelines and reworked land directly after. Beyond the camping ground, there is also a large, forested area that contained a lot of debris which could have potentially interrupted the amount of depth of penetration possible through GPR (<1 m depth).

4.3.2 Transect two

The largest of the transects is transect two (See Figure 4.2). This transect begins on the south-western side of the forested area of the Okains Bay camping ground. This transect then follows a fence line through farmlands while attempting to stay as perpendicular to the beach ridges as possible. The transect then turned to an SSW orientation to stay perpendicular to the ridges. The transect then followed this path until reaching the beginning of the Okains Bay village. Transect two ended before the village due to powerlines that affected the GPR.

4.3.3 Transect three

Transect three began on the south-western side of Okains Bay village next to the Okains Bay Museum. The orientation of transect three ran south. This transect then followed the beach and dune ridges till mid-way through farmland (See Figure 4.2). The transect stopped midway through farmland as seen in Figure 6 due to significant anthropogenic alterations which occurred on the oldest section of beach ridges at Okains Bay. There was therefore no reason for or evidence of beach ridges occurring after this transect.

To further mitigate interferences when performing GPR, measurements of the bay were taken in 100 m increments or as close as possible, with the exception of where fences were. This was necessary because GPR would turn off and reset the current survey if any of the fibreoptic cables were disconnected from the transmitter or receiver. To avoid the risk of data being erased, the GPR lines were ended at the fence lines, the GPR would be disconnected and then restart on the other side of the fence line, therefore, some lines are only 30 m in length.

4.4 Description of GPR

As indicated in Chapter 2, GPR allows for detailed examination of the subsurface without disturbing the earth using electromagnetic energy. The image produced by GPR is represented by a series of various stratigraphy lines that vary in width and illustrate changes in water, sediment density, and deposition of the previously existing surface. Tamura (2016) provided a thorough discussion of GPR and how it works with beach ridges, highlighting frequent

misconceptions and errors committed while using and analysing GPR. GPR is used in conjunction with other methods, such as RTK, to offer changes in surface elevation, therefore slightly modifying what is seen in the subsurface. While GPR is useful for examining the subsurface and changes within the subsurface, it does not offer ages for when events happened.; As such, GPR is used in conjunction with dating techniques such as ^{14}C, and OSL to obtain dates and timing of separate events.

GPR was chosen as the primary approach for this investigation as such method is regarded to be the most reliable contemporary technology for seeing into the subsurface, requiring little time and no trenching, making it a cheap and efficient way (Tamura, 2012). Prior to GPR, trenching through the beach ridges was used to be able to get a cross-section of the strata of the subsurface. Trenching was also used for sea-level studies to gather shell fragments to date using ^{14}C as there is a much higher chance of coming across shell fragments in the subsurface rather than on the surface. This technique is however accompanied with a caveat; ^{14}C dating utilises the time of death rather than the time of deposition, which can substantially distort results.

GPR has been demonstrated in studies on beach ridges in Australia, Denmark, Japan, and China over the last 15 years by researchers (e.g. Neal and Roberts, 2004; Bistow, 2006; Tamura et al., 2008; Nielsen and Clemmensen, 2009; Clemmensen and Nielsen 2010; Tamura, 2016; Gouramanis et al., 2020; Jol (Pers. Comm)). This study looked at a range of various types of beach ridges, all of which produced high-quality data on geomorphic alteration and sea-level changes. Tamura et al. (2008) employed GPR on the Kujukuri Strand plain, Eastern Japan to examine downlapping surfaces in order to acquire low tide information from beach ridges in the past. GPR provides a physical and visible way of testing and displaying intricate subsurface systems that are likely to be missed when using other approaches such as trenching or a modeling approach to observe sea-level rise through the process of beach ridges. GPR was used as the main methodology in this thesis in an attempt to reconstruct the sea-level curve on the Canterbury coastline, following the methodology of Tamura et al. (2008).

The GPR system utilised for this study is of the manufacture, *Sensors and Software*. The next section discusses the usage of GPR and how it was configured to be utilised for this thesis. To obtain the best possible outcomes, GPR configuration was dictated through the technique of grain size, surface compactness, and water table. In 2019, Jol conducted an unpublished investigation on Okains Bay to obtain a reliable GPR configuration and settings (Figure 4.1a and 4.1 b).

4.4.1 The Weather and timing of year

Data for this study were collected between November 8 and November 12th, 2020. The weather and the time of year are significant constraints that must be considered when employing GPR in coastal locations. A time of sunny, clear weather is ideal for GPR since it allows for more subsurface penetration with less constraints due to water conductivity. The summer season is especially ideal for using GPR since it provides the highest possibility of receiving warmer and drier weather, enabling the water table to be lower and the sands above the water table to be drier. The data for this thesis were collected in the end of Autumn, during a period of drier weather, which, while not ideal, generated a scenario close to summer. When operating in coastal locations, it is also necessary to consider tide patterns. When employing GPR on the shoreline during a spring tide, larger amounts of salt water are created, resulting in more conductivity when using GPR. The optimal time to utilise GPR on beaches is during a neap tide, because lower high tides allow for lower saltwater conductivity, which was obtained when data for this thesis was collected.

4.4.2 Type of GPR Survey

There are several types of GPR surveys that produce varying findings depending on what is required. The survey type employed for this thesis is a mid-common point, which is the most often used form of survey in coastal areas, as a result, it is possible to get a 2D representation of the subsurface by cutting a perpendicular line through the beach ridges. A mid-common point survey is when both antennas are located at a fixed position as described in the following sections.

4.4.3 Electrical Permittivity of Okains Bay

The velocity value selected can have a significant impact on whether GPR data is shown accurately. Because Okains Bay is a coastal location with an estuary to the north, the sands would neither be fully wet or completely dry, therefore choosing a velocity between 0.15 and 0.06 would allow the GPR to work optimally. Because of the saturation of the sands and the same velocities attained in the preliminary work by Jol (pers. Comm), 0.1 m/ns was chosen for

this thesis. The results from Jols work on Okains Bay produced clear and precise GPR lines for both 100 MHz and 200 MHz antennas as seen in Figures 4.1a and 4.1b.

4.4.4 Choice of Antennas

At Okains Bay, three alternative signal frequencies could have been employed; the options were 50 Mhz, 100 Mhz, and 200 Mhz, supplied by School of Geography at the University of Otago. As indicated in Chapter Two, the greater the frequency, the lower the depth penetration but higher the vertical resolution collection. Using early research by Jol (pers. Comm) at Okains Bay, the signal frequency was limited down to 100 Mhz or 200 Mhz, with 200 Mhz providing less depth than 100 Mhz (Fig 4.1a and 4.1b). To correspond with the timing of the GPR process for this study, being early November 2020, the 100 MHz signal was chosen because there would be less attenuation from saltwater intrusion if this occurred, allowing for a depth of 10 m. In an ideal situation, both 100 MHz and 200 MHz antennas would be used, supplying further evidence for this thesis, however, time restraints did not allow for this to occur. With a depth of 10 m, all beach ridges may be thoroughly explored, as well as the subsurface of the few dune ridges that exist in Okains Bay. 100 Mhz was the sensible decision here, supplying higher quality data over 200 MHz with as much depth penetration.

4.4.5 Timezero

Timezero is an essential calibration component of GPR. If the user only wants to see a certain portion of the subsurface, time zero will crop the image to begin at that point underground rather than at the ground's surface. GPR allows timezero to be adjusted automatically or manually depending on what the user needs to view underneath the surface. When utilising the automated option, the timezero component will need to be recalibrated on occasion in order to know where the ground's surface is. For timezero to be calibrated correctly for this thesis, it was places 2 m above the surface of the ground as it allows for topography input as well as clearly Figures to be produced during the processing of data. An issue was encountered when using timezero for this study in the instance of the initial use at Okains Bay, timezero was set to automatic, but it was not calibrated and began measurements 8 m below the surface, yielding data insufficient for this study. This error is not visible in the field since the image on the GPR display shows the whole image, but it becomes apparent during data processing. During the

second attempt, timezero was manually placed above the surface in order to see the entire subsurface and prevent the error made during the first attempt. This also enabled a clear separation of the surface to be visible within the photos during data processing, making it simpler to examine just below the ground's surface.

4.4.6 Distance between scans

When addressing horizontal resolution, the distance between each scan is extremely important. Horizontal and vertical resolutions can rapidly alter if scan widths are too wide, resulting in circumstances where lines get mixed owing to subsurface attenuation. When scans are closer together, vertical, and horizontal resolution improves, allowing for greater quality data to be obtained. This is critical in this thesis as the toplaps and downlaps are being investigated to understand historic sea-level from beach ridges at Okains Bay. If the resolution is insufficient, the data may be misunderstood. As the focus of this thesis is on minor changes in the subsurface of beach ridges, a shorter distance between scans allows for improved horizontal resolution. This thesis employed a 0.5 m gap between scans. Jol and Bistow (2003) recommends between 0.25 m and 0.5 m when employing 100 MHz antennas, this being dependent on if stratigraphy lines within the subsurface are continuous or not. If lines are continuous, then a larger gap between scans can be used. The longer distance lines (80 – 150 m) achieved superior horizontal resolution than the shorter distance lines (10–30 m). Such ultimately allowed for more information to be acquired for each scan over a longer distance, thus producing a higher granularity of data to be obtained.

4.4.7 Choice of band width between antennas

The volume of data that may be received depends on the breadth of the band between the transmitter and receiver antennas. As this survey employed dipole antennas, each scan required the antennas to be physically relocated and put on top of the ground in order to work, allowing for the bandwidth to be changed. More data may be captured with a higher bandwidth. An appropriate bandwidth should be between 1 m and 1.5 m, this allows for an ideal 2D image to be produced through. For this study, a bandwidth of 1.25 m was employed. Using this bandwidth was convenient for a single person to perform the GPR research rather than requiring an additional person to relocate the antennas. The data for this thesis was collected

by two people, Associate Professor Wayne Stephenson and myself. Bandwidth was consequently restricted to the width of one person, as the other was using the RTK system, resulting in bandwidth of 1.25 m. It is critical to maintain such bandwidth as consistent as possible across scans in order to keep data identical.

4.4.8 Type of cables used to connect the GPR system to the Antennas

There are two options for connecting the main GPR system to the antennas of the GPR. The two choices are metal cables and fibre optic cables. Both of these cables have positive and negative attributes. Metal cables are conductive of EM energy that is produced by the GPR system, and therefore can affect the imagery produced using the EM signals within a transect, however metal cables are far less prone to breaking compared to fibre optic cables. On the other hand, fibre optic cables do not conduct any EM energy produced through the GPR system, however, are extremely fragile and should be used with utmost care when using fibre optic cables with GPR, as bending these cables or standing on them can break the cables. For this thesis, fibre optic cables were used as the ground that was being surveyed was flat and there was less chance of these fibre optic cables being accidently broken. In the case that they did break, spare cables were brought into the field in the instance that they did break.

4.4.9 Time constraints of data

Setting a constraint duration for electromagnetic radiation to be received helps the user to understand how much subsurface penetration will be applied. If this was not done, there would be no consistency in the data received, and thus data may continue to infiltrate, resulting in a loss of accuracy in outcomes. For the dataset of this research, a time limit of 2 seconds was achieved, allowing for a maximum of 12 m of subsurface penetration. While just 8 m of data was required, it was critical to go over this limit in case there were significant features to be noticed, particularly over the larger dune ridges. In most situations where a beach has both beach and dune ridges, the dune ridge will build on top of the beach ridge, as shown at Okains Bay, although the depth will be substantially lower than all other beach ridges. As a result of imposing a greater limitation, these beach ridges will be visible below the subsurface.

4.5 Real Time Kinematic (RTK)

Real time kinematic (RTK) was used in conjunction with GPR to collect information on the surface's topography. When utilising GPR, the surface topography is required since it might alter the information acquired when processing data. RTK is a surveying technique that may fix typical mistakes in generic global navigation satellite system (GNSS) systems. It operates on the same principles as a standard global positioning system (GPS) system; however, it only uses satellite signals carrier waves for its signal and ignores any other information received from the satellite. As a result, greater resolution data with just 1 cm range of error is now possible. RTK is made up of two distinct parts, specifically a base station and a rover. The base station will be installed at a known location (LINZ, 2021), where coordinates and height are reliably known in relation to either local or national data. The rover will then receive satellite data and transfer it to the base station, which will subsequently make the necessary modifications to obtain high-resolution data. The RTK technique employed in this thesis can also deliver reliable readings over mobile data networks, eliminating the requirement for a base station. The implications of just using mobile data networks are that they require a high level of reception in order to be utilised. Okains Bay did not get any mobile data reception, thus instead employing the base station approach.

The GPS survey sites in Okains Bay were located using the LINZ website (Figure 4.3). Survey points are graded on a scale of 1 to 10, with 1 being the least calibrated to seismic movement of the earth and 10 being the most thoroughly calibrated. On this scale, a score of 5 or above is often sufficient to deliver acceptable outcomes. At Okains Bay, there are two surveying points: one at the bottom of the bay and one at the top. On the LINZ survey scale, both values are a 5 or 6. The bottom marker within the bay was used above the top marker for convenience of access since it was closer to the transect that was being utilised and would be significantly easier to replace in case of errors.



Figure 4.3. Image of RTK base station (right) and rover (left).

4.6 Processing of Data

Following the data collection through GPR and RTK, four basic post-processing approaches are employed. EKKO View and EKKO View Deluxe software were used for data collecting processing in this research. EKKO view and EKKO View Deluxe are computer software that allows for the user to produce high quality imagery of the images of the subsurface produced in the field by GPR. EKKO View and EKKO View Deluxe were the programs chosen for this thesis as they are supplied by the School of Geography at the University of Otago and is one of the leading GPR programs for processing of data. There were 19 lines in total that required to be processed using Static correction, Background removal, changes to contrast and saturation of imagery and the inclusion of Topography using RTK data.

4.6.1 Static correction

When using GPR in the field, the rule is that the further out the electromagnetic band travels, the less energy is absorbed and received. When utilising static correction, the lower energy regions are balanced out by highlighting them more, so areas down in the subsurface are revealed rather than just being black. Automatic Gain Control (AGC) was employed for static data correction in this thesis, with a maximum gain of 500 and a window width of 1.5. The average maximum gain is between 50 and 2000, although it may reach 32767. Placing a maximum gain on AGC enables for deductions about the strength of the subsurface reflectors; if there were no constraints, the smallest reflections would have the same signal intensity as any other reflector within the transect. AGC is often frowned upon for this reason; however, for this thesis, variations in attenuation would not provide any information that might be used for this thesis, and only reflections were employed. AGC was therefore the best fit to use to investigate the beach ridge formation and the subsurface at Okains Bay, Canterbury.

4.6.2 Dewowing of datasets

Background removal is used to eliminate any undesired interruptions from GPR imaging. Dewowing is the most popular method for removing intrusive noises in the data illustration. Dewowing eliminates lower frequency information from GPR, which cleans up the imagery

visible in the final image. When utilising EKKO View Pro, dewowing is an automated procedure. Dewowing of GPR data is utilised in practically every GPR dataset since it cleans up the picture and allows for better interpretation.

4.6.3 Inclusion of Topography

When utilising GPR without an inbuilt GPS system, the findings are programmed to a horizonal line for the surface, affecting what is visible within the subsurface. The incorporation of surface topography is critical to a solid collection of GPR data. These adjustments were made possible thanks to the data acquired by the RTK. Unlike the GPR data, the RTK data was captured in a single continuous line rather than in segments. As a result, the RTK data was dissected to the exact distance associated with each GPR line, in order to align with the data produced with GPR. After RTK was divided up, RTK data had to be inserted in a separate document called a .topo file so that the EKKO deluxe software could read it. As a result, RTK data was integrated with GPR data, reflecting what is seen at Okains Bay. The elevation levels used for the GPR system within this thesis is through the conversion from Lyttelton vertical Datum to NZ vertical Datum to allow this thesis to compare to previous studies performed from the likes of Gibb (1986) and Clement et al. (2016).

4.6.4 Post processing data analysis

Once data has been customised to a legible and correct state, analysis of the data can then be conducted. Analysis of geophysical data, such as GPR, has been a source of conflict, as it is sometimes left to the discretion of the user (Tamura, 2012). The main points that were looked for in this dataset for this thesis are as followed:

1. Downlapping surfaces – This is the lowest point of the beach ridge, where the sand begins to accumulate, also known as an average low tide marker.
2. Toplapping surface – The highest point of the swash build ridge; this can be seen where the higher surface overlaps onto a lower surface and is a high tide point.
3. Areas of disruption – Discussed within the next section “limitations of methodology” these are areas of hyperbolae that are formed through subsurface artifacts such as trees, and underground pipelines, as well as on surface disruptions from electrical and steel

currents, such as fences and powerlines.

4. Contact between aeolian sands deposited onto swash-built beach ridges.
5. Contact between beach ridges and dune ridges
6. Differences in angles of subsurface sands, which are the change in angle of the lines – this represents a difference in wave climate during a period of time. A horizonal line could represent a settling lag ridge whereas a dipping line represents the current beach face and therefore the paleo beach.

Each key point will be further described and analysed within Chapter 5 of this thesis. Similar methodology and layout of results have been performed in the Cham Bay Embayment, Vietnam (Gouramanis et al., 2020), which listed out all different key elements of the GPR lines that they were looking for when looking at the geomorphic change of the embayment through sea-level. In doing so, Gouramanis and his co-workers were able to produce high-quality data and examination of their data through the processes that are listed above. Other papers that used downlapping surfaces are Tamura et al. (2008); Nielsen and Clemmensen (2009) and Clemmensen and Nielsen (2010).

4.7 Limitations of Methodology

While employing GPR and RTK methods for getting sea-level data in the past has been a highly valid methodology, there are several restrictions to using these technologies in order to gather the best possible data.

4.7.1 Estuary and timing

To utilise GPR, the driest circumstances are the best. As a result, it is usually recommended to use GPR near the conclusion of a summer period, when the water table will be at its lowest and there will have been the least amount of rain. Is saltwater very conductive. As a result, the GPR findings can be disrupted. Because electromagnetic waves cannot penetrate through very salty earth, having the lowest feasible water table is critical for concluding investigations. Because fresh water has less electrical characteristics than salt water, it is not as hazardous. However, it is still advised to avoid locations with high water tables for these reasons. The Okains Bay

water level was not a concern for this study since, while data was collected in early November, it was during a period of high dry days, thus the water table was lower than typical for that time of the year. During the final segment of section 2, problems with the water table were encountered. This was the narrowest area of Okains Bay, and the water from the estuary, as well as passing through ancient streambeds, seemed to upset the GPR's conductivity, hence no data was received across this stretch (Figure 4.2, between the purple lines). Small streams passed through this region on their way to the estuary. These places had to be avoided as well throughout this investigation, resulting in a skewed data collection.

To obtain reliable data, the part closest to the existing beach face was completed at the lowest feasible tide. This appeared to function effectively because measurements from the beach showed little saltwater intrusion at the surface, allowing for some subsurface penetration.

4.7.2 Powerlines and Electric Fences

Another major constraint encountered while utilising GPR is the presence of electrical equipment such as power lines and electric fences. Because of the power disparities, the receiver will pick up the electric currents of the powerlines passing over the transmitter. As a result, GPR data could not be obtained through the little township of Okains Bay Village. A powerline was present and traversed down the main street, where the GPR transect had to intersect.

The electric fences that ran through the farmlands near Okains Bay posed no difficulty for this investigation. When requesting permission to utilise property from landowners, it was requested if the electric fences could be turned off for the two days of data collecting. There was no livestock around the transect line through Okains Bay at time of data collection, so all electric fences were already turned off.

4.7.3 Underground Pipes

Another element that might contaminate GPR data is underground pipelines. Because pipe has no porosity, electromagnetic currents are impossible to pass through. Only one pipe was struck during data collection at Okains Bay, however this was only via the portion where there was a significant quantity of salt intrusion within the subsurface and so had no effect on the ultimate outcome of data collection at Okains Bay as this area was simply impossible to be used.

4.7.3 Anthropogenic change of the Landscape

Another major constraint of this study was anthropogenic land modification, which made it impossible to collect data in a continuous line from the beach face to the rear of the bay. Okains Bay Village was avoided for this reason. Farm animals did not present as many challenges as predicted to the final data output since the surface of Okains Bay contains a very little quantity of dirt on top of the sands of Okains Bay below.

4.7.4 Ethical consideration

When obtaining data for this thesis, all farm owners, as well as the residents of Okains Bay community, were acknowledged. All farm owners consented to have their property surveyed, as did the Okains Bay Camping Ground. The little tract of land managed by the Department of Conservation (DOC) was avoided since it was too near to the estuary and so would not be worked on.

4.8 Summary

GPR is the main methodology used within this research project. Validation of the use of GPR occurred through Jol (pers. Comms) preliminary study achieved at Okains Bay in 2019. Through Jols work, the 100 MHz antenna was used instead of the 200 MHz as the resolution of data outweighed the amount of depth penetration needed for this survey. The type of survey used was a mid-common point survey, where the antennas are at a fixed width and moved along the transect line. Understanding the choices of calibration as well as limitations for GPR is crucial to providing a high-quality data collection. Depth penetration achieved a maximum depth of 10 m, however on average, most Figures produced within this research, reached a maximum depth between 5 m and 8 m. The RTK system was used to gather information on topography to provide topographic change for the GPR. Processing of data included, static correction, dewowing, and addition of topography. Lastly, the Estuary, underground pipes, and anthropogenic change of the landscape were the main limitations seen within this study.

The next chapter will provide the data that was gathered within this thesis. Data collected has been analysed and annotated to provide insight into the key features that help understand sea-level change over the Holocene as well as the geomorphic changes that occurred for Okains Bay.

Chapter Five: Results

5.1 Introduction

The capability of GPR in recreating observed sea-level variation over the Holocene has been demonstrated at the case study site of Okains Bay, Canterbury. Following the explanation for the calibration of GPR in Chapter Four. GPR was calibrated accordingly to investigate into the subsurface of Okains Bay, providing insight into the morphological features that have occurred through the processes of progradation, and also the processes that occurred when progradation halted. In doing so, this chapter will aid in investigating this thesis' key questions.

Chapter 5 begins with an analysis of the different formation processes seen within all GPR images at Okains Bay. Such analysis included looking at the different types of geomorphological processes that occurred in order to perform the different types of ridges seen within Okains Bay, namely, Swash built ridges, aeolian build ridges, and the potential of settling lag ridges are all seen within Okains Bay. Afterwards, analysis of each GPR transect was preformed. The GPR Figures used in Chapter Five will have two parts, the first being the GPR transect with no analysis, and the second part of the Figure showing the differences seen within each line. After analysis of GPR, all downlapping and toplapping points from each Figure will be placed into a graph, coupled with RTK data representing the topography of Okains Bay. In doing so, this will produce a sea-level graph for Okains Bay.

5.2 Analysis of beach ridge formation using GPR

Upon analysis of GPR data, it is necessary to understand seven key processes to be able to interpret the sea-level curve of Okains Bay. Specially these seven processes are: Progradational stratigraphy, Downlapping surfaces, Toplapping surfaces, Erosional features, Dune ridges, Hyperbolaes and horizonal stratigraphy. As previously stated in Chapter Two, section 2.6.5, downlapping and toplapping surfaces are only needed to produce an accurate sea-level curve (Tamura et al., 2008; Nielsen and Clemmensen, 2009). However, the other features seen within Okains Bay aid in understanding the geomorphological changes that have occurred throughout the Holocene, further aiding in understanding the sea-level curve for Okains Bay. All GPR elevations have been converted to NZ vertical Datum in order to understand how

Okains Bay's sea-level curve is compared to the rest of New Zealand.

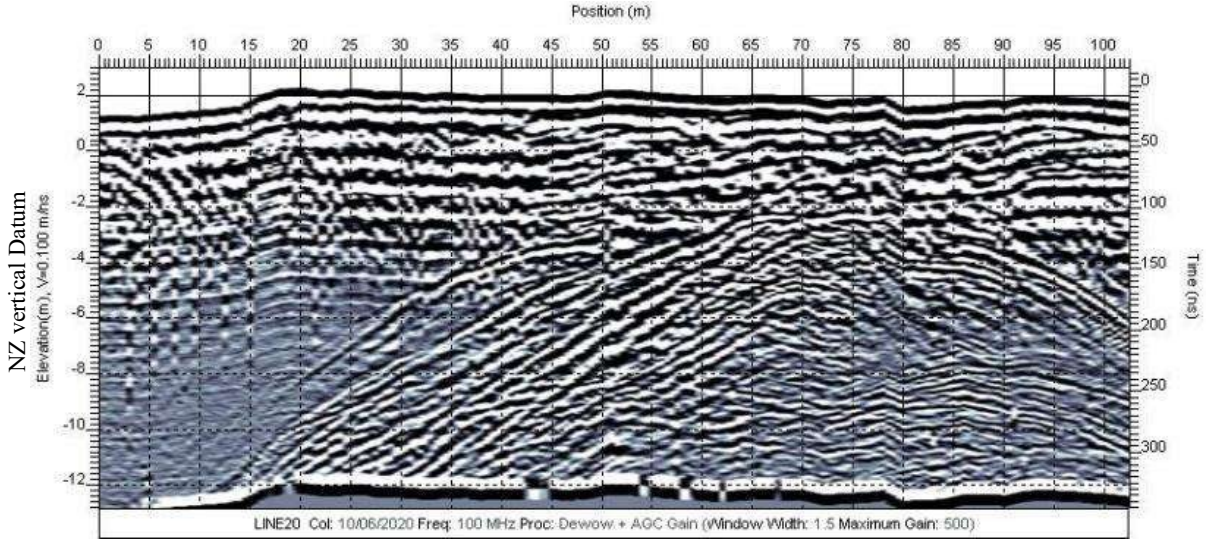
Table 5.1. Key features found within the GPR data with definitions.

Processes	Explanation of process	Colour for Analysis/ Feature
Progradational stratigraphy	Seaward dipping stratigraphy that occurs throughout Okains Bay. Lower angle, representing the historic coastlines at Okains Bay. Found within all Figures	Green
Downlapping surfaces	Areas where two lines diverge from one another, generally the bottom line will be long and continuous, representing low tide. Occurring within a progradational sequence.	
Toplapping surfaces	Areas where two lines converge into one another, occurring at the top of the coming Figures. Toplapping surfaces represent high tidal zones. Occurring within a progradational sequence.	
Erosional features	Landward dipping stratigraphy- overwash deposits from events where swash zone processes go over the older beach ridges near the coastline, creating a cut within stratigraphy.	Red
Dune Ridges	Change in topography, aeolian dominated landforms. Two main aeolian dune ridges are found within Okains Bay transect in Figures 5.7 and 5.11.	Blue
Hyperbolaes (Artifacts)	areas where electromagnetic energy is affected by an artifact in the subsurface. E.g fallen trees, powerlines, electric fences.	Cyan/Purple
Horizontal stratigraphy	areas of deposition that have occurred in low energy zones. Settling lag ridges	Orange

5.3 Transect One of Okains Bay

The first transect of Okains Bay transect (Figure 4.2) is from the current beach face to mid-way through the Okains Bay camping ground. The transect is 105 m as depicted in Figure 5.1. Through this section, the GPR has been shown to produce high-resolution data (Figure. 5.1a). Figure 5.1b shows an interpretation of the different processes that have occurred during the building of Okains Bay. Figure 5.1b first shows three main sections of landward dipping stratigraphy, the first section, has parallel running, high-angle dipping lines, representing the processes that have occurred within the swash zone. From 80 - 105 m in Figure .5.1b, there is also another area of landward dipping lines, albeit at a lower angle. Through the middle of the section, progradation has occurred, represented by the green in Figure. 5.1b, the stratigraphy lines through this section are long and continuous, with some lines reaching 30-35 m in length. Through the area of progradation on Figure 5.1b, clear downlapping surfaces can be seen, the key downlapping surfaces have been highlighted in Figure 5.1b. The largest feature seen within Figures 5.1 is the large hyperbolae (coloured cyan in Figure. 5.1b), the hyperbolae feature covers almost the entire bottom section of Figure 5.1, and reaches a height of – 4 m, it is unknown of the causes of this hyperbolae as the lines underneath do no produce any overlapping stratigraphy or repeating lines that would imply a large artifact to be produced.

5.1a



5.1b

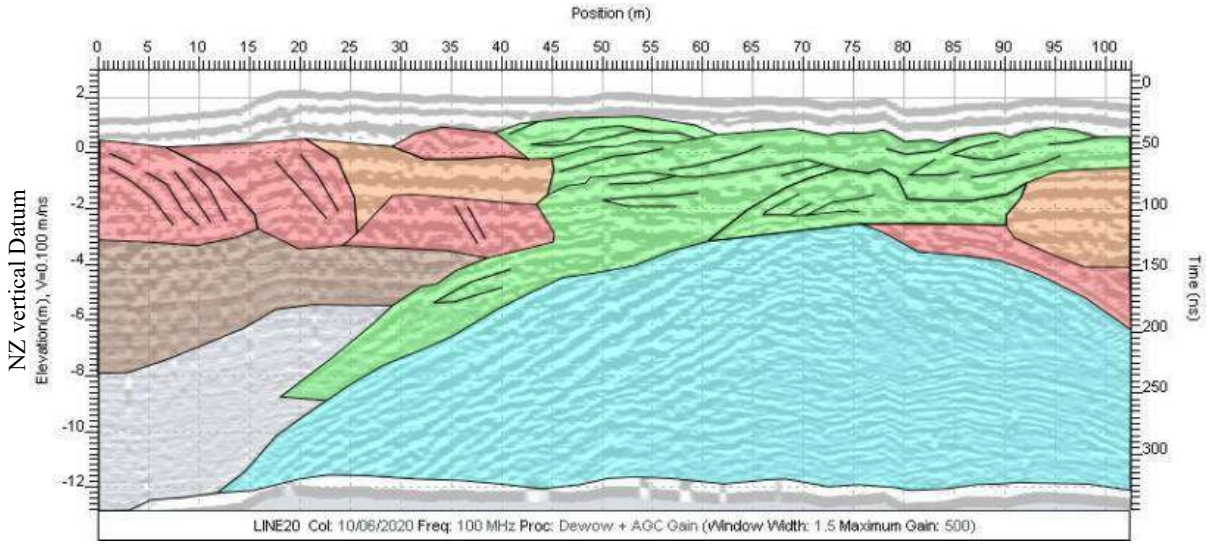


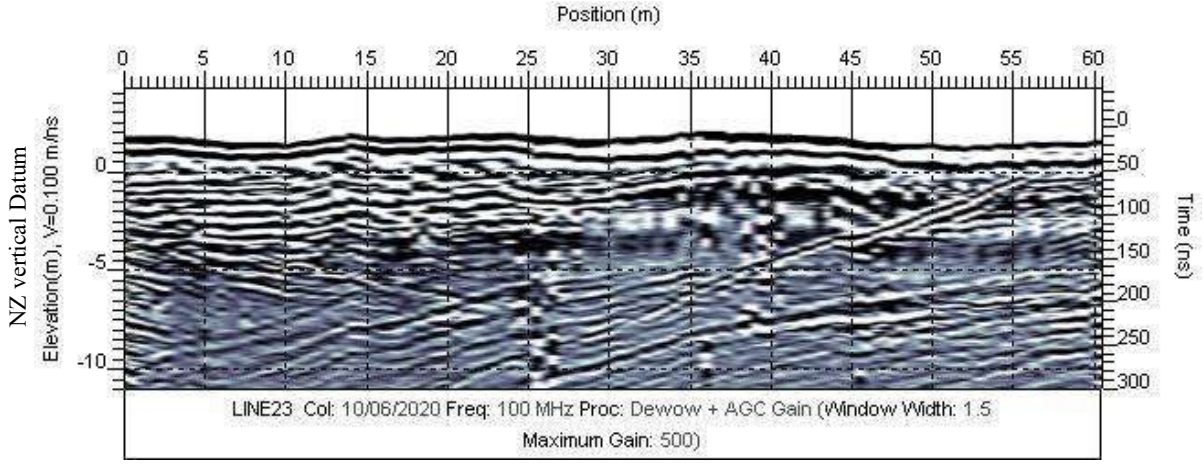
Figure 5.1. Image of GPR through section one of Okains Bay. 5.1a shows imagery from GPR with no analysis. Figure 5.1b shows a schematic of GPR. Red; erosional areas with landward dipping stratigraphy. Green; areas of progradation with downlapping and toplapping points. Orange; areas where stratigraphy is horizontal. Cyan; large hyperbolae, unknown the causes of why this occurred. Brown; unobtainable data.

5.4 Transect Two of Okains Bay

The following set of Figures covers the majority of Okains Bay, beginning with farmland and ending with the township. This section will discuss each Figure individually because each Figure has distinct attributes.

Figure 5.2 is the beginning of the second transect in Okains Bay for this study. The penetration depth on Figure 5.2 is down to -5 m. Progradation can be seen within Figure 5.2b, especially between 0 m and 45 m along the transect. Outside this progradation, there is erosional features seen, highlighted in red. These erosional features are landward dipping stratigraphy. Within the middle of the section, between 20 m and 50 m, there is a large area where GPR has not been able to penetrate and therefore has given no data.

5.2a



5.2b

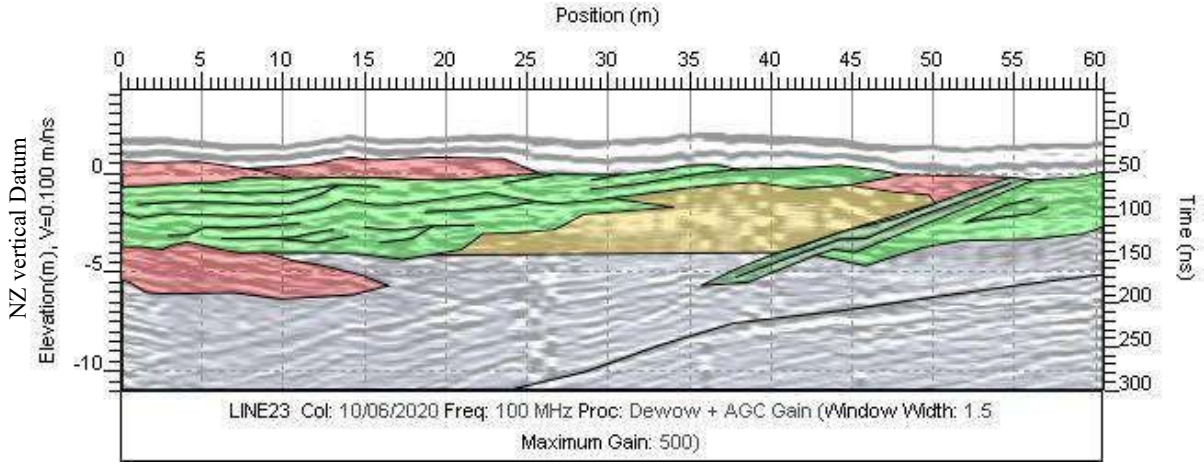
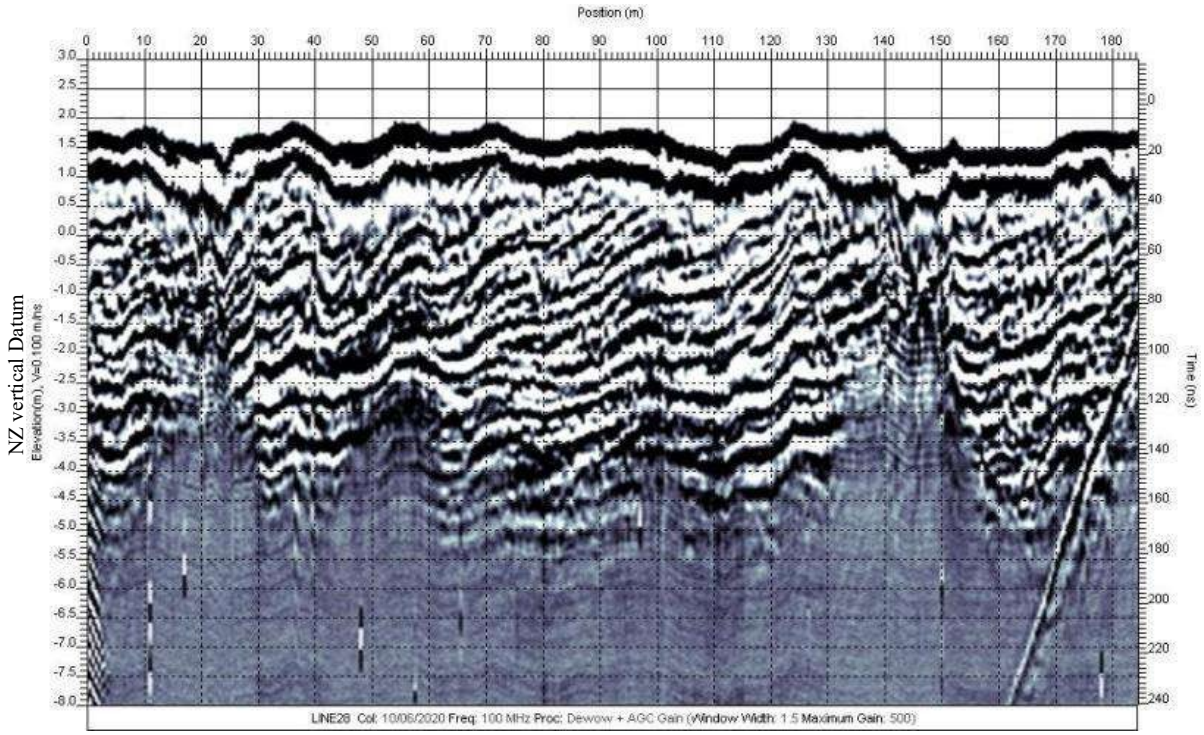


Figure 5.2 GPR Image of 61 m of transect in Okains Bay. A) shows data without annotation. B) shows annotation where green = prograding sequence, red = erosional features, = yellow = unobtainable data.

Figure 5.3 notices an unusual shift in the subsoil. Many of the seaward dipping stratigraphy lines are between 30 and 40 m long, with others exceeding 80 m. The majority of Figure 5.3 transect is a progradational sequence. Three key elements of Figure 5.3 may be identified. The first is 20 m along the transect when the lines converge and the region underneath this becomes grey, where the electromagnetic pulses cannot reach. Another location that should be noted at 0 m is just following this segment, between 40 – 50 m where the lines here have a substantial dip into the surface, with some lines sinking landward, resulting in a pocket just beneath the subsurface with no ordered stratigraphy. Finally, at 130 – 150 m, a similar phenomenon is seen to 20 m, with lines converging on each other at − 1 m and electromagnetic energy penetration was not achieved. Overall, Figure 5.3 illustrates that the angle of the seaward dipping strata changes as it gets larger than previously seen. There are also multiple toplaps and downlaps depicted within Figure 5.3. Almost all lines portraying progradation begin at a lower angle than they do when they conclude.

5.3 a



5.3 b

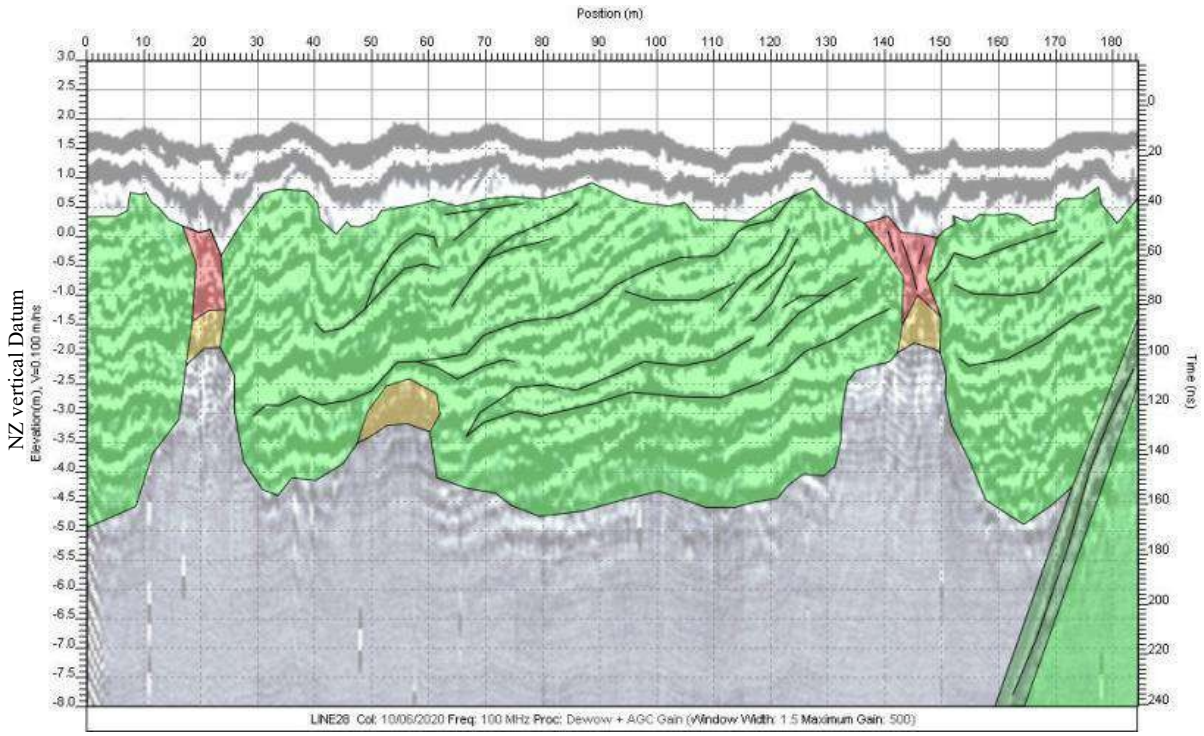
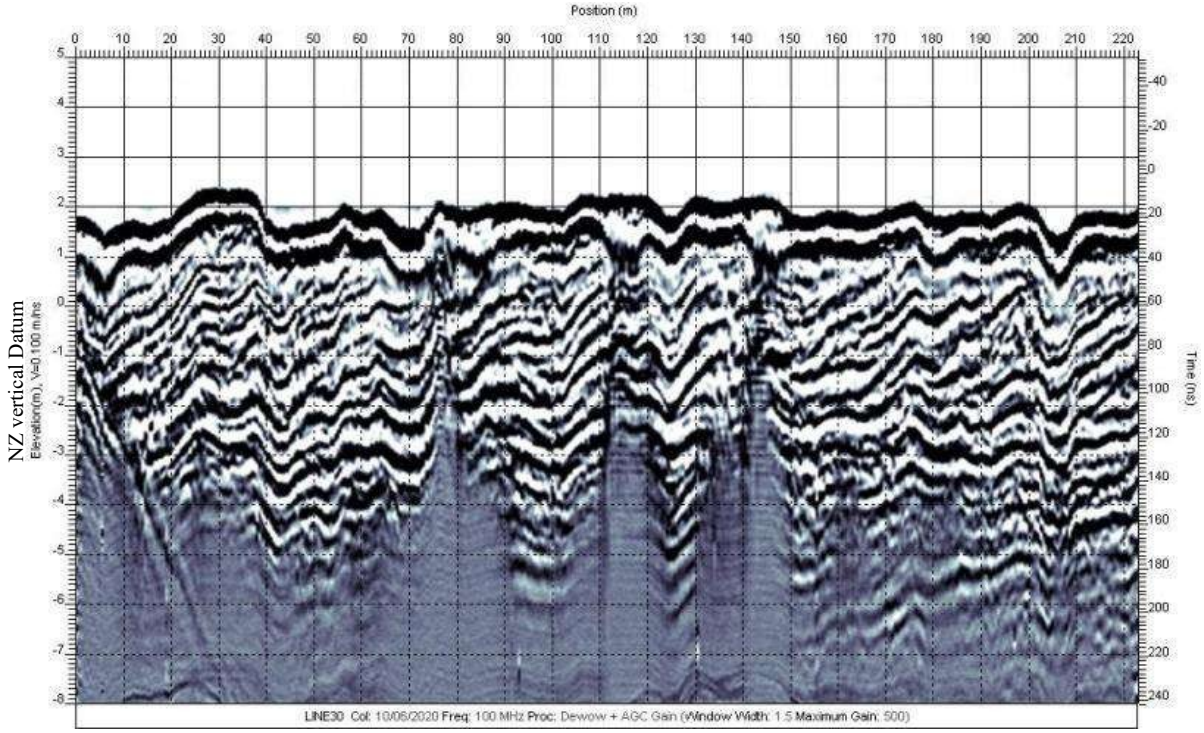


Figure 5.3: Images of GPR transect in Okains Bay showing 185 m. a) is post processed data with no annotation. B) shows annotations. Green = prograding sequence with downlapping points, red = erosional features, yellow = unreadable data.

Figure 5.4 follows a pattern similar to Figure 5.3, with some changes. As indicated in Figure 5.3, several of the lines at the bottom of the picture stretch between 30 and 40 m in length, however at the top, towards the surface, the lines become thinner and shorter in length. When contrasted to the lines above, the huge lines at the bottom are quite thick. Figure 5.4 has very little landward sloping strata, only being at the beginning of the Figure at a depth of – 1 m. Lines are being squeezed in four places along the transect of Figure 5.4. These are in the beginning, when it starts at – 1 m and decreases to – 5 m after 50 m. The second section begins at 78 m and rises to – 1 m. Third, between 110 and 120 m, it reaches -3 and -2 m, and finally, at 140 m, it reaches – 1 m. Following the key areas previously stated, the transect collected high-quality data down to –4 m all the way to the end of the transect line. These downlapping surfaces are plainly visible at 0 m along the whole Figure 5.4b, while toplapping surfaces are not as visible in this image, most likely due to anthropogenic alteration. Anthropogenic alteration is seen right beneath the surface in Figure 5.4 where there is a wider gap between the surface line and the seaward dipping stratigraphy, most likely as a result of reworked soil for farming reasons.

5.4 a



5.4 b

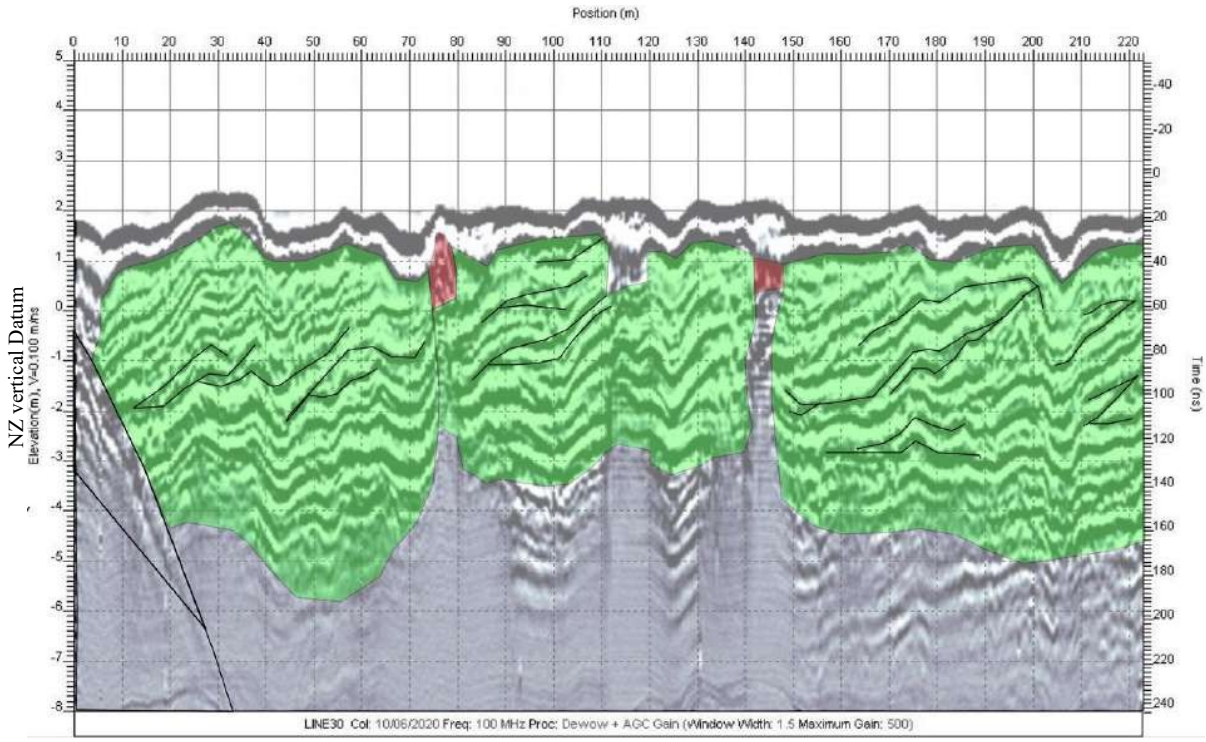
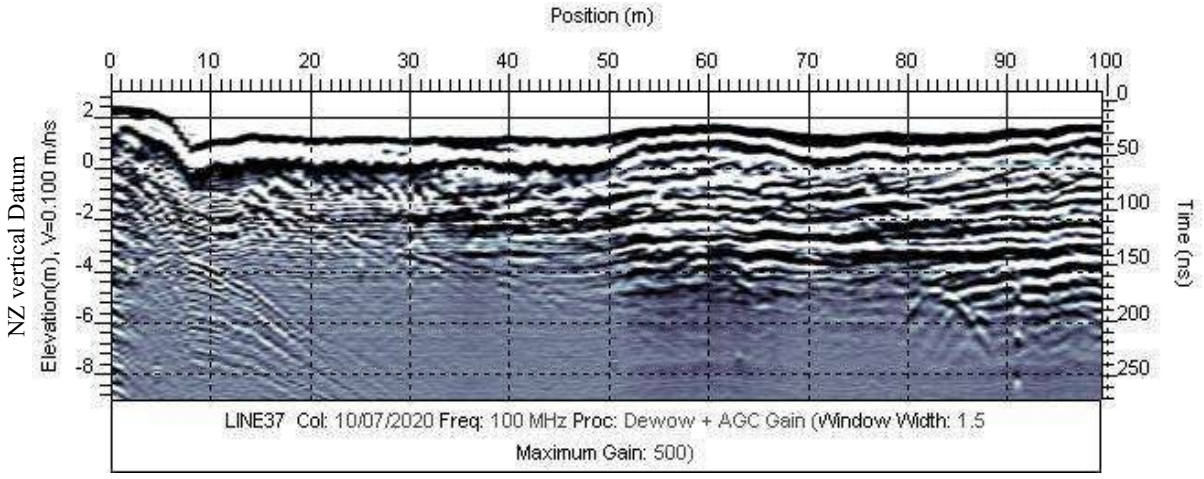


Figure 5.4. Images of GPR transect in Okains Bay showing 222.5 m. a) is post processed data with no annotation. b) shows annotations. Green = prograding sequence with downlapping points, red = erosional features.

Figure 5.5 shows a large amount of disruption slightly below the surface within the first half of the transect. Within the second half, between -2.5 to 0 m is a seaward dipping stratigraphy that stops just below the surface. Between the surface and the seaward dipping stratigraphy, there has been a disruption to the earth can be seen through the thick dark line at 0 m between 8m and 30 m along Figure 5.4. Below the seaward dipping stratigraphy between 40m and 100 m at a depth of -2 m is almost parallel, horizonal running lines, with some slight seaward dip which could have been produced through a process of settling lag. Figure 5.5 has one of the lowest surface sections within the entire line, with some parts reaching down to 1 m.

5.5 a



5.5 b

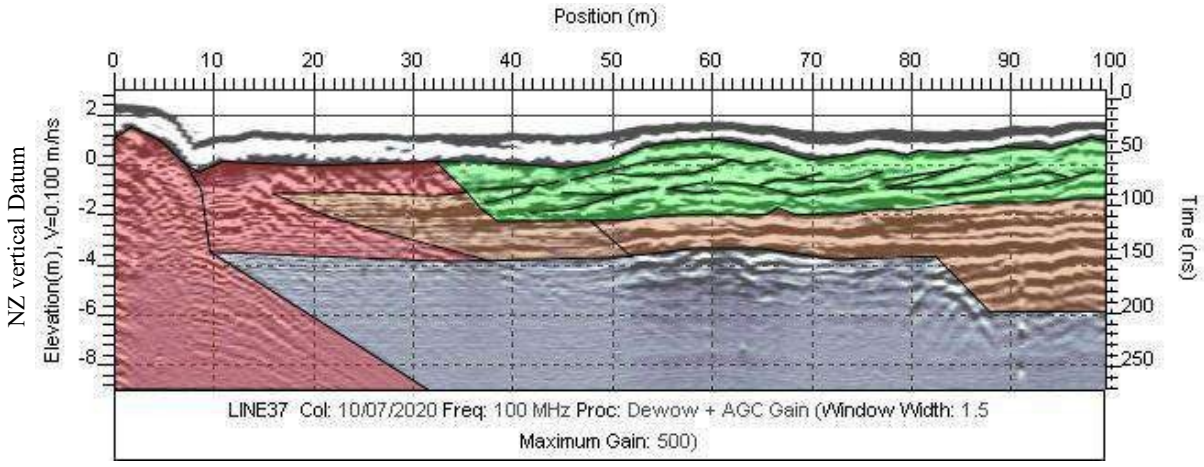
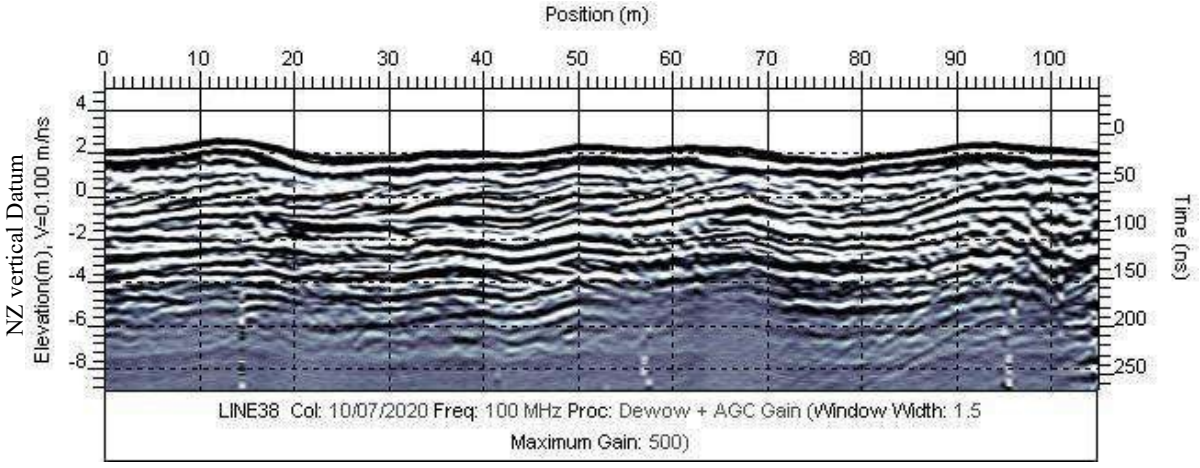


Figure 5.5: GPR image of part of the Okains Bay transect showing 100 m. a) non annotated image. b) showing annotations. Green = prograding sequence, red = erosional sequence and orange showing horizontal stratigraphy.

Figure 5.6 has a surface topography that varies between 2 m and 1.5 m in height. Multiple downlapping points are seen throughout this section as seen in Figure 5.6b, which occur between 0 m and – 2 m. Toplapping points are also seen just under the surface on Figure 5.6a and 5.6b. These toplapping points can be seen to occur between 1 m and 1.5m. Almost no aeolian sediment is seen throughout Figure 5.6 as toplapping surfaces are directly underneath the current surface. The majority of Figure 5.6 is a prograding sequence with only a small section at 100 m showing any signs of erosional features, as seen in Figure 5.6b.

5.6 a



5.6 b

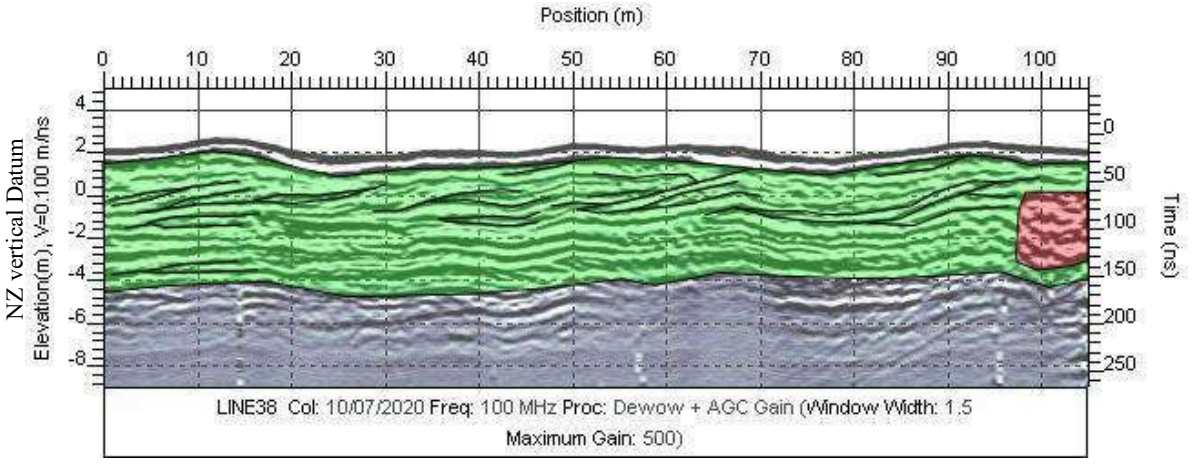
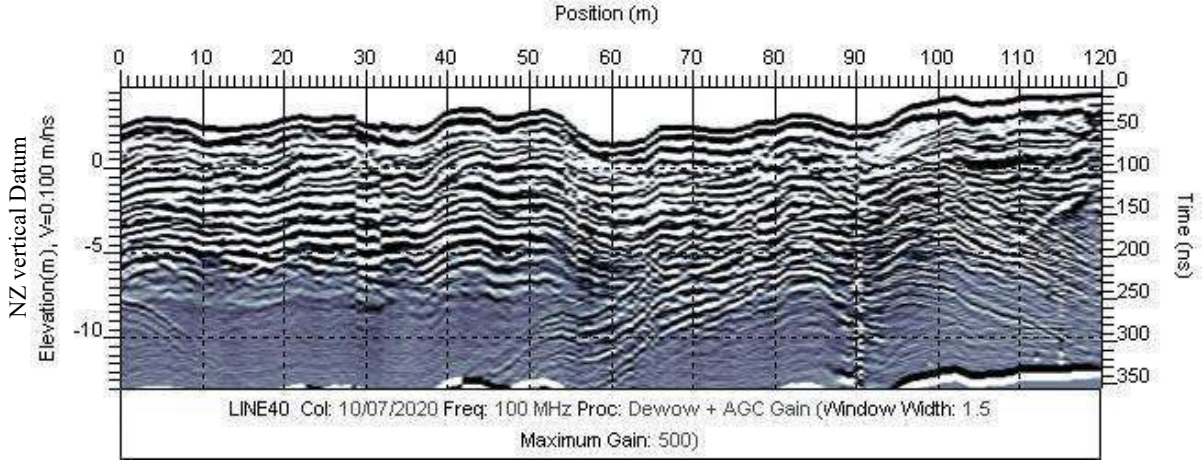


Figure 5.6: GPR image of part of the Okains Bay transect showing 104 m. a) non annotated image. b) showing annotations. Green = prograding sequence, red = erosional sequence.

Figure 5.7 is the Figure that shows the main beach ridge located on the landward side of Chorlton Rd. Compared to the other Figures in this chapter, the topography is much more hummocky than seen throughout the rest of the bay. Figure 5.7 shows the highest point within the bay at just below 5 m. The lines within Figure 5.7 are evenly spaced. Between 60 and 120 m, an overlapping hyperbolae (coloured purple in Figure 5.7b) can be seen under the ground, with its highest point being at 0 m. The left side of this hyperbolae, shows what could have been a historic dune ridge due to the small hump seen between 70 – 90 m. Within Figure 5.7, there are many down lapping surfaces before 60m, with some down laps being on top of the thought to be historic dune ridge. Some of the surfaces within this Figure are very steep, such as the surface slightly before 40 m. Landward dipping lines between 50 m and 60 m are present, slightly before the dune ridge sequence. However, these lines do not intersect any other lines, therefore it is unlikely that these are Erosional features.

5.7 a



5.7 b

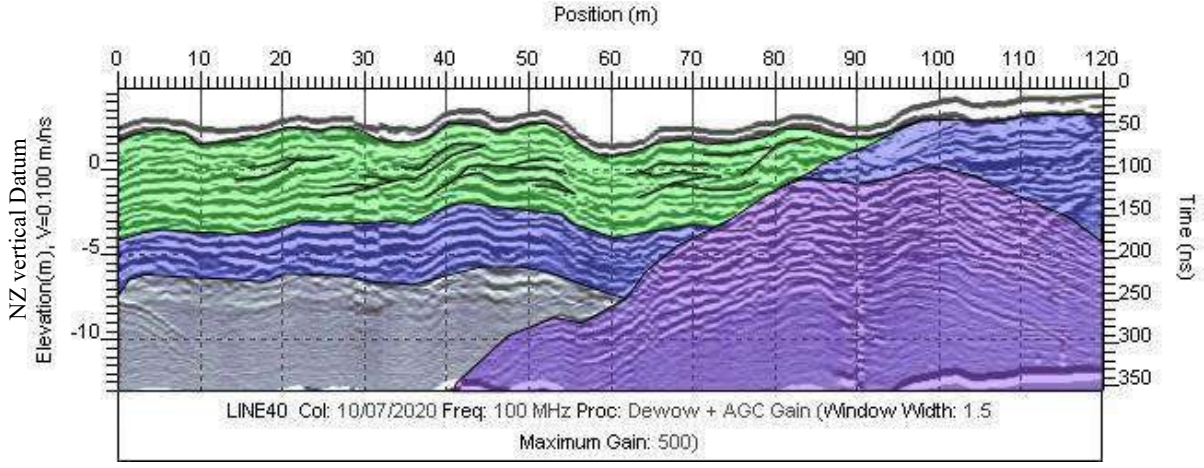
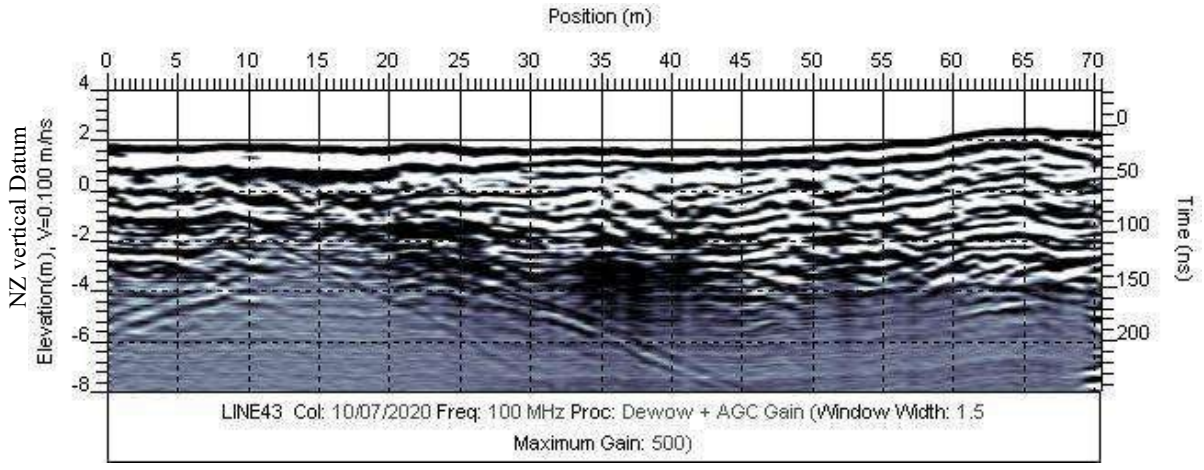


Figure 5.7: GPR image of part of the Okains Bay transect showing 120 m. a) non annotated image. b) showing annotations. Green = prograding sequence, Blue = Showing aeolian sediment deposition and Purple = showing a mix between an artifact within the ground as well as aeolian deposition.

The next four lines though the Okains Bay transect (Figure 5.8, Appendix G, H) ran through the swampiest area of Okains Bay. It is thought to have high salt and water intrusion and therefore was very hard to get a signal though this section of transect 2. However, within these Figures, there are some important features that can be noted. Firstly, the surface topography through this section is very flat to almost horizonal and all slightly above or below 2m above sea-level. Through this section in Figure 5.8, and Appendices 7 and 8 see only a small amount of down lapping surfaces that can be used to present historic low tide and even less amounts of toplapping surfaces. This is mainly due to the angle of the stratigraphy being very close to horizonal.

5.8 a



5.8 b

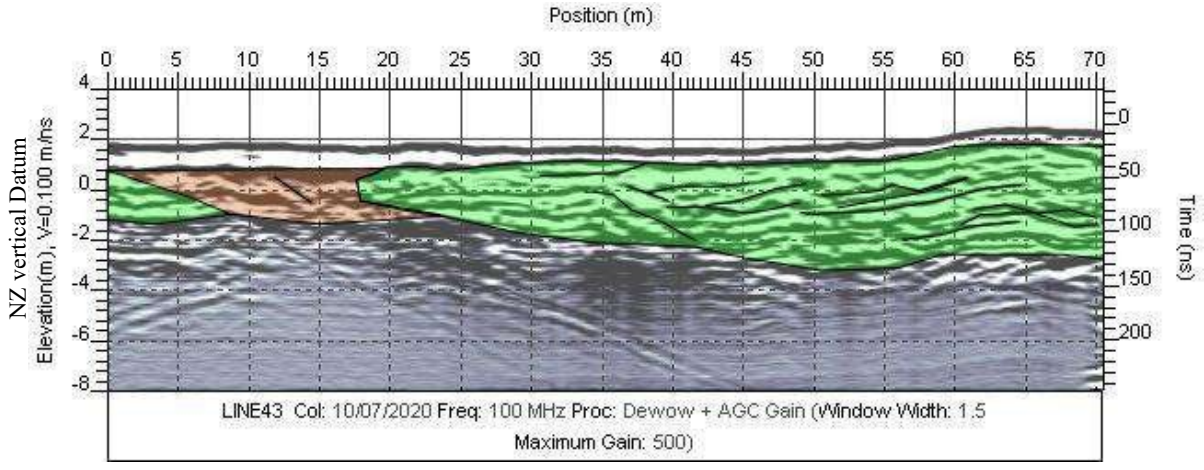
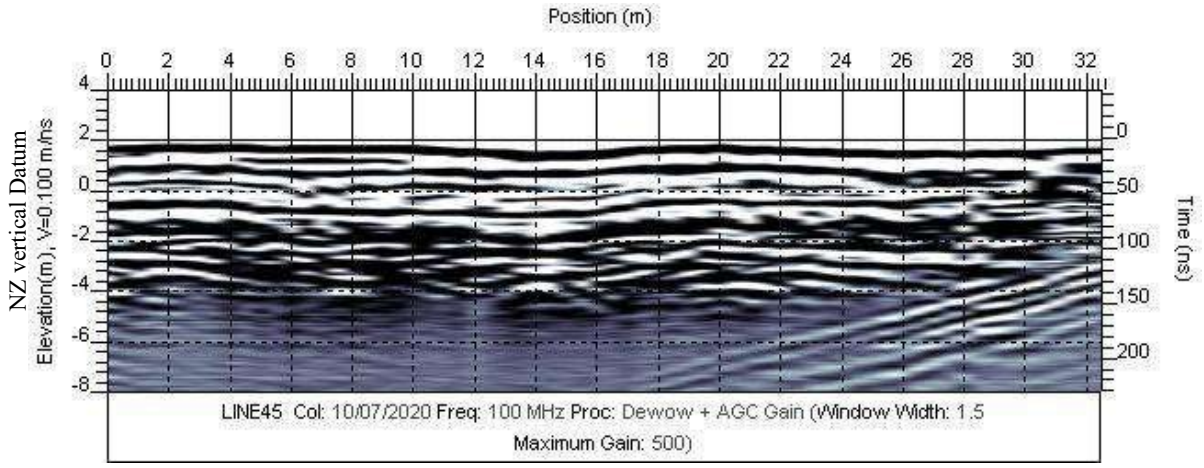


Figure 5.8 GPR image of part of the Okains Bay transect showing 71 m. a) non annotated image. b) showing annotations. Green = prograding sequence, and orange showing horizontal stratigraphy.

Figure 5.9 is the end of the swampy area described above. Figure 5.9 does not show any sign of progradation through the entire image. The stratigraphy lines through this section have horizontal lines, two stratigraphy lines reach from 0 m to 32 m, the first being just below 0 m and the second being at – 2 m extending over 32 m and 29.5 m respectively (see Figure 5.9b and the continuous black lines that annotated onto the diagram). The stratigraphy at – 3 m is highly attenuated which could have been induced by two possible reasons. The first being that saltwater intrusion affected the electromagnetic waves throughout the sequence, therefore not producing any changes in stratigraphy. The second being that the sediment was deposited through the process of settling lag.

5.9 a



5.9b

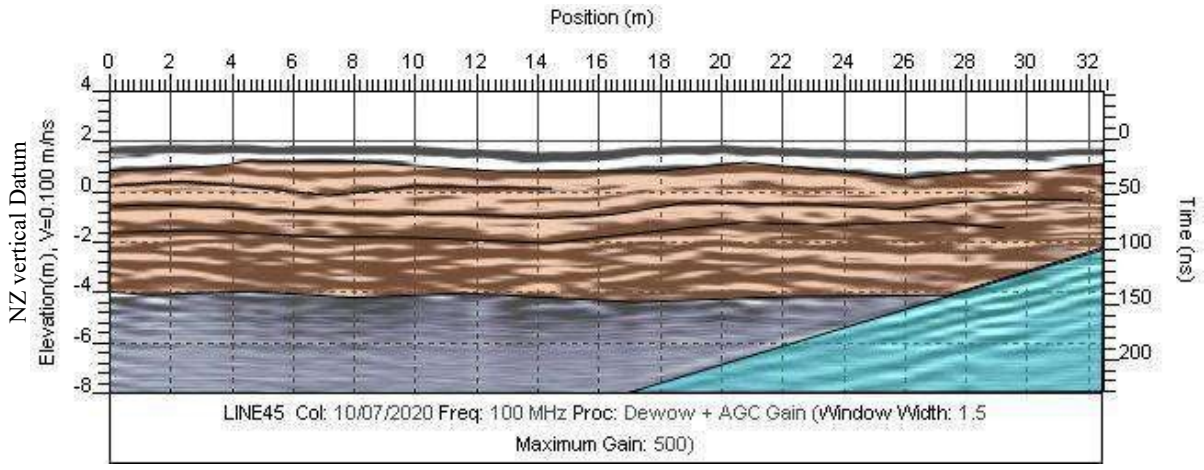
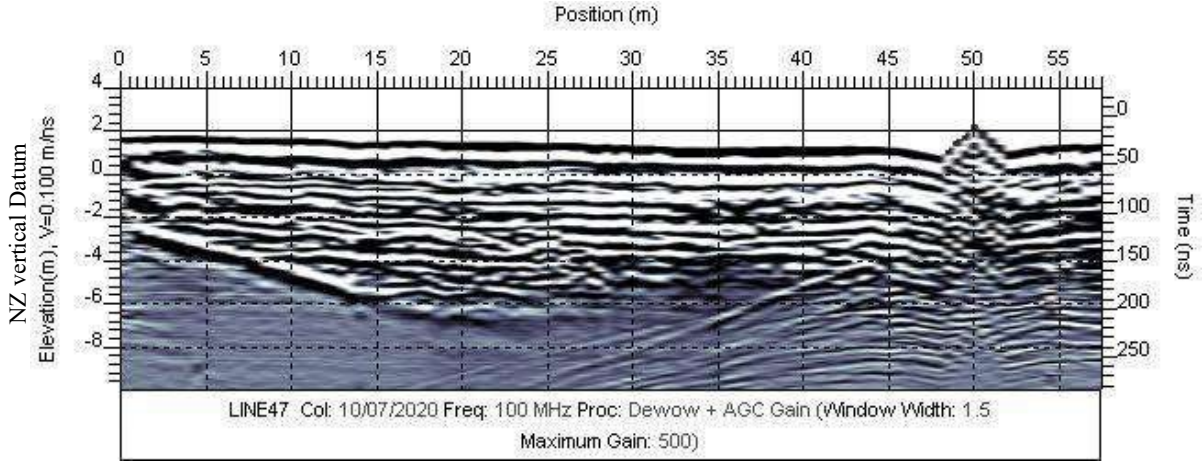


Figure 5.9: GPR image of part of the Okains Bay transect showing 32.5 m. a) non annotated image. b) showing annotations. Orange = horizontal stratigraphy and cyan = unreadable imagery due to electrical disturbances.

5.5 Transect Three of Okains Bay

Transect three of the GPR line begins directly after the Okains Bay village. Figure 5.10 shows horizonal lines, compared to the previous lines seen dipping seaward. Throughout Figure 5.10, there are only two downlapping surfaces due to this landward dipping orientation. Between 48 m and 52 m, there is a section of data unobtainable due to malfunctions with the RTK system. This malfunction was caused due to losing signal with the base station. At this point, the RTK had to be reset, however data was lost for this point.

5.10a



5.10 b

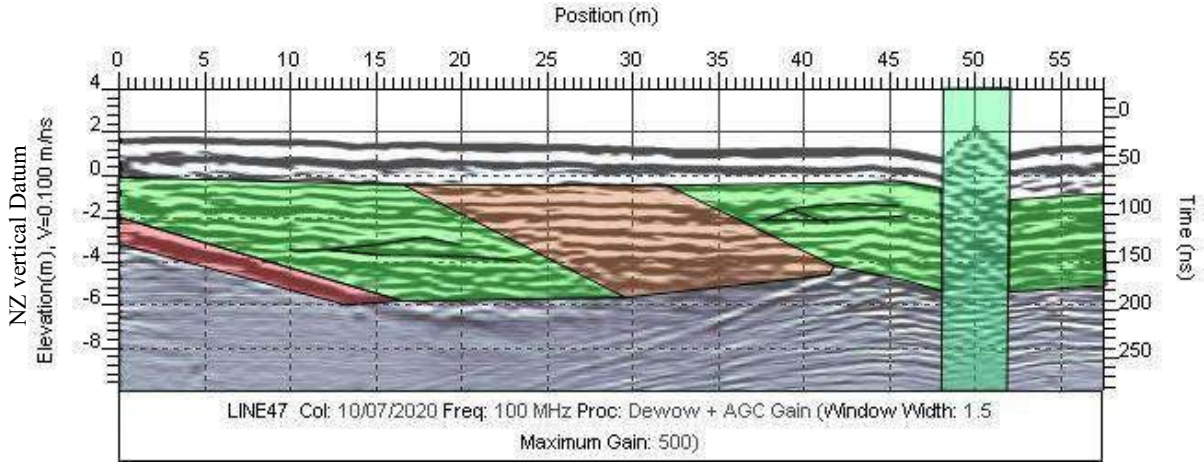


Figure 5.10: GPR image of part of the Okains Bay transect showing 57.5 m. a) non annotated image. b) Showing annotations. Green = prograding sequence, red = erosional sequence and orange showing horizontal stratigraphy, Blue/green = area where RTK results misread topography.

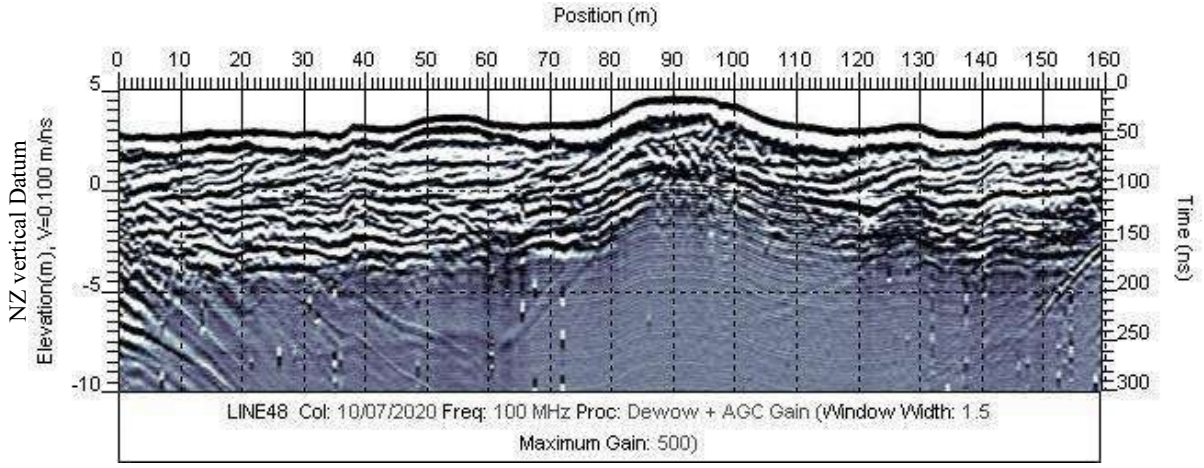
Figure 5.11 shows a transition between beach and dune ridges directly after the Okains Bay village. The left side of Figure 5.11 shows downlapping and toplapping surfaces within a progradation sequence which are seen at 0 m, specifically at 10m and 20m. The lines that are seaward dipping are low lying, rising 1 m over a 40 m distance (especially between 30 m – 70 m), similar to the coastline at Okains Bay present day. Below these prograding lines (0 m to -4 m depth) are a series of landward dipping stratigraphy. These surfaces suggest that a large amount of erosion occurred within Okains Bay at some point, most likely as the dune ridge sequence on the landward side of this was being built, as these are not seen on the landward side of the dune ridge sequence.

Between 70 and 110 m, topography is much higher than usual, reaching a height of 4 m, suggesting a dune ridge sequence. The internal structure of the dune ridge is a series of landward dipping stratigraphy that are steeply dipping.

The gap between the air line and the ground surface line in Figure 5.11 is very wide apart. This was because of the large amounts of grass that sat on the surface and therefore was difficult to place the GPR exactly onto the ground surface. This is prominent from 70m to the end of the transect at 160m. On the landward side of the dune ridge (110 m onwards), the series of progradational lines continue, still being above the 0 m line. It is expected that sea-level resided between the downlapping and toplapping surface through this section, with a rise in sea-level during the dune ridge sequence where aeolian sands took over from the progradational record. The angle of the lines on the right side of the dune ridge are at a similar angle to the stratigraphy that is between 0 – 40 m in Figure 5.11.

The date of 7500 +\- 1200 years resides exactly on top of the dune ridge sequence of Figure 5.11 by Stephenson and Shulmeister (1999). This date is a ^{14}C date by an unidentified shell fragment.

5.11a



5.11b

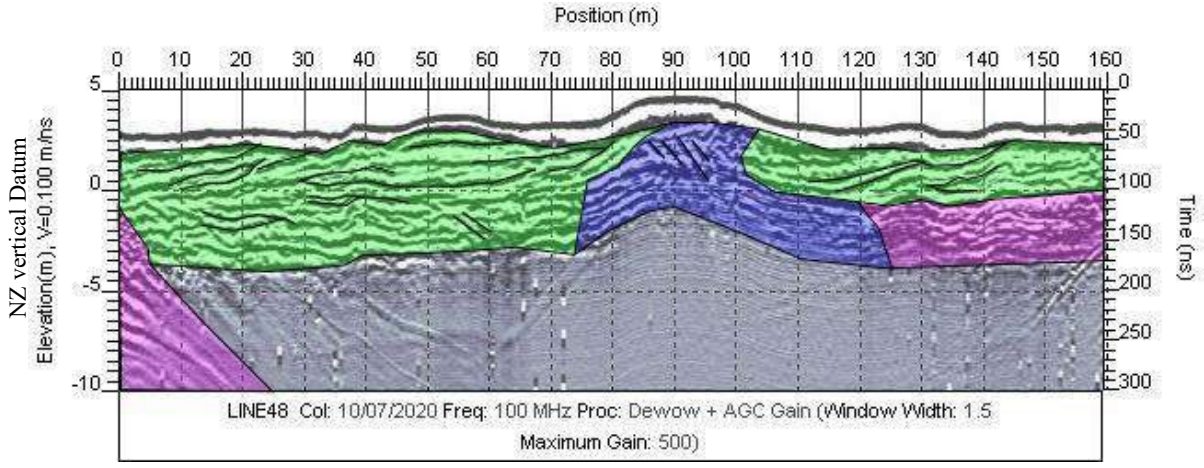


Figure 5.11: GPR image of part of the Okains Bay transect showing 100 m. a) non annotated image. b) showing annotations. Green = prograding sequence, Blue = aeolian deposition and pink = mix between aeolian and swash zone mixing.

5.6 Other GPR images Obtained in Okains Bay

Many other lines were produced for this GPR survey, however only showed progradation through them. Therefore, the use of these Figures was only to analyse the downlapping and toplapping surfaces to produce the sea-level curve (Figure 5.12) and not for geomorphological changes. These images can be seen in Appendix A, B, C, D, E, F, G.

5.7 Sea-level curve for Okains Bay

The important points visible within the sea-level curve for Okains Bay are listed in the following section. This section begins with section three, which is the oldest portion of the Okains Bay sequence (7500 +\- 1200) and goes seaward to the present-day shoreline. A rolling average of 30 points was utilised to characterise sea-level in order to create the sea-level curve (Figure 5.12). Such allowed for an easier interpretation of the sea-level curve than if no average points were produced during the sequence.

5.7.1 Transect Three

At the completion of the transect, the oldest piece of Okains Bay within this thesis has been dated to 7500 +/- 1200 years. This date is based on an TSL date found on a dune crest (Stephenson and Shulmeister, 1999). The sea-level was at its highest point within Figure 5.11, with a high tide average of 2.5 m and a low tide average of 0.2 m. High tides can be observed falling swiftly throughout this segment, with high tide lying at 1.1 m at the conclusion of section 3 and low tide only lowering 0.2 m to 0 m. The Okains Bay Village is located in the large gap between sections 3 and 2, making it difficult to get any results as stated in Chapter 4. Predictions may be formed by connecting the ends of sections 3 and 2, which could suggest a dropping sea-level for high tides and particularly for low tides.

5.7.2 Transect Two

Section two is the Okains Bay sequences' body. The oldest date in this segment is 1674 +/- 76 years, and it is located landward of the biggest dune crest in the Okains Bay series. The sea-level at this location is slightly lower than it is now, with an average high tide of 0.5 m and a decreasing low tide of – 1.5 to – 2 m. This section marks the conclusion of the present dip in sea-level from Section 3 to the beginning of Section 2 (Figure 5.12). Points of interest within section two indicate that there is fluctuation within the low tide points compared to the high tide points moving seaward. Sea-level trends following the dune ridge show a dropping sea-level from high tide locations, and fluctuations in low tide locations. High and low tides reach their closest point in the series at 1250 m, with high tides averaging 0.5 m, dropping to 0 m, and low tides rising to -0.3 m (Figure 5.12). This location has the lowest average high tidal

zone and one of the greatest low tidal zones in the Okains Bay series at 1250 m. Low tide begins to decline after tidal points get near together, but high tide remains at comparable levels about 0.2 m. The average gap between high and low tides here is slightly more than 2 m. This 2 m difference between high and low tides is consistent throughout the series until reaching the present-day shoreline. From this low point, there is a substantial rise in sea-level, with high tides reaching an average height of 1.5 to 2 m and low tides reaching a maximum height of 0 m. Following this, there is a steady fall in sea-level until the end of section 2, where the earliest date from Stephenson and Shulmeister (1999) reveals 672 +/- 63 years from a radiocarbon date. The sea-level was somewhat lower than at PMSL at this location, with a maximum high tide point of 0.8 m and an average low point of − 2 m. The timing of these occurrences is still uncertain owing to the inability to date throughout this section due to COVID-19.

5.7.3 Transect One

Section One is Okains Bays newest and shortest section, extending from the present low tide zone to 100 m landward into the Okains Bay Camping Ground (Figure 5.12). The progradation of Okains Bay is between 2.4 and 3.9 m (Dingwall, 1966; Martin, 1969; Stephenson, 1992), indicating that this survey line is between 25 and 41 years old, allowing for analysis and data to be checked against historic tidal data from the Lyttelton tidal gauges, provided by NIWA's tide forecaster model (NIWA, 2021). These data are comparable to current high and low tide levels since they are located at similar locations. As shown in Figure 5.12, sea-level varies from 0 to 1.2 m for high tidal marks and from -1 to -2 for low tidal zones.

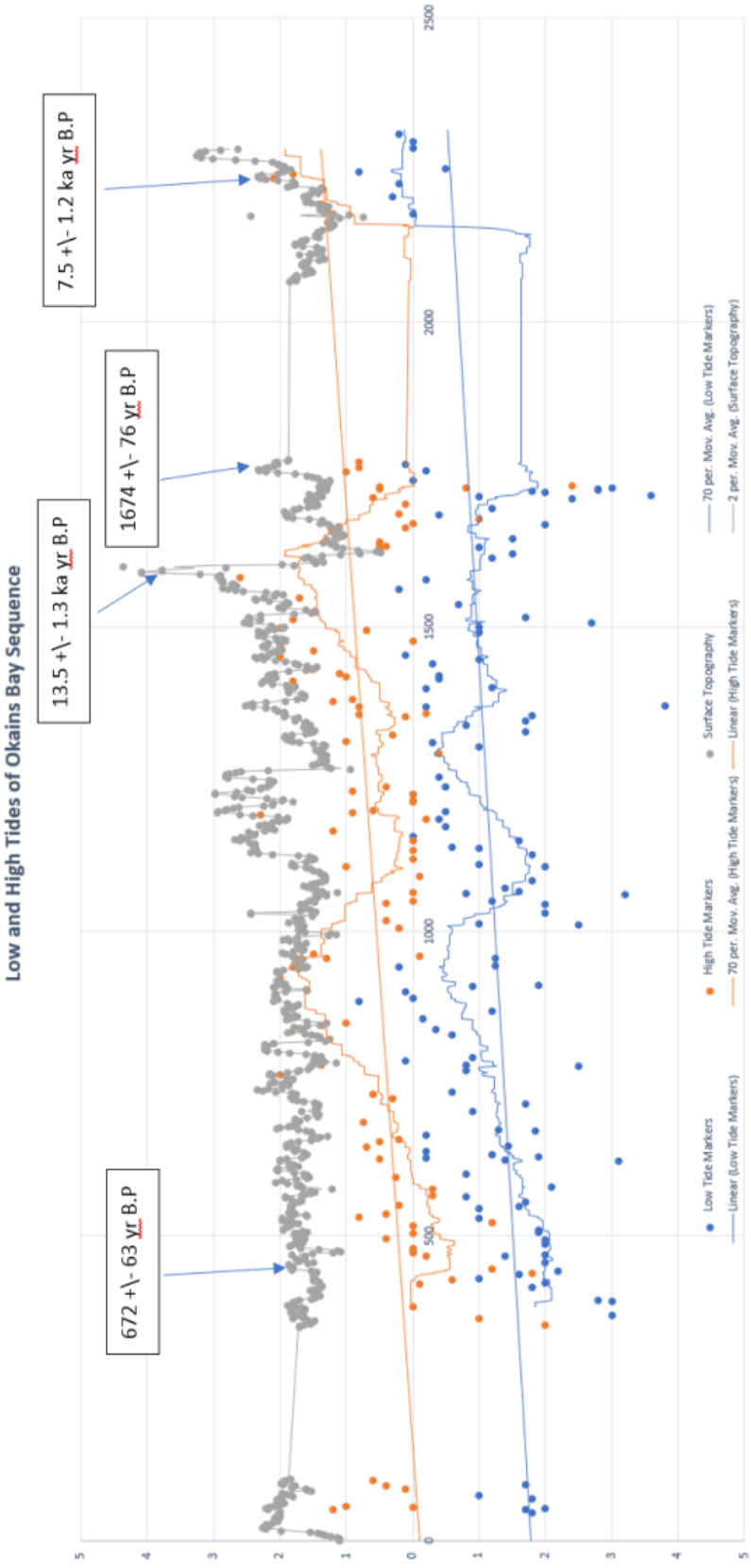


Figure 5.12. Image of the sea-level history using the downlapping and toplapping surfaces from GPR data collected in this research. Dates from Stephenson and Shulmeister (1999).

5.8 Summary

Chapter Five reported the results from GPR work achieved on Okains Bay, Canterbury which aimed to observe the key features within the subsurface, as well as provide evidence for producing a sea-level curve thus answering the first research question posed in Chapter One. In total, 19 GPR lines were produced throughout the three transects within Okains Bay, Canterbury. Downlapping and toplapping points within GPR imagery provided, revealed a sea-level curve, showing low tides and high tides between 7.5 ka and present day. The study by Stephenson and Shulmeister (1999) provided dates for this thesis that allows for further analysis. For the next chapter, Chapter Six provides a discussion on the implications of the findings. Specifically, evidence of geomorphic change using GPR imagery, and the sea-level curve provided in this chapter will be discussed in relation to the findings from Gibb (1986) and Clement et al. (2016).

Chapter Six: Discussion

6.1 Introduction

This thesis set out to provide further evidence of Holocene sea-level history for the Canterbury coastline using GPR methodology. The chosen site, Okains Bay, Canterbury provided the ideal opportunity to employ GPR methodology on a series of beach ridges and dune ridges to explore sea-level using the internal structure of beach ridge formation.

Chapter Five allowed for the analysis of GPR imagery on Okains Bay beach ridges and dune ridges, allowing for a sea-level history to be formed for Okains Bay and in turn, showing that Okains Bay held a fractured sea-level curve using GPR, with missing areas of the Okains Bay Village and the Forested area that is between the current beach face and the beginning of the farmlands.

Two research questions (Q2 and Q3 Chapter One) remain for this study concern the validity of the sea-level curve and the areas that were missed in relation to limitations, as well as providing insight into the slowing of progradation discussed within Stephenson and Shulmeister (1999). While discussing this missing gap due to a change in progradation, the geomorphological changes that occurred between 7.5 ka and present day will be discussed. Finally, using the sea-level curve provided within Chapter Five, discussion will revolve around the validity of this research sea-level curve in relation to sea-level curves produced for New Zealand by Gibb (1986) as well as regional sea-level curve provided by Clement et al. (2016).

6.2 Okains Bay sea-level history

The next section will explain if Okains Bay preserves a complete mid to late Holocene sea-level curve. Using the GPR and RTK data supplied in Chapter Five, a sequence of downlaps and toplaps were employed as limits to the high and low tides inside Okains Bay, allowing for the visualisation of historic sea-level data across the Holocene.

6.2.1 Toplapping and Downlapping surfaces

Tamura et al. (2008) and Nielsen and Clemmensen (2009) demonstrated the utilisation of downlapping surfaces inside the subsurface of beach ridges. These two publications showed that when downlapping surfaces are accurately gathered, these points may be used to determine the low tide points of sea-level. Clemmensen and Nielsen (2009) utilized downlapping points compared to tidal data on the coast Denmark for the previous 100 years. Such showed that the downlapping locations within their study corresponded to local tidal data recorded by tide gauges with 95% accuracy (Clemmensen and Nielsen, 2009). While doing so, Clemmensen and Nielsen (2009) demonstrated that Tamura et al. (2008) were accurate when they stated that downlapping surfaces may be employed with sea-level data. This thesis expands on the notion of employing downlapping surfaces, however, dating back 7500 years. This thesis presents a novel technique of interpreting toplapping surfaces as high tide indicators to deduce the sea- level curve along with downlapping surfaces as low tide indicators. Toplapping surfaces are the direct opposite of downlapping surfaces, where the overlying sediment cuts over previously deposited sediment therefore depicting the interface between high tide and aeolian wind-driven sediments, or topsoil deposited on the surface for farming. Okains Bay contains a significant succession of beach ridges dated back to the mid-Holocene (Stephenson and Shulmeister, 1999). Instead of only a maximum low point, restricting the sea-level between high and low points provides further information to enable an accurate picture of sea-level change over the Holocene. The accuracy of sea-level may be demonstrated in Section 5.7, where high and low tides for Okains Bay are at current day sea-level. This is critical because tidal disparities fluctuate over extended periods of time rather than being constant throughout history.

When using both toplaps and downlaps to present sea-level data on the same curve, it needs to be noted that the downlapping surfaces representing the low tide zones would inherit a lag time dependent on the angle of the current beach face throughout the Holocene. Present-day beach face at Okains Bay can be used as an excellent example of this, with the swash zone being approximately 50 m in length. This is because the angle of the present-day beach face is at a low angle, and a change in tides presents a large change in the present-day beach face. When taking this into account, an average tidal regime would be unknown, as the angles of the beaches would differ throughout time, similar to how the difference between high and low tides differ. Therefore, the sea-level curve presented within this thesis was only an estimate of high and low points of sea-level instead of an exact measurement.

6.2.2 Sea-level analysis

The highest peak of sea-level was attained at the oldest recorded date in the Okains Bay sequence, with an average height of 1.4m, limited by a high tide of 2.5 m and a low tide of 0.1 m. Low tides remained higher than at any other point in the series throughout the rest of the Okains Bay sequence. The 7500-year point from this study was consistent with earlier study done in New Zealand by Clement et al. (2016), who theorised that sea-level reached present-day sea-levels for the Canterbury coastline at 8000 years BP and a high stand at 7000 years BP. The toplap and downlap points from this location demonstrate that sea-level changed throughout the rest of the segment. This change in sea-level indicates that high and low tides were not consistent throughout the series, instead getting closer together at spots along the sequence, such as at 1250 m in Figure 5.12 and farther apart on either side of this segment. The cause of these changes is uncertain; however, it is conceivable that the beach had lower intensity waves throughout this period when sea-levels were closer together, resulting in a lower angled beachface.

Okains Bay sees a higher sea-level midway through the process of progradation due to variations in sea-level. Due to the increasing sea-level, sand progradation into Okains Bay was severely interrupted, and aeolian sands, rather than swash build sands, began to dominate the beach. As a result, a piece of the Okains Bay sea-level curve, also known as the dune ridge in Figure 6.1, indicates lost time. This missing period is critical when addressing sea-level since essential sea-level information is then lost. Since no dates were gathered on either side of this missing portion of progradation, it is uncertain of how long the Okains Bay coastline's progradation remained interrupted. According to Stephenson and Shulmeister (1999), this area is lacking around 4000 years of progradation, between 2000 and 6000 years BP, therefore 4000 years of missing sea-level variation. This idea was developed by utilising the 1674 date, which is further into the sequence and closer to the 7500 date than the oldest date of 674 years BP. The date of 1674 years BP, on the other hand, might be an indication of sea-level increase at point b in Figure 6.3. Because the estuary to the north was still there throughout this period of sea-level rise, hightides would have filled it, creating a region higher than the beach ridges that were deposited at an unknown time. This would explain the 1674 +\- 74 ^{14}C date. As a result, the missing gap in time is thought to be directly on the dune ridge sequence at position in Figure 6.2. As the water level began to decrease again, progradation onto the Okains Bay shoreline resumed, and the sea-level curve was restored afterward. The forested area and the municipality of Okains Bay are two more locations that are overlooked in this thesis. Sea-level predictions

can be established by looking at either side of the missing portions in order to connect high and low tides via these parts. Through the settlement of Okains Bay. On the landward side of Okains Bay village, sea-level is higher, with a low tide height of 0 m and a high tide height of 1.2 m. The sea-level is much lower on the seaward side of Okains Bay village, with peak tides 0.4 m above present-day sea-level and low tides -1.4 m below sea-level. Such implies that the water level progressively lowered across the Okains Bay community, syncing up the sites on each side. The forested area on the landward side of Okains Bay Camping Ground is the opposite of what may be observed in Okains Bay Village. The landward side is at a lower sea-level than the seaward side, and the increase low tide of 1.3 m and an increase in high tide of 1 m (Figure 5.12).

Okains Bay does, in reality, includes a large number of downlapping and toplapping points necessary to construct a sea-level curve for the Canterbury coastline. The sea-level curve for Okains Bay is however not intact throughout the Holocene period due to several missing gaps across the township and forested areas, as well as the possibility of a shift in sea-level regime owing to rising sea-levels affecting the sediment budget and therefore progradation. Stephenson and Shulmeister (1999) proposed that the sediment budget altered due to the shift in erosional forces that occurred on the South Canterbury cliff faces, which is one of the primary theories for the reasons of a change in sediment budget on Banks Peninsula, and hence Okains Bay. Using a fragmented sea-level curve only offers insight for sections of the sea-level curve, and more study, such as dating techniques around the wider dune ridge, will be required in order to restrict where a halt in progradation may have happened.

6.3 Holocene coastal evolution of Okains Bay

The coastline evolution and changes of geomorphology of Okains Bay throughout the Holocene time period is explored in this section. The total number of years that Okains Bay has been prograding since is around 8 ka (Stephenson and Shulmeister, 1999). Due to the shift in sea-level over this time, the rates of progradation have varied dramatically. Understanding the changes in geomorphology of the Okains Bay shoreline is not possible through dates as there are only three dates utilised in this thesis; instead, it can only be done by using what is visible within the data supplied by GPR to make sense of the dates. Between 6000 and 2000 years ago, there was a disturbance in progradation inside Okains Bay, according to Stephenson

and Shulmeister, (1999) and such could have been caused by either a higher or lower sea-level. The formation of coastlines within a bay region is directly impacted by bay morphology, such as narrower portions of the bay providing varying levels of erosion and deposition than larger locations.

Okains Bay is a 3.2-kilometer-long intricate system composed of dune ridges and beaches. GPR was utilised to survey 2.3 km of the 3.2 km. As a result, Okains Bay was determined to have a broken sea-level curve, with an unknown duration of missing time occurring midway through the series (Figure 6.1). Okains Bay appears to have had a semi-continuous amount of progradation from 7500 years ago. As a result of this progradation, many beach ridges formed until the sea-level began to rise by approximately 1.8 m, progradation either slowed or halted for an unknown amount of time and aeolian sands began to dominate the coastline, generating a large dune crest in comparison to the adjacent beach ridges. After the unknown period of slowed progradation, sea-levels began to lower again, and progradation continued throughout the rest of the bay until reaching where the present-day beach face is currently.

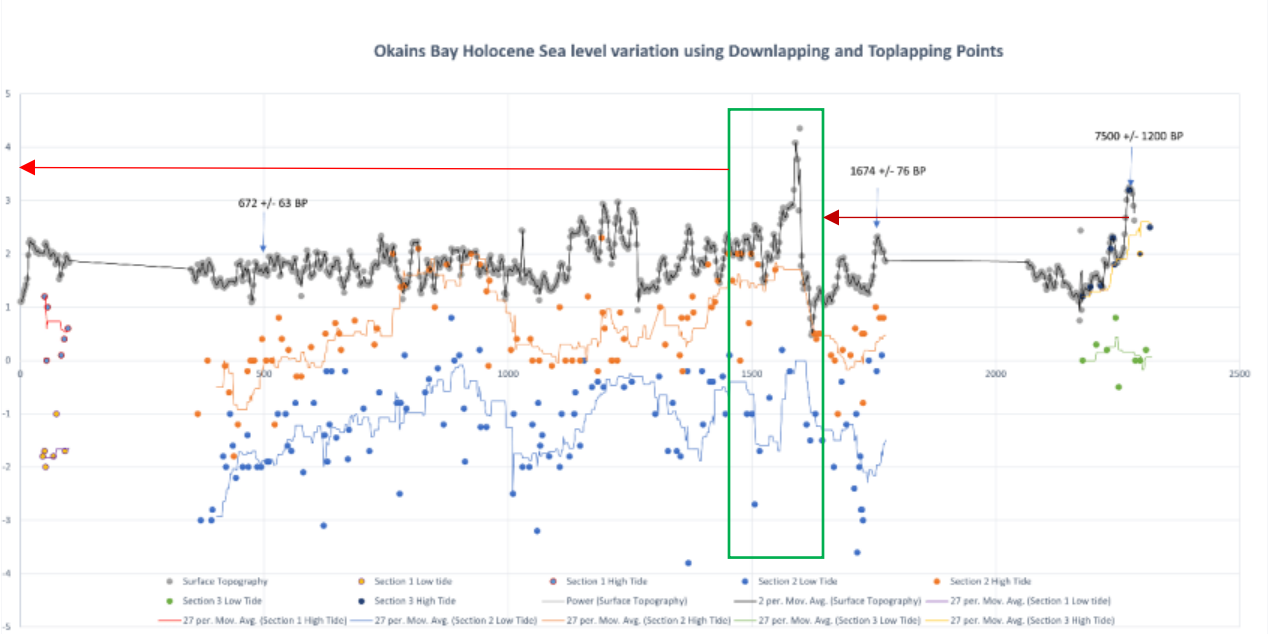


Figure 6.1. schematic of Okains Bay sea-level history. The red arrows represent consistent amounts of progradation. The green box represents the area of unknown time due to a rising sea-level and progradation only occurred through the building of dune ridges.

According to Stephenson and Shulmeister (1999), a dramatic slow in progradation that occurred at point B in Figure 6.3 was caused by a difference in sediment supply from coastal erosion in coastal South Canterbury, as well as alterations and development in the banner bank directly offshore of Okains Bay. Using GPR to map toplaps and downlaps (Figure 5.12), it is possible to observe that there were multiple occurrences of sea-level rise and decline from the mid to late Holocene. Figure 6.1 and Figure 6.2 depicts the effects of this alteration on Okains Bay, where sea-level at point A was significantly higher than at point B. Because point A has a higher sea-level than point B, flooding of the point B region was more likely to happen when high tides occur, which is made possible by the estuary and Opara stream to the north of the beach and dune ridge sequence. As the tides rose and filled the region at point B (Figure 6.3), sea levels generated an area of deposition, most likely of very low energy since it was not impacted by the wave environment and was shielded by the dune ridge before point B.

Evidence of this sediment fill at point B can be seen within Figures 5.8, 5.9 and 6.3, where the stratigraphic lines within the GPR work are very close to horizonal (Figure 5.8 and Figure 5.9), which is evident of settling lag ridges, rather than swash-built ridges. This could explain why the date is 1674 years BP at point B in Figure 6.3 and why the shoreline was at point A about 1674 years instead of where the date was discovered through Stephenson and Shulmeister (1999). Such a similar impact may also be observed in Figure 6.2, where the estuary is undermining the current beach system. When sea-levels rise, lower topographic are threatened with a rising sea-level.

The missing time gap of sea-level still holds true to the area depicted in Figure 6.1, since the high tide sea-level curve produces a big leap in a small amount of space when looking at the sea-level curve created for Okains Bay (Figure 5.12 and Figure 6.1). The chronology of occurrence of the missing time gap on the left side of point B (Figure 6.3) is however unclear, future research around this critical point in Okains Bay will be needed to be done in order to understand sea-level throughout the Holocene at Okains Bay.

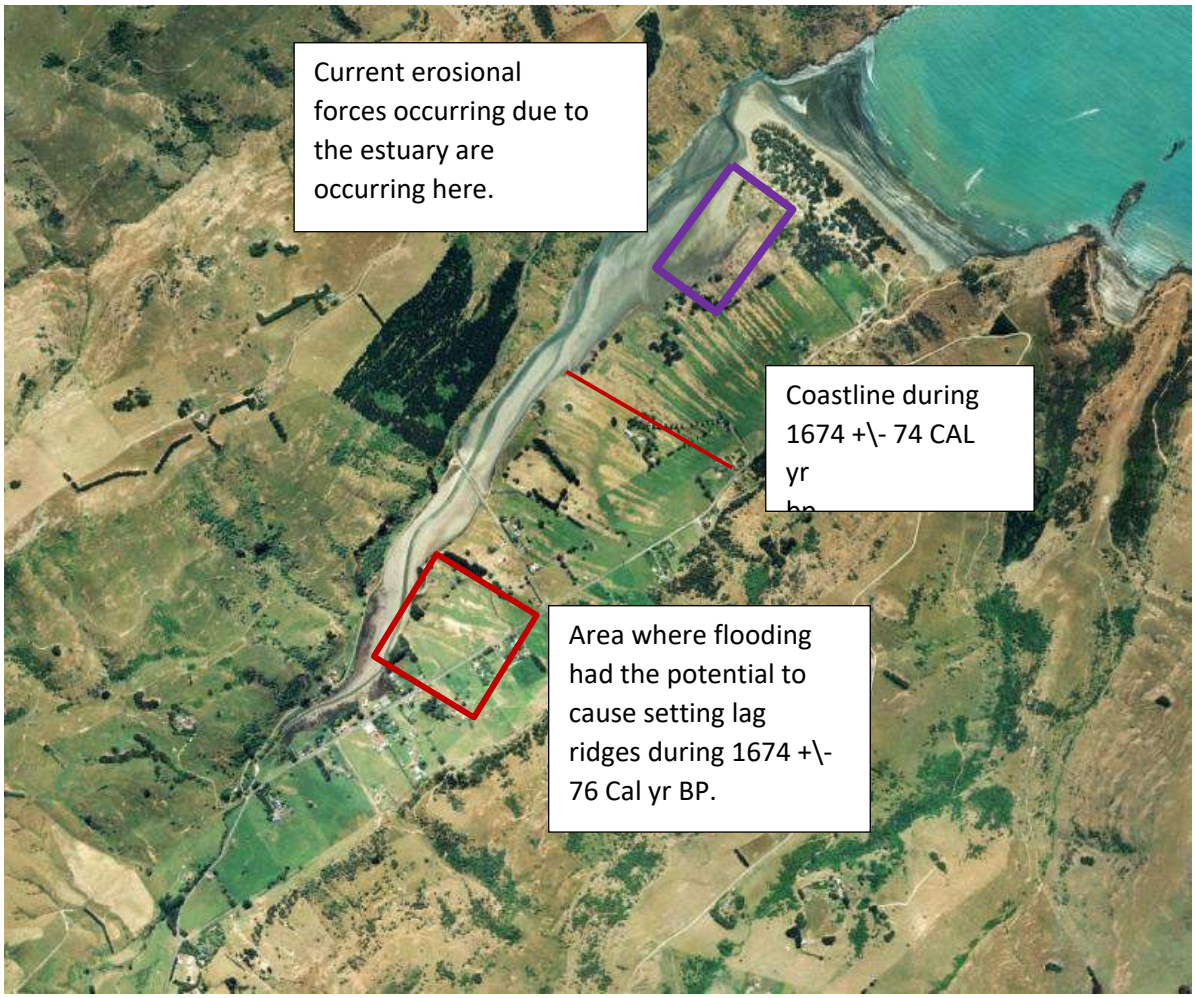


Figure 6.2. Aerial photograph of Okains Bay showing the area where a higher sea-level had the potential to flood during 1674 date, as well as where the coastline would have been 1674 years ago (date from Stephenson and Shulmeister, 1999).

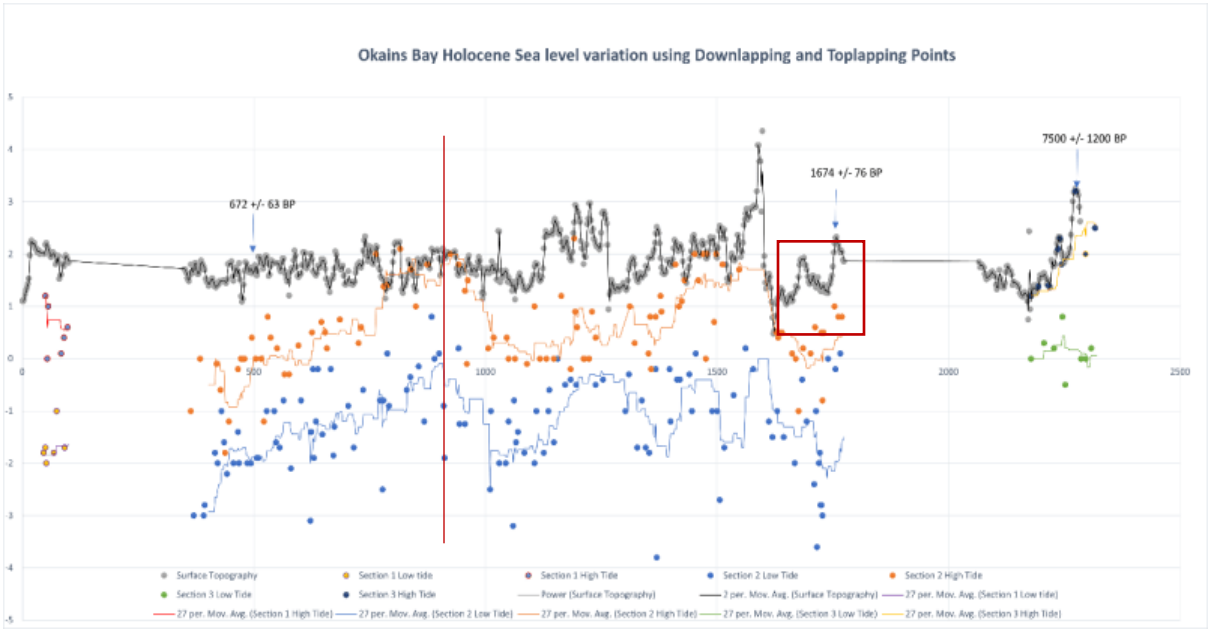


Figure 6.3. Showing the sea-level curve. The red line represents point A and the red square represents point B.

An increase in sea-level was observed along the Canterbury coastline at point A on Figure 6.3. This influence on sea-level rise would affect not just the coasts, but also the offshore locations where sediment is accumulated and subsequently carried onto Okains Bay, such as the banner bank.

With the rise in sea-level, the banner bank would have been further from the sea's surface, and therefore the wave energy may have been reduced or insufficient to suspend the sediment. This mechanism would have a direct impact on sediment movement along coasts, resulting in a slower rate of sediment deposition in Okains Bay and the surrounding bays of Banks Peninsula. This mechanism would have a direct impact on sediment movement along coasts, resulting in a slower rate of sediment deposition in Okains Bay. In doing so, aeolian sands would have been the main supply to Okains Bay, where a dune ridge sequence resides. To recommence sediment transfer, either sand deposition on the banner bank would have had to catch up to where sea-level is at a point where it could occur, greater energy waves had to occur to suspend sediment into the ocean, or sea-level had to drop to a point where the wave climate could affect the banner bank again. The transition between dune ridges and beach ridges is difficult to be seen, as within Figure 6.2 and 6.3, the prograding sands have overlayed on top of aeolian sands, creating a much higher sequence of dune ridges than seen anywhere else in Okains Bay. As shown in Figure from Figures 5.7 and 5.11, there are two primary places within Okains Bay

that have been dominated by dune ridges over beach ridges, both occurring at a greater sea-level than when beach ridges were created. The lag effect of sediment reaching the beach is more pronounced on dune ridge B and less pronounced on dune ridge A (Figure 6.3). Stephenson and Shulmeister (1999) proposed that the growth and development of the banner bank near the mouth of Okains Bay had a direct influence on the progradation of the Okains Bay shoreline. There was, however, insufficient evidence of sea-level change to support this notion during the time of Stephenson and Shulmeister (1999) publication. Using evidence supported by this thesis, it can be stated that this was the most likely cause of the change in progradation records of sands onto Okains Bay throughout the Holocene.

6.3.1 Future changes of coastal evolution at Okains Bay

The processes of progradation of sands onto Okains Bay, the equilibrium between progradation and the shape of Okains Bay, and the anthropogenic alterations within this area are drivers of potential future changes in Okains Bay's shoreline development. The first step could be a change in sea-level, which would impact the amount of sand that is prograded onto the Okains Bay shoreline, as discussed in the preceding section. The processes of progradation onto Okains Bay appear to thrive at a constant, dropping sea-level or a modest increase in sea-level, and have done so since the last dune ridge series. The coastline's equilibrium is the second mechanism that influences the quantity of progradation that happens. If Okains Bay continues to prograde, it will begin to open up due to the shape of the bay. This increase in breadth would need a significant increase in sediment delivery onto the shore. Furthermore, when the coastline approaches the opening of Okains Bay, the beach face will be subjected to greater intensity waves that may not been dispersed from the shallow entry. In most circumstances, prograding coasts achieve an equilibrium limit when deposition and erosional processes equalise and the beach face remains stationary. The final process that will have a significant impact on Okains Bay is the anthropogenic alterations currently happening. The Christchurch City Council is now planting pingau grass along the latest beach ridge to function as a sand trap for the shoreline. Planting grasses in this location will have a direct impact on the amount of aeolian sediment stored, resulting in a greater dune ridge. As the grasses continue to vegetate, they will spread to adjacent beach ridges, altering the geomorphology and character of Okains Bay and resulting in a mix of aeolian and swash zone deposition sands on the existing shoreline.

6.3.2 Historic storm events on Okains Bay

Storm events can have direct erosional impacts on Beach ridges as they are low-lying formations that are easily destroyed by larger storm waves. Large storm events impacting Okains Bay are extremely unusual due to the bay's direction to the north - northeast, protecting it from large storm waves coming from the south, which is the dominant direction for storm fronts to reach the Canterbury region. North – north-eastern storm occurrences are often created in New Zealand through tropical cyclone processes (Kirk, 1979). These storms are often strong in the northern North Island and dissipate before reaching the northern parts of the South Island (Adam et al., 2020).

Tsunamis may strike Okains Bay from the north-eastern direction (Kain et al., 2014; Goff et al., 2008; Donnelly et al., 2017). However, based on historical data, many of the tsunamis that reach New Zealand's east coast are caused by massive earthquakes on the continents of North and South America's west coasts. A substantive body of literatures (e.g. Kain et al., 2014; Goff et al., 2008; Donnelly et al., 2017) shows that tsunamis do arrive onto the east coast of New Zealand, however evidence suggests through GPR imagery that these tsunamis have dissipated to less energetic waves. As such, large storm events are extremely unlikely to have produced the erosion of 4000 years of beach ridges inside Okains Bay. When studying the progradational record of Okains Bay, Stephenson and Shulmeister (1999) came to the same conclusion, indicating that erosional documented within Holocene sedimentary strata is often inconclusive. Truncation surfaces, lag deposits, and bigger foredune ridges produced right after the storm events are not seen within the GPR data produced in this thesis, therefore not affecting the progradational record of Okains Bay.

Alternatively, it is thought that a number of different processes all influenced the geomorphology and change that occurred on Okains Bay throughout the Holocene, specifically the rising of sea-level and the effects that sea-level rise would have on sediment supply from the banner bank just offshore of Okains Bay. These occurrences would have explained why there were several transitions between beach ridge formations and dune ridge formations inside Okains Bay. This section explored the changes in geomorphology, which contributed to revealing past coastal environments which aids in explaining why there was a gap within the progradational record at point B in Okains Bay.

6.4 Comparing Okains Bay sea-level history to Gibb (1986) and Clement et al. (2016)

Using the dating methods provided by Stephenson and Shulmeister (1999), the GPR and RTK methods used in this thesis, and discussion on geomorphological change over the Holocene in Okains Bay, it can be assumed that the sea-level trendline in this thesis closely follows what is seen in Clement et al. (2016), but at a much lower level (See Figure 5.12). The findings from both Gibb (1986) and Clement et al. (2016) follow a pattern of two higher sites after 7 ka when sea-level increased over current levels, and one lower point between these two areas where sea-level dipped marginally below current levels. Gibb's (1986) findings, however, did not align with Clement et al. (2016) due to the demonstrated stability of sea-level from 6 ka to the present.

6.4.1 Comparing to Gibb (1986) national sea-level curve

This section compares the sea-level curve obtained from this study to the sea-level curve constructed by Gibb (1986). The majority of dates used by Gibb (1986) ranged from 9ka to 7.5ka, with only six dates occurring after 6.2ka, when Gibb (1986) argued that sea-level is steady. These dates presented a difficulty for Gibb's to offer a reasonable estimate of sea-level following the end of the Holocene high stand, which is thought to have occurred at approximately 6.2 ka (Figure 6.4).

Gibb (1986) proposed that sea-level declined to below present-day sea-level after the highstand, which reached a maximum of 2 m. The results are substantially different, not just in terms of sea-level heights and highstand times, but also in terms of the trendlines seen within the sea-level curves (Figure). Interpretative comparisons between Gibb's (1986) and this study's sea-level curve starts from 7.5 ka due to unobtained/obtainable data prior to 7.5 ka. At 7.5 ka Okains Bay (Figure 5.12), sea-level was between 0.2 m and 1.8 m, which is 6 m higher than Gibb proposed sea-level in his study. Sea-level dropped from where it was at 7.5 ka in this study from an average of 1m to below present day sea-level, with an average height of -0.5 m. Evidence of this drop in sea-level have not been seen in studies such as Clement et al. (2016). The sea-level then fluctuated, rising to 1 m, lowering to 0 m, and then rising again to an average of 0.8 m, before declining to where it presently. Such change in sea-level is not seen in Gibb (1986), owing to a lack of evidence of shell pieces.

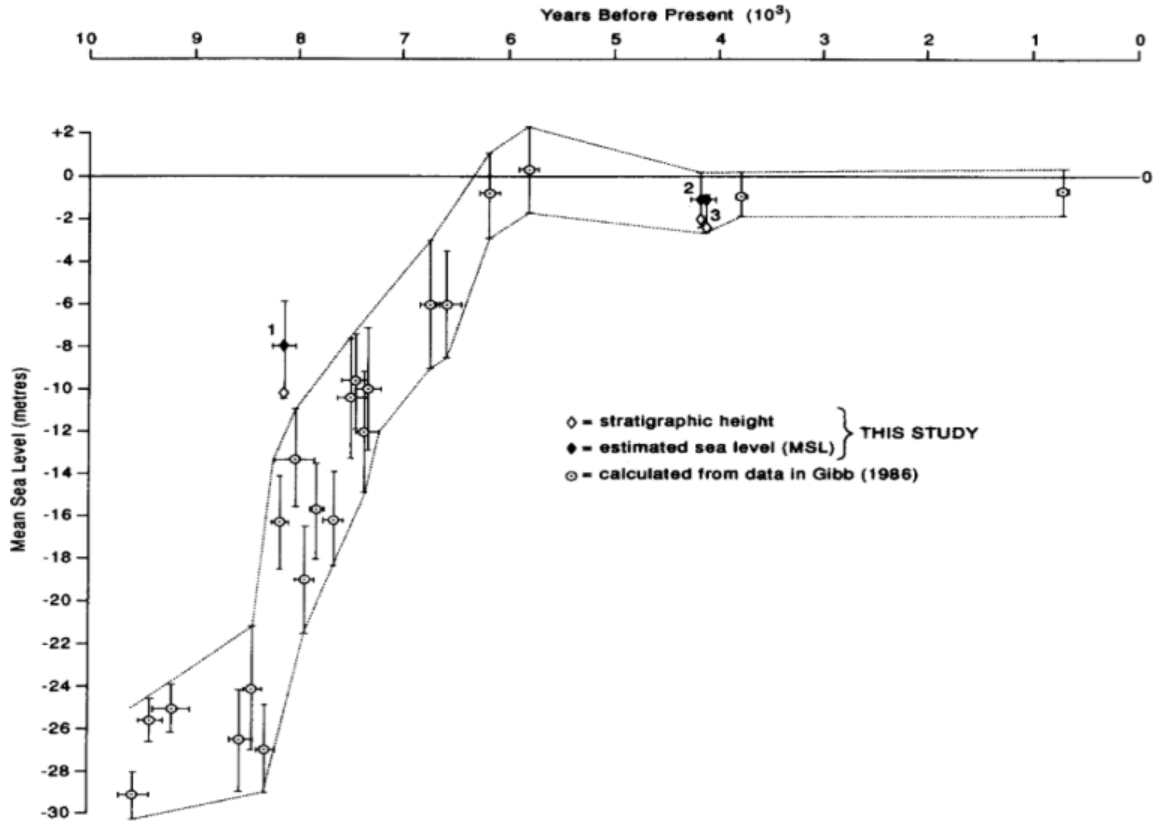


Figure 6.4. Sea-level curve produced by Gibb (1986) further dates and heights added by Shulmeister and Kirk, 1993).

While the sea-level curve in this thesis is difficult to understand due to the absence of dating methodologies utilised in the study from Covid – 19 restrictions, the trend line of the sea-level curve, regardless of the dates, is substantially different from Gibb's findings. The disparity between this study to Gibb (1986) with the changes made from Kirk and Shulmeitser (1993) research in terms of the stability of sea-level is apparent due to the differences in methodologies used. Both Gibb (1986) and Kirk and Shulmeister (1993) used ^{14}C dating techniques to find out where sea-level was in the Holocene. In doing so, shell fragments are needed to be identified which will give a range of where these shell organisms lived during the Holocene. The findings from this thesis are believed to be more accurate compared to Gibb (1986) because downlapping points have been shown to produce exact points instead of a range for low tide indicators by Nielsen and Clemmensen (2009) who used a similar methodology as this research project. The interpretation for high tide points formed by toplapping stratigraphy has received limited research however still shows considerable validity (e.g Engels and Roberts, 2005).

6.4.2 Comparison of Okains Bay sea-level history to Clement et al. (2016) Canterbury Holocene sea-level curve

Clement et al. (2016) created a sea-level curve for the Canterbury coastline that differed greatly from Gibb (1986) by using dates from five separate publications totaling 31 dates. Clement et al. (2016)'s comments on Gibb's work are summarised in Chapter Two:

1) No Holocene sea-level highstand was observed at 8ka.

2) No occurrence of regional variation in sea-level change across New Zealand.

3) Lack of supporting explanation for differences and contrasting assumptions for differences between Gibb's 1983 and 1986 studies.

4) The unorthodox dating techniques utilized.

The sea-level curve provided by Clement et al. (2016) reached present-day sea-level on the Canterbury shoreline at 8 ka, 1800 years before Gibb's study. Clement et al. (2016) proposed that sea-level continued to rise from 8 ka to 2 m above present-day sea-level at 7ka, before reaching a halt for 2000 years. After these 2000 years, sea-level increased slightly again, by around 0.5 m between 5000 and 4000 years ago. Following then, the sea-level progressively lowered to where it is now

Compared to the sea-level curve in this thesis, the curbed obtained from Clement et al. (2016) demonstrates similar timing of events at the beginning with a higher sea-level at 7.5 ka as well as a greater sea-level than the current sea-level. The gap between the two sea-level curves is the number of data points available to comprehend the sea-level between now and 7.5 ka. There is a total of 12 data points between 7.5 ka and present-day in Clement et al. (2016), but all data points acquired in this research project are situated between the studied dates of 7.5 ka to present day. Apart from few maximum indicator shells, Clement et al. (2016) do not exhibit a minimum and maximum sea-level curve (Figure 2.4). It is feasible that if Clement et al. (2016) used a maximum and minimum sea-level curve then it would follow closer to the trend seen within this thesis. Such would allow a more thorough sea-level curve, which Clement et al. (2016) and Gibb (1986) as updated by Shulmeister and Kirk (1993) do not have. Clement et al. (2016) Canterbury sea-level curve does not exhibit the fluctuation observed in the sea-level curve illustrated within this research project, however, there are times in the Okains Bay sea- level curve may have comparable timings of sea-level increase to those shown in Clement et al. (2016). The sea-level curve from Clement et al. (2016) likewise

indicates a greater sea-level than Gibb's (1986) study, with the majority of his high sea-level indicators being higher with the sea-level curve being above PMSL. The average sea-level curve obtained within this research is lower to what was suggested by Clement et al. (2016), with only two points on this study's sea-level curve surpassing 2 m during instances of high tide. There is a complexity and difficulty to provide an exact comparison of this thesis' sea-level curve to the findings by Clement et al. (2016) due to the inability of employing dating techniques due to limited research funds and Covid-19 restrictions. The comparison among the trends of the sea-level curves obtained from Gibb (1986), Clement et al. (2016) and this study is possible, with the latter illustrating a sea-level trend that contains specific similarities to both literature.

Specifically, this research shows a similarity to Gibb's sea-level curve which is demonstrated by sea-level indicators reaching an average of ~ 0 m, as seen in Figure 5.12. Meanwhile, several sea-level markers found in this research are above 0 m, thus aligning with what was observed in Clement et al. (2016).

Parts of this research that is not seen in neither Gibb (1986) nor Clement et al. (2016) is when mean sea-level goes below 0 m (Figure 5.12). However, due to the lower points seen within Figure 2.4 of Clement et al. (2016) for Canterbury, it is possible that these areas of lower sea-level were possible and therefore linking my sea-level curve closer to Clement et al. (2016).

Different methodologies between Gibb (1986) and Clement et al. (2016) could be a main factor as to why this thesis has produced differing results. Both Gibb (1986) and Clement et al. (2016) used ^{14}C dating in order to gather an understanding of what occurred during the Holocene in regard to sea-level variation whereas this research project looked into the exact heights of sea-level changes using both downlaps for lowtide indicators and toplaps for high tide indicators though GPR.

6.5 Future Research

Future work on Okains Bay can be driven by opportunities for additional GPR work. GPR can be employed onto prograding coastlines around New Zealand that have a series of swash-built ridges. Calibration of GPR will need to be done dependent on grain size, attenuation, type of grains and is dependent on how much water is within the subsurface. Beach ridges are known to also form on mixed sand and gravel beaches so therefore allowing for further beach ridges to be viable for GPR work. GPR needs to be coupled with some type of dating technique to provide answers to when changes in sea-level occurred rather than only what happened. This was a crucial point within this research project as lack of dates did not allow for precise timings of certain events, especially when looking into where progradation slowed seen in Figures 6.1, and 6.3. Using GPR allows for a different approach compared to strictly using radiocarbon dating methods to understand sea-level, such as Clement et al. (2016). This thesis shows that using GPR achieves different results, providing a more accurate image of localised sea-level variation on the Canterbury coastline.

Future work can stem from the questions discussed within this thesis. In order to understand the progradational and sea-level record over the Holocene for Okains Bay. More dating evidence will be needed to be used to gather further insight into the coastal evolution of Okains Bay. Using the data gathered from GPR in this study, the use of dating techniques needs to be done at Point B in Figure 6.3. This will allow for an understand how long progradation slowed or halted during this time. Further dates should be taken at Point A to compare to Point B to see if these were in fact settling lag ridges that formed behind the dune ridge during a time of higher sea-levels. In doing so, future work should be achieved on the Banner bank, outside the mouth of Okains Bay. Further understanding of where this sediment comes from as well as the movement of sediments off the banner bank and onto the canterbury coastlines would allow for better understands of geomorphological change. Models for the banner bank to see how it is affected by a change in sea-level height will also aid in answering the progradational record of Okains Bay.

Future research should be achieved on the surrounding bay on Banks Peninsula, especially Le Bons Bay, which has the potential to hold a similar sea-level history at Okains Bay. Le Bons Bay is 5.3 km south of Okains Bay and faces an eastern direction rather than the northeast of Okains Bay. Prograding beaches also form Le Bons Bay and is much larger in area than Okains Bay, reaching 2-4 m in height in some places. The height of these ridges,

however, suggests that there has been much more aeolian sediment accumulation than what is/has been observed in Okains Bay, which could cause complications such as not being able to distinguish the swash build and aeolian build sand contact. Being able to look at the sequence of beach ridges at Le Bons Bay would deduce the timing and the processes of sediment movement around Banks Peninsula, as well as further insight into the changes of sea-level during the Holocene, not only on Banks Peninsula, but also contributing to observing changes within the wider Canterbury coastline region.

Different methodology at Okains Bay would also be able to aid in understanding sea-level variation and sand movement. Using LiDAR would provide Okains Bay with high resolution analysis of the changes in spacing between ridges, and the morphology of the ridges. In doing LiDAR, the spacing between the ridges would allow for further understanding of coastline change, as well as being able to understand the structure of historic coastlines.

Chapter Seven: Conclusion

This thesis aimed to answer three primary questions through using GPR methodology at Okains Bay, New Zealand. These questions were:

1. Does Okains Bay hold a preserved and intact sea-level curve for the Canterbury coastline line and what does this sea-level curve look like?
2. What are the changes in coastal evolution that have occurred with a changing sea-level over the Holocene at Okains Bay?
3. Does the sea-level curve at Okains Bay fit more to Gibb (1986) or Clement et al. (2016)?

Question One showed that GPR produced a fragmented sea-level history for Okains Bay, Canterbury, New Zealand. The research was achieved using GPR methodology, looking into the subsurface of beach ridges. This thesis adds to the New Zealand Holocene sea-level history by employing a methodology that has not been used as much as radiocarbon dating techniques. The images provided by GPR allowed for the investigation of downlapping and toplapping surfaces within the subsurface which represent low tide and high tide markers, respectively. However, lack of dating techniques did not allow any strong conclusions to be provided to exact timings of events.

Question two showed that GPR imagery was able to produce some theories on previous geomorphic events that occurred within Okains Bay, New Zealand. Prior research from Stephenson and Shulmeister (1999) showed that beach ridge progradation had been occurring since 7.5 ka, with a gap in progradation occurring between 6000-2000 years. However, this research project suggests that the timing of these events may be at a different through the evidence that sea-level was higher at Point A than Point B in Figure 6.3. Potential for flooding of point B could have occurred through the Opara Stream on the northern side of Okains Bay. Despite the findings affirming a different rate of progradation compared to Stephenson and Shulmeister (1999), these rates of progradation remained inconclusive and unknown. Further research would be needed to uncover further information.

Question Three aimed to answer if this thesis could help aid in understanding current and previous theories by Gibb (1986) and Clement et al. (2016) on how sea-level varied through the mid to late Holocene. Through this research topic, it is shown (Figure 5.11) that the sea-level curve produced within this thesis differs from both Gibb (1986) and Clement et al. (2016). However, sea levels were higher than Gibb (1986) suggested at 7.5 ka, similar to what is shown in Clement et al, (2016).

Clement et al. (2016) emphasized a need for further research to be achieved on the Canterbury coastline in order to aid in New Zealand's sea-level history over the Holocene, although Clement et al. (2016) did not suggest to use GPR, it has been shown by Tamura (2008) and Nielsen and Clemmensen (2009) to be a valid methodology to use when collecting data for historic sea-level research. Clement et al. (2016) research gathered a large amount of data on sea-level in New Zealand through the process of compiling all ^{14}C over the past 30 years of Holocene sea-level research, producing findings that resulting in a different curve seen from this research project.

GPRs validation was achieved for Okains Bay through Jol (Pers.comms) who presented data of 100 MHz and 200 MHz 100 m transects. Calibration of GPR was achieved using data presented within Jols work and used throughout Okains Bay. Similar studies, such as Tamura (2008) and Nielsen and Clemmensen (2009) both used downlapping surfaces to provide sea-level data for their respective locations. GPR imagery for Okains Bay presented high quality data using a mid-common point survey over 2.3 km. GPR then produced the basis for examining downlapping and toplapping surfaces within the subsurface that in turn provided an in-depth sea-level history from 7.5 ka till present day. GPR does not produce an ideal sea-level curve by itself, and therefore shows a critical need to gain further dates at the large dune ridge seen in 6.1.

7.1 Key Findings

A number of key findings have emerged from this research project, which are as follows:

- The sea-level curve presented for this thesis is fragmented, with gaps in progradation occurring and therefore producing areas of missing time. As such, Okains Bay does not hold an intact sea-level curve, with an unknown amount of missing time occurring as seen discussed in section 6.2 and 6.3.
- Progradational changes that occurred throughout the sequence have been highlighted, theories attempting to understand the causes of these progradational changes have been thought to be due to a change in sea-level height, therefore affecting the suspension of sediment off the Banner bank, outside of the Mouth of Okains Bay.
- The sea-level curve presented in this thesis provides insight into the last 7.5 ka, in doing so, the trend of this thesis' sea-level curve can represent both Clement et al. (2016) and Gibb's (1986) with some areas showing that average sea-level height was at 0 m during the Holocene, similar to Gibb's (1986) whereas other parts of the sea-level curve being above present-day sea-level, similar to what is shown in Clement et al. (2016). Sea levels at 7.5 ka within this research project are shown to be higher than present-day sea- level, which means that PMSL was attained before 7.5 ka, as seen in Clements et al. (2016) and not Gibb (1986).
- GPR revealed past coastal environments at Okains Bay, showing swash – built ridges, aeolian dunes and settling lag ridges. Only minor amounts of erosional processes were seen within the GPR imagery, therefore showing that large storm events have not affected progradation throughout the Holocene on Okains Bay.
- Certain areas of Okains Bay were not able to be surveyed, such as the Okains Bay Village between transect 3 and 2 (Figure 4.2) and the forested section between transect one and transect two (Figure 4.2). Further research will need to be achieved within these sections in order to gather a more complete sea-level curve for Okains Bay and the Canterbury coastline.
- GPR does provide an in-depth look into the subsurface and does provide accurate data that can be used for historic sea-level research.

7.2 Implications of Findings

The key results of this study relating to both GPR methodology have practical outcomes for future management on the Canterbury coastline, although consideration of GPR limitations need to be addressed. Such methodology can be used in order to aid in management schemes as looking into the past events of sea-level can help academics predict what may occur within the future. Given future GPR studies on prograding coastal regions, GPR can produce reliable readings and a different methodology to the commonly used ^{14}C dating methods to observe sea-level curves, however GPR should be used in conjunction with other dating methods to provide accuracy for sea-level curves. Findings within this study have lent credibility towards past sea-level studies. validity of this thesis has been shown by previously cited work that have shown that GPR works on coastlines, both by investigating geomorphological change as well as sea-level change.

Reference list

Adam, R.J., Hilton, M.J., Jowett, T. and Stephenson, W.J. (2020). The magnitude and frequency of storm surge in southern New Zealand. *New Zealand Journal of Marine and Freshwater Research*, pp.1–16.

Anderson, J.B., Shipp, S.S., Lowe, A.L., Wellner, J.S. and Mosola, A.B. (2002). The Antarctic Ice Sheet during the Last Glacial Maximum and its subsequent retreat history: a review. *Quaternary Science Reviews*, 21(1-3), pp.49–70.

Andrews, J.T. and Peltier, W.R. (1976). Collapse of the Hudson Bay ice center and glacio-isostatic rebound. *Geology*, 4(2), p.73.

Annan, A.P. (2002). GPR - History, Trends, and Future Developments. *Subsurface Sensing Technologies and Applications*, 3, pp.253–270.

Baker, R.G.V., Haworth, R.J. and Flood, P.G. (2001). Inter-tidal fixed indicators of former Holocene sea levels in Australia: a summary of sites and a review of methods and models. *Quaternary International*, 83-85, pp.257–273.

Barber, D.C., Dyke, A., Hillaire-Marcel, C., Jennings, A.E., Andrews, J.T., Kerwin, M.W., Bilodeau, G., McNeely, R., Southon, J., Morehead, M.D. and Gagnon, J.-M. . (1999). Forcing of the cold event of 8,200 years ago by catastrophic drainage of Laurentide lakes. *Nature*, 400(6742), pp.344–348.

Bard, E., Hamelin, B., Arnold, M., Montaggioni, L., Cabioch, G., Faure, G. and Rougerie, F. (1996). Deglacial sea-level record from Tahiti corals and the timing of global meltwater discharge. *Nature*, 382(6588), pp.241–244.

Bard, E., Hamelin, B. and Delanghe-Sabatier, D. (2010). Deglacial Meltwater Pulse 1B and Younger Dryas Sea Levels Revisited with Boreholes at Tahiti. *Science*, 327(5970), pp.1235–1237.

Berger, A. (1988). Milankovitch Theory and climate. *Reviews of Geophysics*, 26(4), pp.624–657.

Bird, E.C.F. (1960). The formation of sand beach ridges. *Australian Journal of Science*, 22, pp.349–350.

Blanchon, P. and Shaw, J. (1995). Reef drowning during the last deglaciation: Evidence for catastrophic sea-level rise and ice-sheet collapse. *Geology*, 23(1), p.4.

Brown, A.F. (1976). *Beach and nearshore dynamics, Pegasus Bay*. Unpublished MA thesis.

Brown, L.J. (1995). Holocene shoreline depositional processes at Poverty Bay, a tectonically active area, northeastern North Island, New Zealand. *Quaternary International*, 26, pp.21–33.

Buis, A. (2020). *Milankovitch (Orbital) Cycles and Their Role in Earth's Climate*. [online] Climate Change: Vital Signs of the Planet. Available at: https://climate.nasa.gov/news/2948/milankovitch-orbital-cycles-and-their-role-in-earths-climate/ [Accessed 16 Feb. 2022].

Carlson, P.R., Karl, H.A. and Edwards, B.D. (1991). Mass sediment failure and transport features revealed by acoustic techniques, Beringian margin, Bering Sea, Alaska. *Marine Geotechnology*, 10(1-2), pp.33–51.

Carter, L. and Herzer, R.H. (1979). The hydraulic regime and its potential to transport sediment on the Canterbury continental shelf. *New Zealand Oceanographic Institute Memoir 8*, p.33.

Clague, J.J. and James, T.S. (2002). History and isostatic effects of the last ice sheet in southern British Columbia. *Quaternary Science Reviews*, 21(1), pp.71–87.

Clarke, G.K.C., Leverington, D.W., Teller, J.T. and Dyke, A.S. (2004). Paleohydraulics ofthe last outburst flood from glacial Lake Agassiz and the 8200BP cold event. *Quaternary Science Reviews*, 23(3-4), pp.389–407.

Clement, A. (2011). *Holocene sea-level change in the New Zealand archipelago and the geomorphic evolution of a holocene coastal plain incised-valley system : the lower Manawatu valley, North Island, New Zealand*. [Unpublished PhD] Available at: https://mro.massey.ac.nz/handle/10179/2678.

Clement, A.J.H., Whitehouse, P.L. and Sloss, C.R. (2016). An examination of spatial variability in the timing and magnitude of Holocene relative sea-level changes in the New Zealand archipelago. *Quaternary Science Reviews*, 131(Part A), pp.73–101. doi:10.1016/j.quascirev.2015.09.025.

Clemmensen, L.B. and Nielsen, L. (2010). Internal architecture of a raised beach ridge system (Anholt, Denmark) resolved by ground-penetrating radar investigations. *Sedimentary Geology*, 223(3-4), pp.281–290. doi:10.1016/j.sedgeo.2009.11.014.

Daniels, D.J. (2004). *'Ground penetrating radar'*. 2nd ed. London, UK: The Institution of Electrical Engineers.

Davies, J.L. (1957). The importance of cut and fill in the development of sand beach ridges. *Australian Journal of Science*, 20, pp.105–111.

DAVIS, J.L. and ANNAN, A.P. (1989). Ground-penetrating radar for high-resolution mapping of soil and rock stratigraphy. *Geophysical Prospecting*, 37(5), pp.531–551.

Davis, R.A. and Healy, T.R. (1993). Holocene coastal depositional sequences on a tectonically active setting: southeastern Tauranga Harbour, New Zealand. *Sedimentary Geology*, 84(1-4), pp.57–69.

Denton, G.H. and Hughes, T.J. (1983). Milankovitch Theory of Ice Ages: Hypothesis of Ice-Sheet Linkage Between Regional Insolation and Global Climate. *Quaternary Research*, 20(02), pp.125–144.

Dingwall, P.R. (1966). *Bay head sand beaches of Banks Peninsula*. Unpublished MA.

Dingwall, P.R. (1974). Bay head sand beaches of Banks Peninsula. *New Zealand Oceanographic Institute Memoir 15*, New Zealand Department of Scientific and Industrial Research.

Donnelly, J., Goff, J. and Chagué-Goff, C. (2016). A record of local storms and trans-Pacific tsunamis, eastern Banks Peninsula, New Zealand. *The Holocene*, 27(4), pp.496–508.

Dougherty, A.J. and Dickson, M.E. (2012). Sea-level and storm control on the evolution of a chenier plain, Firth of Thames, New Zealand. *Marine Geology*, 307-310, pp.58–72.

Edwards, R.L., Beck, J.W., Burr, G.S., Donahue, D.J., Chappell, J.M.A., Bloom, A.L., Druffel, E.R.M. and Taylor, F.W. (1993). A large drop in atmospheric 14C/12C and reduced melting in the Younger Dryas, Documented with 230Th ages of corals. *Science*, 260, pp.962–968.

Engels, S. and Roberts, M.C. (2005). The Architecture of Prograding Sandy-Gravel Beach Ridges Formed During the Last Holocene Highstand: Southwestern British Columbia, Canada. *Journal of Sedimentary Research*, 75(6), pp.1052–1064.

England, J., Atkinson, N., Bednarski, J., Dyke, A.S. and O'Cofaigh, C. (2006). The Innuitian Ice Sheet: configuration, dynamics and chronology. *Quaternary Science Reviews*, 25, pp.689–703.

Evans, R.D. (2009). *Optimising Ground Penetrating Radar (GPR) to Assess Pavements*. EngD Thesis.

Fairbanks, R.G. (1989). A 17,000-year glacio-eustatic sea level record: influence of glacial melting rates on the Younger Dryas event and deep-ocean circulation. *Nature*, 342(6250), pp.637–642.

Fairbridge, R.W. (1982). The Pleistocene-Holocene boundary. *Quaternary Science Reviews*, 1(3), pp.215–244.

Fleming, K., Johnston, P., Zwartz, D., Yokoyama, Y., Lambeck, K. and Chappell, J. (1998). Refining the eustatic sea-level curve since the Last Glacial Maximum using far- and intermediate-field sites. *Earth and Planetary Science Letters*, 163(1-4), pp.327–342.

Gehrels, W.R., Callard, S.L., Moss, P.T., Marshall, W.A., Blaauw, M., Hunter, J., Milton, J.A. and Garnett, M.H. (2012). Nineteenth and twentieth century sea-level changes in Tasmania and New Zealand. *Earth and Planetary Science Letters*, 315-316, pp.94–102.

Gibb, J.G. (1983). Sea levels during the past 10000 years BP from the New Zealand Region, South Pacific Ocean. *International symposium on coastal evolution in the Holocene*, pp.28–31.

Gibb, J.G. (1986). A New Zealand regional Holocene eustatic sea-level curve and its application to determination of vertical tectonic movements. *Royal Society of New Zealand Bulletin*, 24, pp.377–395.

Goff, J., McFadgen, B., Wells, A. and Hicks, M. (2008). Seismic signals in coastal dune systems. *Earth-Science Reviews*, 89(1-2), pp.73–77.

Gouramanis, C., Switzer, A.D., Bristow, C.S., Pham, D.T., Mauz, B., Hoang, Q.D., Lam, D.D., Lee, Y.S., Soria, J.L.A., Pile, J., Chi, N.T.K., Nghiem, D. and Sloss, C. (2020). Holocene evolution of the Chan May coastal embayment, central Vietnam: Changing coastal dynamics associated with decreasing rates of progradation possibly forced by mid- to late-Holocene sea-level changes. *Geomorphology*, 367, p.107273.

GSSI (2006). *GSSI handbook for the radar inspection of concrete*. Salem, New Hampshire, USA: Geophysical Survey Systems, Inc.

Hayward, B.W., Grenfell, H.R., Sabaa, A.T., Kay, J., Daymond-King, R. and Cochran, U. (2010). Holocene subsidence at the transition between strike-slip and subduction on the Pacific-Australian plate boundary, Marlborough Sounds, New Zealand. *Quaternary Science Reviews*, 29(5-6), pp.648–661.

Hayward, B.W., Grenfell, H.R., Sabaa, A.T., Southall, K.E. and Gehrels, W.R. (2007). Foraminiferal evidence of Holocene subsidence and fault displacements, coastal South Otago, New Zealand. *Journal of Foraminiferal Research*, 37(4), pp.344–359.

Heap, A.D. and Nichol, S.L. (1997). The influence of limited accommodation space on the stratigraphy of an incised-valley succession: Weiti River estuary, New Zealand. *Marine Geology*, 144(1-3), pp.229–252.

Herzer, R.H. (1977). *Late Quaternary geology of the Canterbury continental terrace.* Unpublished PhD thesis.

Hicks, H. and Nichol, S.L. (2007). A marine to freshwater sediment succession from Kowhai Beach wetland, Northland: Implications for Holocene sea level. *Journal of the Royal Society of New Zealand*, 37(3), pp.91–107.

Isla, M.F., Moyano-Paz, D., FitzGerald, D.M., Simontacchi, L. and Veiga, G.D., (in press). Contrasting beach ridge systems in different types of coastal settings. *Earth Surface Processes and Landforms*.

Jol, H.M. and Bristow, C.S. (2003). GPR in sediments: advice on data collection, basic processing and interpretation, a good practice guide. *Geological Society, London, Special Publications*, 211(1), pp.9–27.

Kain, C.L., Gomez, C., Hart, D.E., Wassmer, P., Goff, J. and Starheim, C. (2014). Assessing topographic controls on flow direction in washover deposits using measurements of Magnetic Fabric. *Marine Geology*, 350, pp.16–26.

Kennedy, D.M. (2008). Recent and future higher sea levels in New Zealand: A review. *New Zealand Geographer*, 64(2), pp.105–116.

L. M. J. U. van Straaten, Ph. H. Ku (1958). Tidal Action as a Cause of Clay Accumulation. *SEPM Journal of Sedimentary Research*, Vol. 28.

Lajeunesse, P. and St-Onge, G. (2008). The subglacial origin of the Lake Agassiz–Ojibway final outburst flood. *Nature Geoscience*, 1(3), pp.184–188.

Lambeck, K., Yokoyama, Y. and Purcell, T. (2002). Into and out of the Last Glacial Maximum: sea-level change during Oxygen Isotope Stages 3 and 2. *Quaternary Science Reviews*, 21(1-3), pp.343–360.

Laskar, J., Fienga, A., Gastineau, M. and Manche, H. (2011). La2010: a new orbital solution for the long-term motion of the Earth. *Astronomy and Astrophysics*, 532, p.A89.

Lawrie, A. (1993). Shore platforms at +6–8 m above mean sea level on Banks Peninsula and implications for tectonic stability. *New Zealand Journal of Geology and Geophysics*, 36(4), pp.409–415.

Leventer, A., Domack, E., Dunbar, R., Pike, J., Stickley, C., Maddison, E., Brachfeld, S., Manley, P. and McClennen, C. (2006). Marine sediment record from the East Antarctic margin reveals dynamics of ice sheet recession. *GSA Today*, 16(12), p.4.

Leverington, D.W., Mann, J.D. and Teller, J.T. (2002). Changes in the Bathymetry and Volume of Glacial Lake Agassiz between 9200 and 7700 14C yr B.P. *Quaternary Research*, 57(2), pp.244–252.

Lewis, S.E., Sloss, C.R., Murray-Wallace, C.V., Woodroffe, C.D. and Smithers, S.G. (2013). Post-glacial sea-level changes around the Australian margin: a review. *Quaternary Science Reviews*, 74, pp.115–138.

Liggett, K.A. and Gregg, D.R. (1918). The Geology of Banks Peninsula. *Geological Magazine*, 5(11), pp.523–525.

LINZ (2021). *LINZ Geodetic database - spatial view*. [online] www.geodesy.linz.govt.nz. Available at: https://www.geodesy.linz.govt.nz/gdb/ [Accessed 26 Oct. 2021].

Liu, J.Paul., Milliman, J.D., Gao, S. and Cheng, P. (2004). Holocene development of the Yellow River's subaqueous delta, North Yellow Sea. *Marine Geology*, 209(1-4), pp.45–67.

Mackenzie, P. (1958). The development of beach sand ridges. *Australian Journal of Science*, 20, pp.213–214.

Mackintosh, A., Golledge, N., Domack, E., Dunbar, R., Leventer, A., White, D., Pollard, D., DeConto, R., Fink, D., Zwartz, D., Gore, D. and Lavoie, C. (2011). Retreat of the East Antarctic ice sheet during the last glacial termination. *Nature Geoscience*, 4(3), pp.195–202.

Martinez, A. and Byrnes, A.P. (2001). Modeling Dielectric-Constant Values of Geologic Materials. *Current Research in Earth Sciences*, pp.1–16.

McGlone, M.S., Turney, C.S.M., Wilmshurst, J.M., Renwick, J. and Pahnke, K. (2010). Divergent trends in land and ocean temperature in the Southern Ocean over the past 18,000 years. *Nature Geoscience*, 3(9), pp.622–626.

McSaveney, M.J., Graham, I.J., Begg, J.G., Beu, A.G., Hull, A.G., Kim, K. and Zondervan, A. (2006). Late Holocene uplift of beach ridges at Turakirae Head, south Wellington coast, New Zealand. *New Zealand Journal of Geology and Geophysics*, 49(3), pp.337–358.

Munk, W.H. and Revelle, R.R.D. (1952). Sea level and the rotation of the earth. *American Journal of Science*, 250(11), pp.829–833.

Nakada, M. and Lambeck, K. (1989). Late Pleistocene and Holocene sea-level change in the Australian region and mantle rheology. *Geophysical Journal International*, 96(3), pp.497–517.

Neal, A. and Roberts, C.L. (2000). Applications of ground-penetrating radar (GPR) to sedimentological, geomorphological and geoarchaeological studies in coastal environments. *Geological Society, London, Special Publications*, 175(1), pp.139–171.

Nesje, A., Dahl, S.O. and Bakke, J. (2004). Were abrupt Lateglacial and early-Holocene climatic changes in northwest Europe linked to freshwater outbursts to the North Atlantic and Arctic Oceans? *The Holocene*, 14(2), pp.299–310.

Neumann, B., Vafeidis, A.T., Zimmermann, J. and Nicholls, R.J. (2015). Future Coastal Population Growth and Exposure to Sea-Level Rise and Coastal Flooding - A Global Assessment. *PLOS ONE*, 10(3).

Nielsen, L. and Clemmensen, L.B. (2009). Sea-level markers identified in ground-penetrating radar data collected across a modern beach ridge system in a microtidal regime. *Terra Nova*, 21(6), pp.474–479.

NIWA (2022). *NIWA Tides*. [online] tides.niwa.co.nz. Available at: https://tides.niwa.co.nz/ [Accessed 29 Mar. 2022].

Oliver, T.S., Dougherty, A.J., Gliganic, L.A. and Woodroffe, C.D., 2015. Towards more robust chronologies of coastal progradation: optically stimulated luminescence ages for the coastal plain at Moruya, south-eastern Australia. The Holocene, 25(3), pp.536-546.

Oliver, T.S., Thom, B.G. and Woodroffe, C.D., 2017. Formation of beach-ridge plains: an appreciation of the contribution by Jack L. Davies. Geographical Research, 55(3), pp.305-320.

Oliver, T.S., Donaldson, P., Sharples, C., Roach, M. and Woodroffe, C.D., 2017. Punctuated progradation of the Seven Mile Beach Holocene barrier system, southeastern Tasmania. Marine Geology, 386, pp.76-87.

Oliver, T.S., Tamura, T., Short, A.D. and Woodroffe, C.D., 2019. Rapid shoreline progradation followed by vertical foredune building at Pedro Beach, southeastern Australia. Earth Surface Processes and Landforms, 44(2), pp.655-666.

Oliver, T.S., Murray-Wallace, C.V. and Woodroffe, C.D., 2020. Holocene shoreline progradation and coastal evolution at Guichen and Rivoli Bays, southern Australia. The Holocene, 30(1), pp.106- 124.

Otvos, E.G. (2000). Beach ridges — definitions and significance. *Geomorphology*, 32(1-2), pp.83–108.

Peltier, W.R. and Fairbanks, R.G. (2006). Global glacial ice volume and Last Glacial Maximum duration from an extended Barbados sea level record. *Quaternary Science Reviews*, 25(23-24), pp.3322–3337.

Pirazzoli, P. A. World Atlas of Holocene Sea-level Changes. (1991). Amsterdam: Elsevier.

Postma, H. (1961). Transport and accumulation of suspended matter in the Dutch Wadden Sea. *Netherlands Journal of Sea Research*, 1(1-2), pp.148–190.

Rial, F.I., Pereira, M., Lorenzo, H., Arias, P. and Novo, A. (2009). Resolution of GPR bowtie antennas: An experimental approach. *Journal of Applied Geophysics*, 67(4), pp.367–373.

Ritchie, J.C., Cwynar, L.C. and Spear, R.W. (1983). Evidence from north-west Canada for an early Holocene Milankovitch thermal maximum. *Nature*, 305(5930), pp.126–128.

Schallenberg, M., Goff, J. and Harper, M.A. (2012). Gradual, catastrophic and human induced environmental changes from a coastal lake, southern New Zealand. *Sedimentary Geology*, 273-274, pp.48–57.

Scholfield, J.C. (1960). Sea level fluctuations during the last 4,000 years as recorded by a chenier plain, Firth of Thames, New Zealand. *New Zealand Journal of Geology and Geophysics*, 3(3), pp.467–485.

Shulmeister, J. and Head, J. (1993). Aspects of the emplacement, evolution and 14C chronology of ridges on a coastal spit, Groote Eylandt, Northern Australia. *Marine Geology*, 111(1-2), pp.159–169.

Shulmeister, J. and Kirk, R.M. (1993). Evolution of a mixed sand and gravel barrier system in North Canterbury, New Zealand, during Holocene sea-level rise and still-stand. *Sedimentary Geology*, 87(3-4), pp.215–235.

Sloss, C.R., Jones, B.G., Switzer, A.D., Nichol, S., Clement, A.J.H. and Nicholas, A.W. (2010).

The Holocene infill of Lake Conjola, a narrow incised valley system on the southeast coast of Australia. *Quaternary International*, 221(1-2), pp.23–35.

Smith, D.E., Harrison, S., Firth, C.R. and Jordan, J.T. (2011). The early Holocene sea level rise. *Quaternary Science Reviews*, 30(15-16), pp.1846–1860.

Soons, J.M., Shulmeister, J. and Holt, S. (1997). The Holocene evolution of a well nourished gravelly barrier and lagoon complex, Kaitorete 'Spit', Canterbury, New Zealand. *Marine Geology*, 138(1-2), pp.69–90.

Stapor, F.W. (1975). Holocene beach ridge plain development, northwest Florida. *Zeitschrift fur Geomorphologie*, 22, pp.116–144.

Stephenson, W. and Shulmeister, J. (1999). A Holocene progradation record from Okains Bay, Banks Peninsula, Canterbury, New Zealand. *New Zealand Journal of Geology and Geophysics*, 42(1), pp.11–19.

Stephenson, W.J. (1992). *Morphology and morphodynamics of a bay head sand beach, Okains Bay, Banks Peninsula.* Unpublished MSc.

Tamura, T. (2012). Beach ridges and prograded beach deposits as palaeoenvironment records. *Earth-Science Reviews*, 114(3-4), pp.279–297.

Tamura, T., Murakami, F., Nanayama, F., Watanabe, K. and Saito, Y. (2008). Ground-penetrating radar profiles of Holocene raised-beach deposits in the Kujukuri strand plain, Pacific coast of eastern Japan. *Marine Geology*, 248(1-2), pp.11–27.

Tanner, W. (1995). Origin of beach ridges and swales. *Marine Geology*, 129, pp.149–161.

Tanner, W.F. and Demirpolat, S. (1988). New Beach Ridge Type: Severely Limited Fetch, Very Shallow Water: ABSTRACT. *AAPG Bulletin*, 72.

Teller, J.T. and Leverington, D.W. (2004). Glacial Lake Agassiz: A 5000 yr history of change and its relationship to the δ18O record of Greenland. *Geological Society of America Bulletin*, 116(5), p.729.

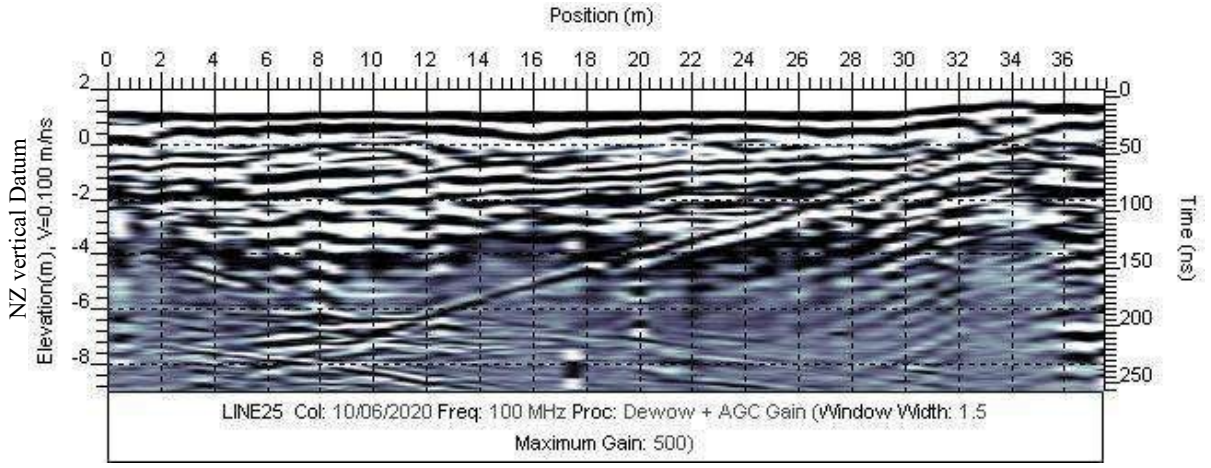
Thom, B.G. (1984). Transgressive and regressive stratigraphies of coastal sand barriers in southeast Australia. *Marine Geology*, 56(1-4), pp.137–158.

Ullman, D.J., Carlson, A.E., Hostetler, S.W., Clark, P.U., Cuzzone, J., Milne, G.A., Winsor, K. and Caffee, M. (2016). Final Laurentide ice-sheet deglaciation and Holocene climate-sea level change. *Quaternary Science Reviews*, 152, pp.49–59.

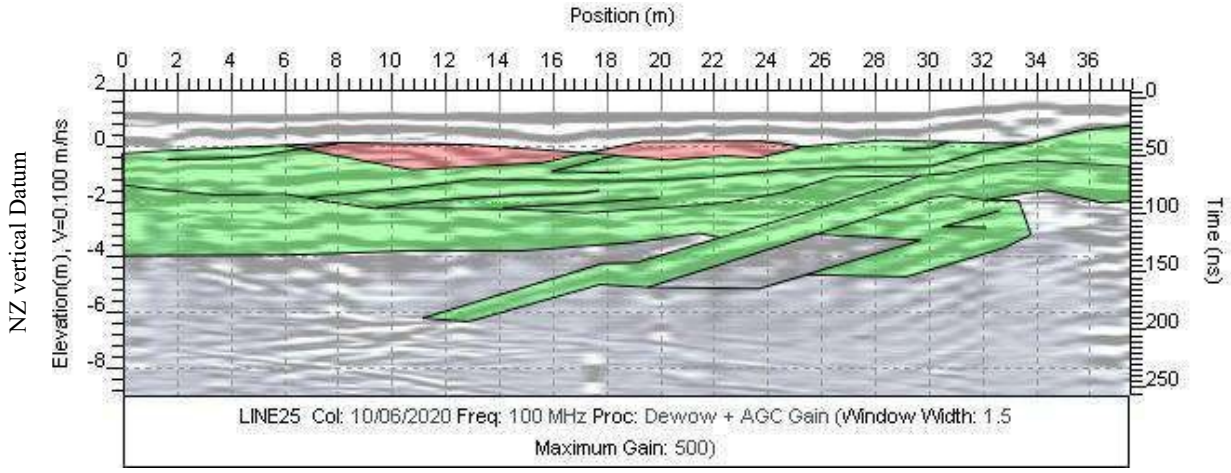
Woodroffe, S.A. (2009). Testing models of mid to late Holocene sea-level change, North Queensland, Australia. *Quaternary Science Reviews*, 28(23-24), pp.2474–2488.

Appendix A: GPR image for Okains Bay showing 37.5 m

a



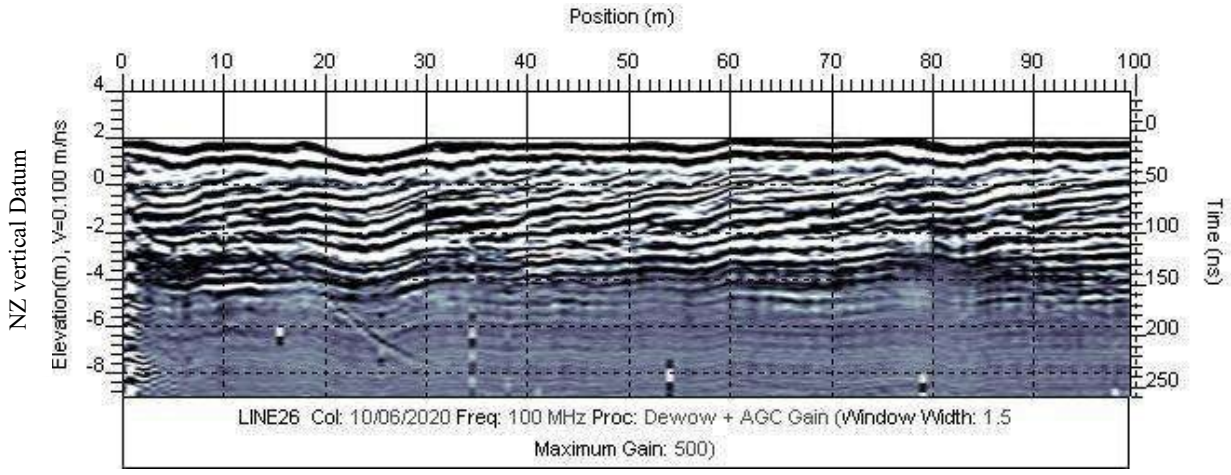
b



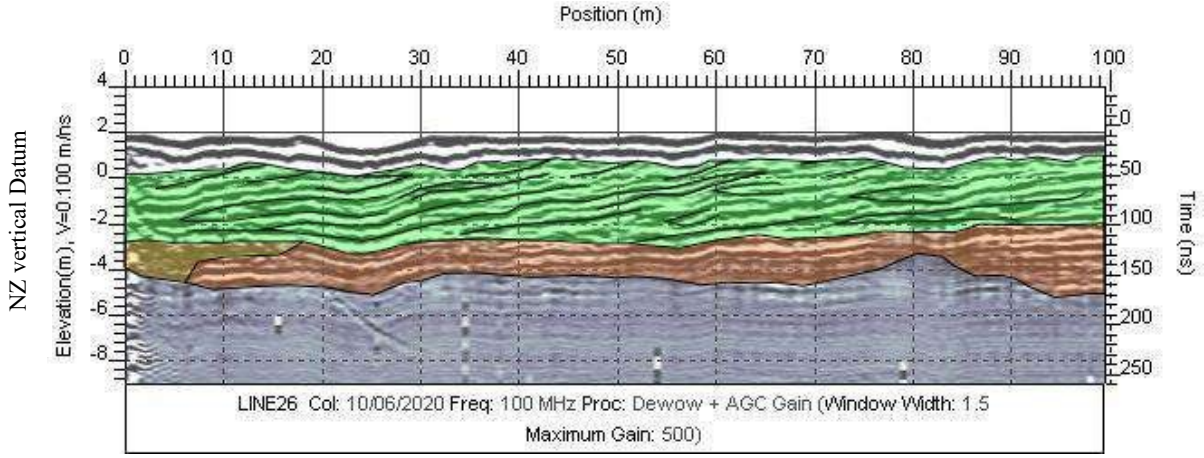
Appendix A: GPR image of part of the Okains Bay transect showing 37.5 m. a) non annotated image. b) showing annotations. Green = prograding sequence, red = erosional surfaces.

Appendix B: GPR image for Okains Bay showing 100 m

a



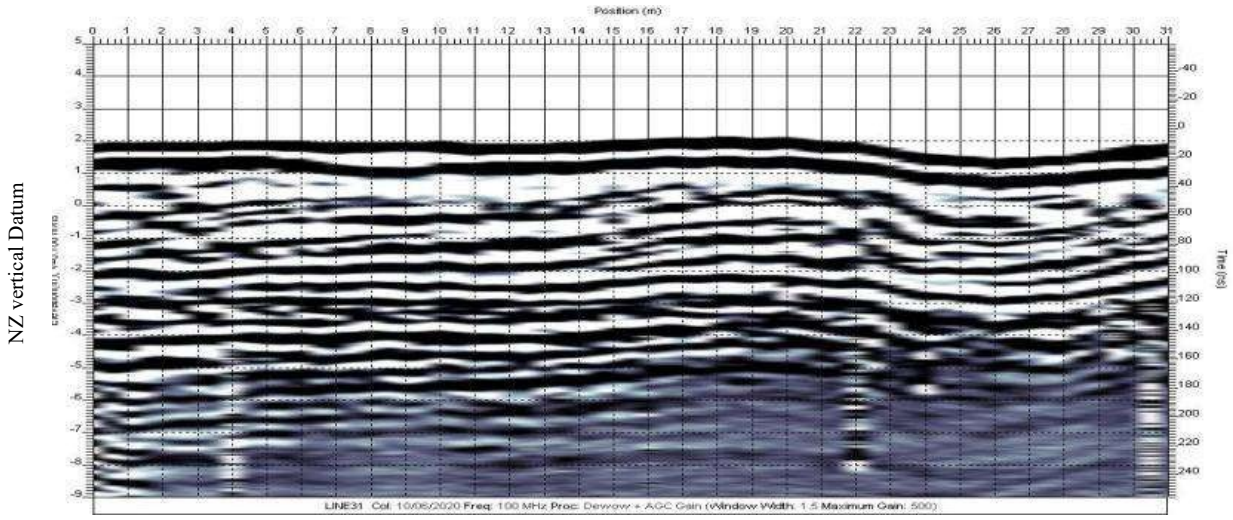
b



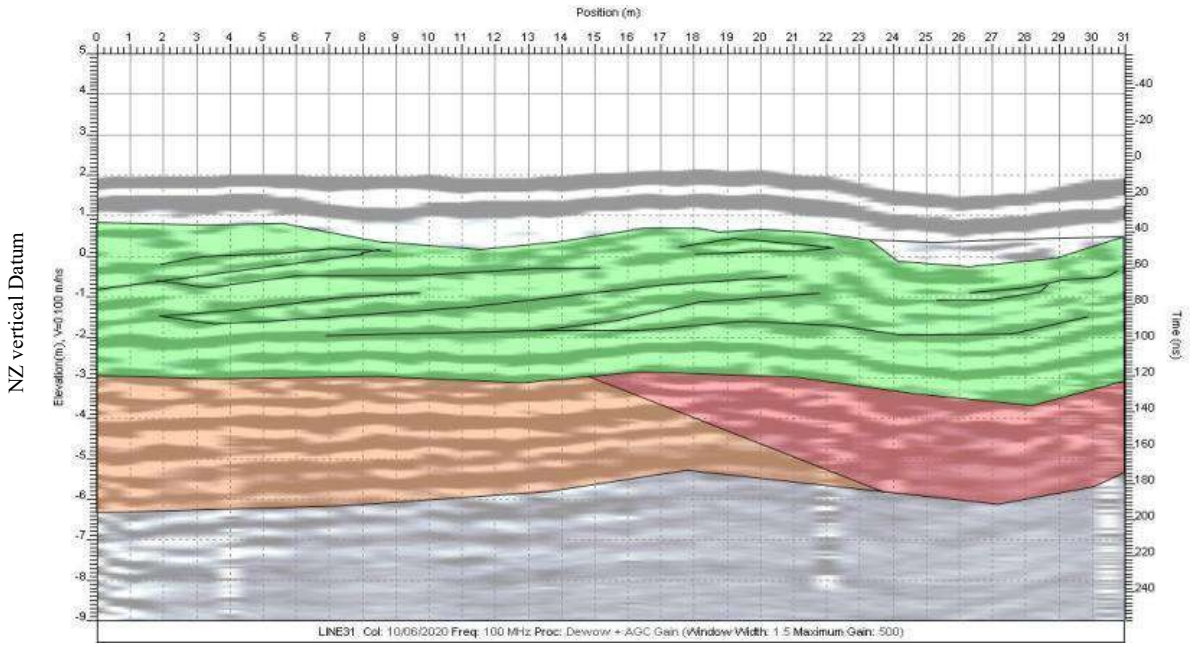
Appendix B: GPR image of part of the Okains Bay transect showing 100 m. a) non annotated image. b) showing annotations. Green = prograding sequence, Orange = horizonal stratigraphy, and yellow = unreadable data.

Appendix C: GPR image for Okains Bay showing 31 m

a



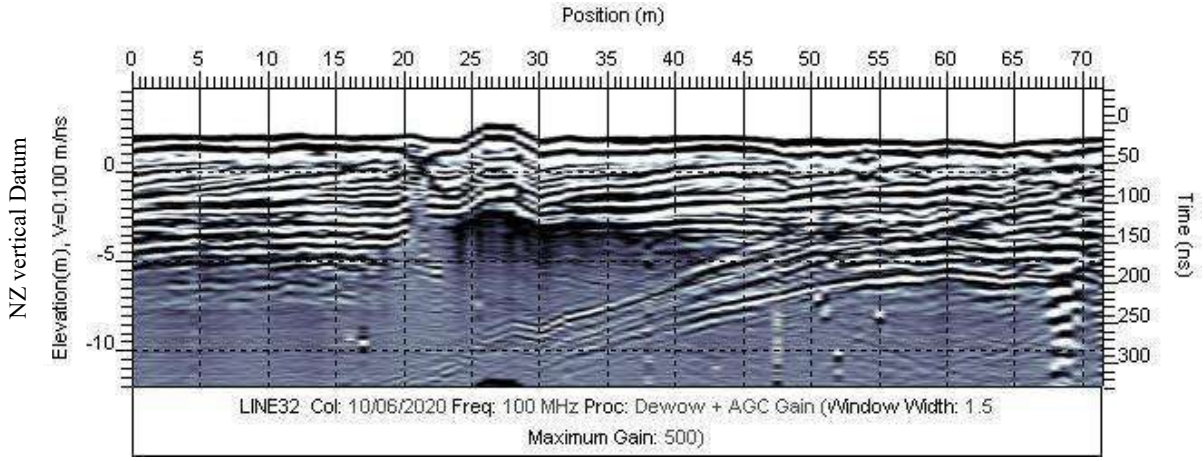
b



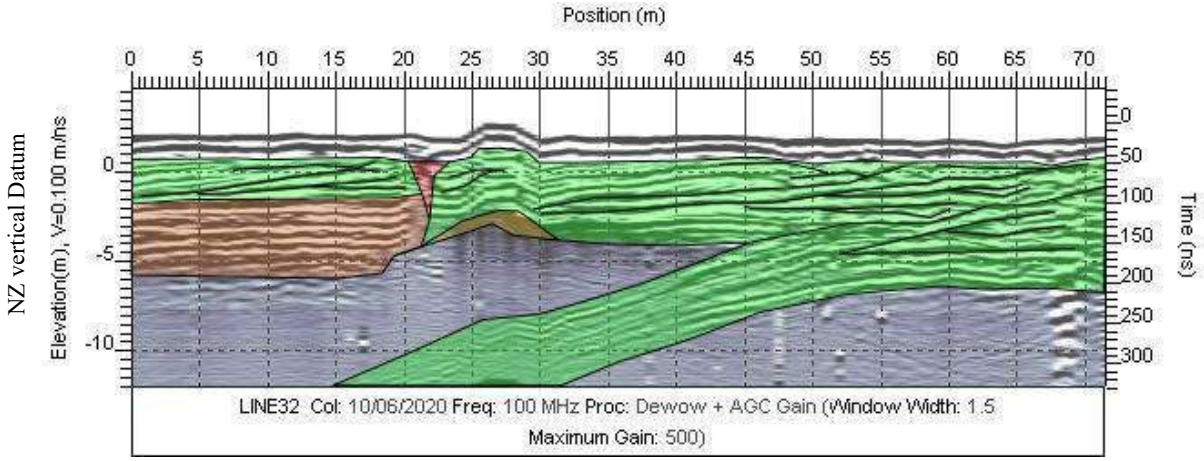
Appendix C: GPR image of part of the Okains Bay transect showing 31 m. a) non annotated image. b) showing annotations. Green = prograding sequence, red = erosional surfaces, and orange = horizontal stratigraphy.

Appendix D: GPR image for Okains Bay showing 72 m

a



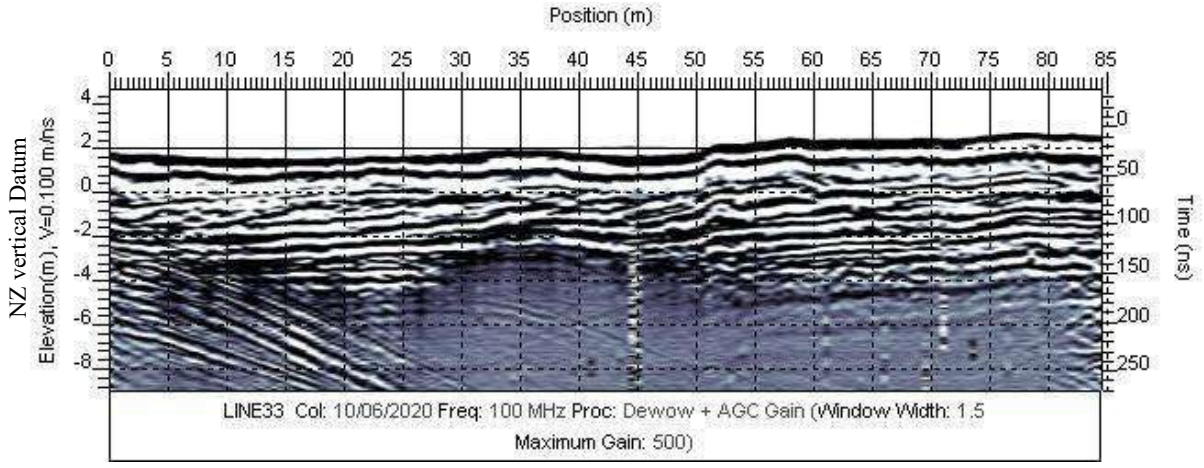
b



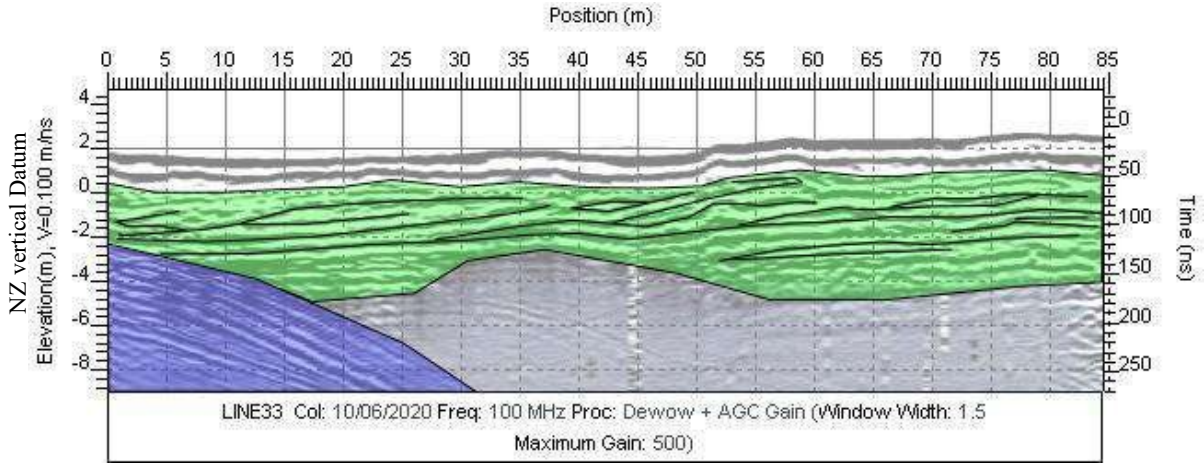
Appendix D: GPR image of part of the Okains Bay transect showing 72 m. a) non annotated image. b) showing annotations. Green = prograding sequence, red = erosional surfaces, yellow = unreadable data, and orange = horizontal stratigraphy.

Appendix E: GPR image for Okains Bay showing 85 m

a



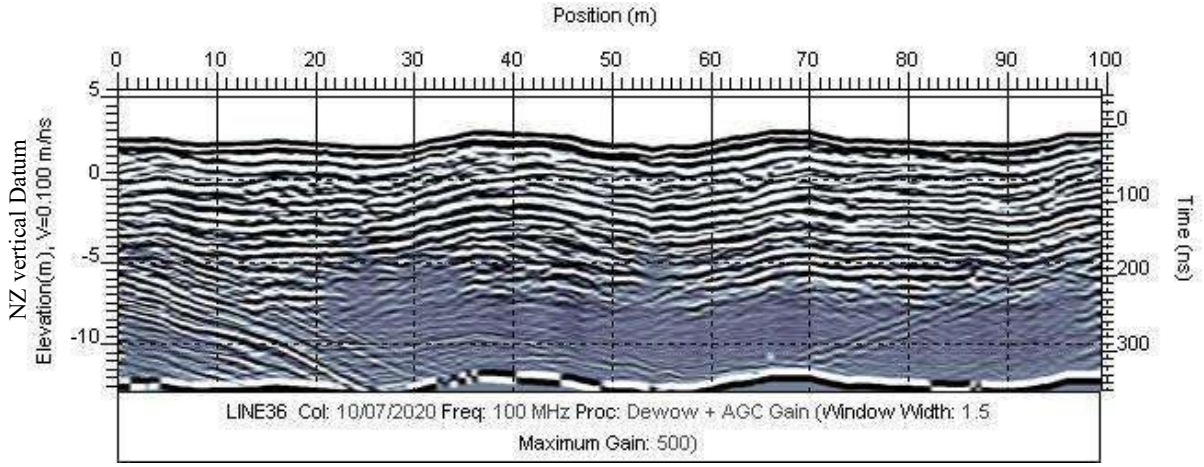
b



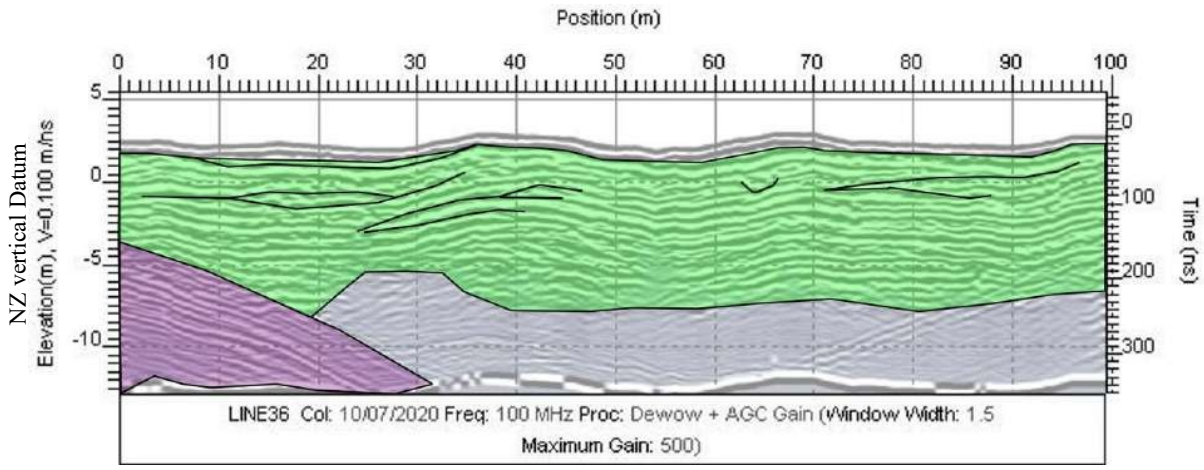
Appendix E: GPR image of part of the Okains Bay transect showing 85 m. a) non annotated image. b) showing annotations. Green = prograding sequence, purple = aeolian sediment with unknown artifact.

Appendix F: GPR image for Okains Bay showing 100 m

a

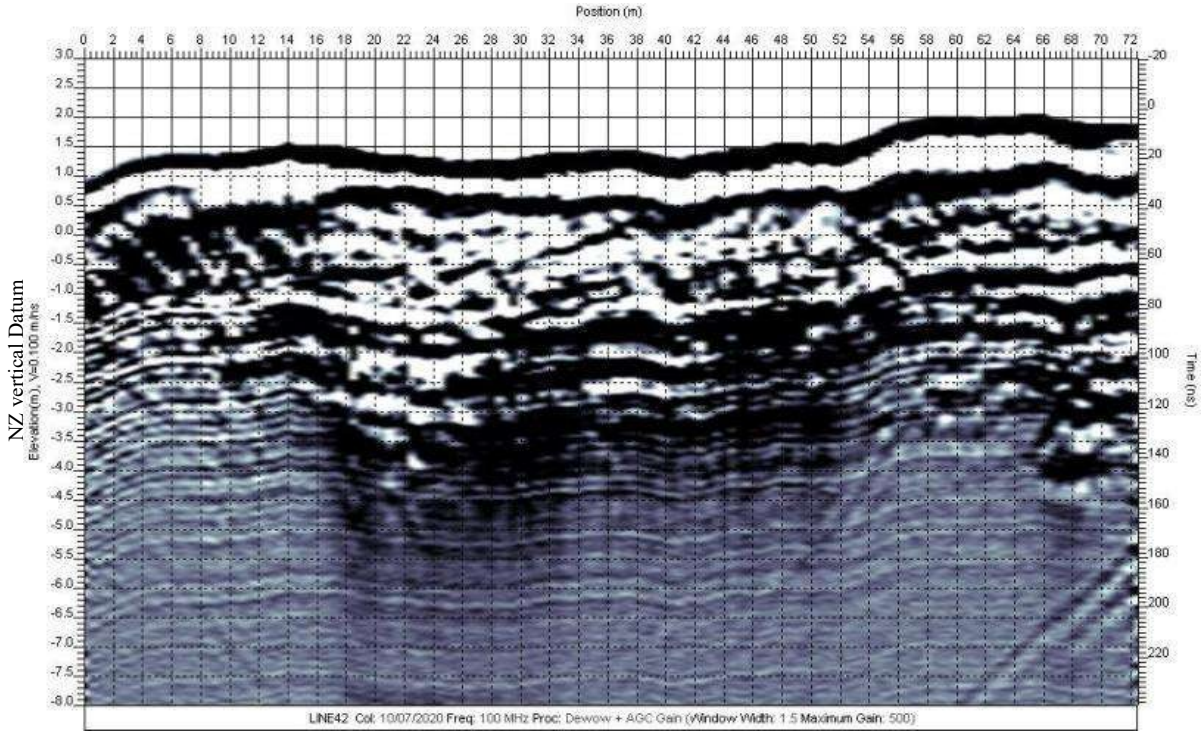


b



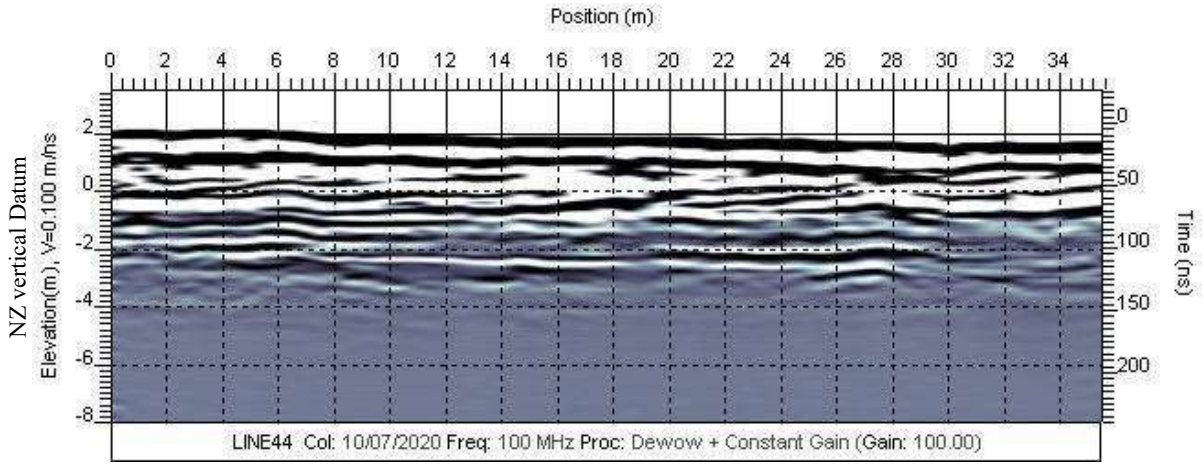
Appendix F: GPR image of part of the Okains Bay transect showing 100 m. a) non annotated image. b) showing annotations. Green = prograding sequence, and pink = unknown stratigraphy as too close to start of transect.

Appendix G: GPR image for Okains Bay showing 72.5 m



Appendix G: GPR image of part of the Okains Bay transect showing 72.5 m.

Appendix H: GPR image for Okains Bay showing 35 m



Appendix H: GPR image of part of the Okains Bay transect showing 35 m.